



**International Committee for Future Accelerators**

Sponsored by the Particles and Fields Commission of IUPAP

# **Beam Dynamics Newsletter**

**No. 36**

**Issue Editor:  
A.M. Lombardi**

**Editor in Chief:  
W. Chou**

**April 2005**



## Contents

<b>1</b>	<b>FOREWORD.....</b>	<b>7</b>
1.1	FROM THE CHAIRMAN.....	7
1.2	FROM THE EDITOR .....	8
<b>2</b>	<b>INTERNATIONAL LINEAR COLLIDER (ILC).....</b>	<b>9</b>
2.1	THE BIRTH OF THE GLOBAL DESIGN EFFORT (GDE) FOR THE ILC .....	9
2.2	THE CHALLENGES OF THE CLIC TECHNOLOGY – EXPERIMENTAL PROGRAM AND FIRST RESULTS OF THE TEST FACILITY CTF3 .....	11
2.2.1	Introduction .....	11
2.2.2	Previous Experimental Results .....	12
2.2.3	Status of the CTF3 complex .....	14
2.2.3.1	<i>Injector and linac</i> .....	15
2.2.3.2	<i>The PETS beam line and the High Power Test Stand</i> .....	16
2.2.3.3	<i>Chicane and end-of-linac diagnostics</i> .....	16
2.2.4	Commissioning and First Experimental Results .....	17
2.2.4.1	<i>Injector and linac performances</i> .....	17
2.2.4.2	<i>Full Beam Loading Operation</i> .....	18
2.2.4.3	<i>30 GHz power production</i> .....	18
2.2.4.4	<i>Chicane and bunch length measurements</i> .....	19
2.2.5	Conclusions and Outlook .....	20
2.2.6	Acknowledgment.....	20
2.2.7	References .....	20
<b>3</b>	<b>THEME SECTION.....</b>	<b>21</b>
3.1	ION SOURCES FOR SYNCHROTRON INJECTORS .....	21
3.1.1	Introduction .....	21
3.1.2	Ionisation .....	21
3.1.2.1	<i>Plasma and ionisation</i> .....	21
3.1.2.2	<i>Ionisation of hydrogen</i> .....	22
3.1.2.3	<i>Multiply charged ions</i> .....	22
3.1.3	Proton Sources.....	23
3.1.3.1	<i>Background</i> .....	23
3.1.3.2	<i>Plasmatrons</i> .....	23
3.1.3.3	<i>Surface negative ion sources</i> .....	24
3.1.3.4	<i>Volume negative ion sources</i> .....	26
3.1.4	Multi charged ions .....	27
3.1.4.1	<i>The Electron Cyclotron Resonance Source (ECRIS)</i> .....	27
3.1.4.2	<i>Electron Beam Ion Source (EBIS)</i> .....	28
3.1.5	Final Remarks.....	29

3.1.6	References.....	29
3.2	R&D OF RFQ DRIFT-TUBE PROTON LINACS IN IHEP-PROTVINO .....	30
3.2.1	Introduction.....	30
3.2.2	Acceleration and focusing in RFQ-DTL .....	31
3.2.3	Operational RFQ-DTL Facilities .....	33
3.2.4	References.....	34
3.3	BEAM HALO IN HIGH INTENSITY PROTON/H <sup>-</sup> LINEAR ACCELERATORS .....	35
3.3.1	Introduction.....	35
3.3.2	Halo Mechanisms in Linacs.....	35
3.3.3	The Particle-Core Model .....	36
3.3.3.1	<i>Basic equations</i> .....	36
3.3.3.2	<i>Initial mismatch</i> .....	37
3.3.4	3D Mismatch Modes.....	38
3.3.5	Simulations & Experiments.....	40
3.3.6	Recent Developments .....	41
3.3.7	Summary .....	41
3.3.8	References.....	41
3.4	RECENT ADVANCES ON THE MULTI-TURN EXTRACTION USING STABLE ISLANDS OF TRANSVERSE PHASE SPACE.....	43
3.4.1	Introduction.....	43
3.4.2	Further Developments .....	46
3.4.2.1	<i>Analysis of the Capture Process for the Fourth-Order Resonance</i> .....	46
3.4.2.2	<i>Extension to Other Resonances</i> .....	48
3.4.2.3	<i>Multi-Turn Injection Using Stable Islands</i> .....	50
3.4.3	Experimental Results .....	51
3.4.3.1	<i>Overall Measurement Strategy</i> .....	51
3.4.3.2	<i>Special Measurements</i> .....	55
3.4.4	Towards an Operational Version of the Multi-Turn Extraction .....	57
3.4.5	References.....	58
3.5	BEAM TESTS OF A STOCHASTIC SLOW EXTRACTION IN THE U70 .....	60
3.5.1	Introduction.....	60
3.5.2	Specifics of the scheme .....	60
3.5.3	Beam observations.....	61
3.5.4	Further prospects .....	62
3.5.5	References.....	62
3.6	IDRA: DESIGN STUDY OF A PROTON THERAPY FACILITY .....	62
3.6.1	Introduction.....	62
3.6.2	IDRA .....	64
3.6.2.1	<i>IDRA overview</i> .....	64
3.6.2.2	<i>LIBO: the Linac BOster</i> .....	65
3.6.2.3	<i>Beam energy modulation</i> .....	67
3.6.2.4	<i>LIBO-30 transverse beam optics</i> .....	69
3.6.2.5	<i>Beam injection in LIBO and multi-particle computations</i> .....	70
3.6.3	Acknowledgment.....	72

3.6.4	References .....	72
<b>4</b>	<b>ACTIVITY REPORTS.....</b>	<b>73</b>
4.1	THE RAL FRONT END TEST STAND.....	73
4.1.1	Introduction .....	73
4.1.2	The Front End Test Stand.....	73
4.1.2.1	<i>H</i> ion source .....	74
4.1.2.2	LEBT.....	75
4.1.2.3	RF frequency choice.....	75
4.1.2.4	RFQ.....	75
4.1.2.5	The high-speed beam chopper.....	76
4.1.3	Diagnostics .....	77
4.1.4	Summary.....	78
4.1.5	References .....	78
4.2	ACCELERATION OF BEAM IN A FOUR-CELL PLANE WAVE TRANSFORMER (PWT) LINAC STRUCTURE.....	79
4.2.1	Introduction .....	79
4.2.2	The Plane Wave Transformer (PWT) linac.....	79
4.2.3	Simulations and cold tests .....	80
4.2.4	Acceleration trials.....	82
4.2.5	Future plans .....	83
4.2.6	Acknowledgements .....	84
4.2.7	References .....	84
<b>5</b>	<b>WORKSHOP AND CONFERENCE REPORTS.....</b>	<b>84</b>
5.1	SUMMARY OF THE 33RD ICFA ADVANCED BEAM DYNAMICS WORKSHOP ON "HIGH INTENSITY AND HIGH BRIGHTNESS HADRON BEAMS" (ICFA-HB2004) .....	84
5.1.1	Lattices, Beam Loss Handling and Collimation & Diagnostics and Instrumentation.....	86
5.1.2	High Intensity Linacs / Front End & Proton Drivers .....	89
5.1.3	Space Charge Simulation and Experiment .....	90
5.1.4	Electron Clouds and Desorption.....	91
5.1.5	Injection, Instabilities and Feedback .....	93
5.1.6	Beam cooling and high brightness .....	97
5.1.7	Advanced Techniques .....	98
5.1.8	FFAGs and Cyclotrons.....	100
<b>6</b>	<b>FORTHCOMING BEAM DYNAMICS EVENTS.....</b>	<b>101</b>
6.1	WORKSHOP COULOMB 05 – HIGH INTENSITY BEAM DYNAMICS .....	101
6.2	34 <sup>TH</sup> ICFA ADVANCED BEAM DYNAMICS WORKSHOP - HIGH POWER SUPERCONDUCTING ION, PROTON, AND MULTI-SPECIES LINACS, "HPSL 2005" .....	103
6.3	JOINT 38TH ICFA ADVANCED BEAM DYNAMICS AND 9TH ADVANCED & NOVEL ACCELERATORS WORKSHOP ON LASER-BEAM INTERACTIONS AND LASER AND PLASMA ACCELERATORS .....	105

<b>7</b>	<b>ANNOUNCEMENTS OF THE BEAM DYNAMICS PANEL.....</b>	<b>108</b>
7.1	ICFA BEAM DYNAMICS NEWSLETTER.....	108
7.1.1	Aim of the Newsletter.....	108
7.1.2	Categories of Articles .....	108
7.1.3	How to Prepare a Manuscript .....	109
7.1.4	Distribution .....	109
7.1.5	Regular Correspondents.....	110
7.2	ICFA BEAM DYNAMICS PANEL MEMBERS .....	111

# 1 Foreword

## 1.1 From the Chairman

Weiren Chou, Fermilab  
 mail to: [chou@fnal.gov](mailto:chou@fnal.gov)

At the annual joint ICFA – Lab Directors meeting on February 10-11, 2005 in Vancouver, Canada, ICFA unanimously approved offering the position of ILC GDE (International Linear Collider Global Design Effort) Director to Professor Barry Barish (Caltech, U.S.A.). On March 18 Prof. Barish accepted the offer and was invited to write an article on the GDE plan. One important feature of his plan is that the GDE will have a “virtual” central site, i.e., no physical location. He believes this is the right approach to get the best people to work for the GDE without asking them to relocate. Barry’s article can be found in Section 2 of this newsletter.

At the same meeting five ICFA Advanced Beam Dynamics Workshops (ABDWs) were proposed and approved:

- 34<sup>th</sup>: High Power Superconducting Ion, Proton, and Multi-Species Linacs (HPSL2005), May 22-24, 2005, Northern Illinois University, Naperville, Illinois, U.S.A.
- 35<sup>th</sup>: Physics and Applications of High Brightness Electron Beams, October 9-14, 2005, Erice, Sicily, Italy. (Jointly sponsored with the ICFA Advanced and Novel Accelerator Panel)
- 36<sup>th</sup>: Nanobeam 2005, October 17-21, 2005, Uji Campus of Kyoto University, Japan.
- 37<sup>th</sup>: Future Light Sources 2006, May 15-19, 2006, DESY, Hamburg, Germany.
- 38<sup>th</sup>: Laser-Beam Interactions and Laser and Plasma Accelerators (LBI-LPA 2005), December 12-16, 2005, National Taiwan University, Taipei, Taiwan. (Jointly sponsored with the ICFA Advanced and Novel Accelerator Panel)

ICFA also approved Dr. Chris Prior (Rutherford Appleton Lab, U.K.) to be a new member of the Beam Dynamics Panel. Chris is a well-known accelerator physicist. On behalf of the Panel, I welcome Chris on board and look forward to working with him in the coming years. The current Panel member list can be found at the end of this newsletter.

At the Vancouver meeting, the *ICFA Beam Dynamics Newsletter* received high marks from the ICFA Chairman, Prof. J. Dorfan (SLAC, U.S.A.). He praised the Newsletter for its rich content and high quality of articles. The credit belongs to all the issue editors (C. Biscari, D. Rice, K. Ohmi and M. Furman, J. Gao, Y. Funakoshi, and other previous issue editors) as well as to all the contributors and distributors (S. Kamada, R. Wanzenberg, etc.). The editor of this issue, Dr. Alessandra Lombardi (CERN, Switzerland), has kept up with the good work and produced another high quality issue. You will find a number of interesting papers, workshop reports and other articles. We thank Alessandra for her efforts in editing this newsletter.

In order to report the accelerator activities from every corner of the world, we are in the process of recruiting more regular correspondents from those institutions and

countries where the accelerator community is small. Dr. Sameen Ahmed Khan (MECIT, Oman) recently accepted our invitation to be a correspondent. We encourage more volunteers to come forward and join this team.

During PAC2005, this Panel will hold a meeting on May 16, 2005. A majority of the Panel members (or their delegates) are expected to attend. It will review the work in the past two years and make a plan for the following two years. Suggestions or comments from the readers concerning the Panel's activities are welcome.

## 1.2 From the Editor

Alessandra Lombardi, CERN  
mail to: [Alessandra.Lombardi@cern.ch](mailto:Alessandra.Lombardi@cern.ch)

Issues linked to high intensity proton machines constitute the main theme of this beam dynamics newsletter. In particular, I have collected articles on the less-known mechanisms of intensity limitation as well as the most astute tricks to overcome them. This issue also contains a complete overview of particle sources. Sources, too often forgotten or taken for granted, are really the first stage of acceleration where the initial beam emittance and distribution of particles within the beam are determined. The theme section also contains a description of the beam dynamics in a new "mixed" structure (the Radio Frequency Quadrupole-Drift Tube Linac), a promising structure for the early stages of acceleration. Finally a report on an application of hadron acceleration to medical machines closes the section.

This issue contains a section dedicated to linear collider with a message from Barry Barish, the newly appointed Director of the International Linear Collider Global Design Effort. In addition there is a report on the CLIC test facility.

I have received two activity reports: a contribution on the upcoming test stand facility for the high intensity pulsed proton beam at Rutherford Laboratories and a preliminary report on the ever-expanding accelerator activities in India from our regular correspondent S. Krishnagopal.

A comprehensive summary of the issues discussed at HB2004 together with the announcement of three upcoming ICFA workshops complete the issue.

Editing this issue has been a pleasure and I would like to thank all the contributors for the high quality of the material and, last but not least, for providing the material by the deadline.

## 2 International Linear Collider (ILC)

### 2.1 The Birth of the Global Design Effort (GDE) for the ILC

Barry C. Barish, Director of the GDE  
mail to: [barish@ligo.caltech.edu](mailto:barish@ligo.caltech.edu)

Last August 2004, a crucial milestone was reached in making the choice of which technology to pursue for linear collider. The International Technology Recommendation Panel (ITRP), which I chaired, submitted its recommendation to the International Linear Collider Steering Committee (ILCSC) chaired by Maury Tigner and to its parent body, ICFA, chaired by Jonathan Dorfan. The recommendation read:

*“We recommend that the linear collider be based on superconducting rf technology. This recommendation is made with the understanding that we are recommending a technology, not a design. We expect the final design to be developed by a team drawn from the combined warm and cold linear collider communities, taking full advantage of the experience and expertise of both.”*  
(From the ITRP Report Executive Summary)

Since this recommendation followed a decade of intensive R&D on both technologies, we were concerned how the recommendation would be received and whether the community would, in fact, be able to get behind it. Our recommendation was submitted during the Beijing ICHEP Conference and both ILCSC and ICFA immediately and unanimously accepted and endorsed the recommendation. The three laboratory directors for the proponent laboratories: Yoji Totsuka of KEK, Albrecht Wagner of DESY and Jonathan Dorfan of SLAC each strongly backed the recommendation in their own laboratories. All of these were crucial elements in bringing the community and our large laboratories together for the next step toward a linear collider.

An amazingly short time after the decision, the laboratories began to reorganize themselves to jointly develop a global design based on the cold technology. A workshop at KEK last October provided a forum for the community to self-organize toward the design goal. Working groups were formed, alternate schemes for key systems in the machine design were identified and the ILC R&D programs were redirected. During this period I went back to my “day job,” the LIGO experiment to detect gravitational waves, feeling that things had gotten on the right track.

In addition to the research and design programs organized at the KEK workshop, ILCSC and ICFA kept busily working toward organizing the global design effort. They developed a plan for doing the global design, solicited proposals for host sites for the design phase and began a search for someone to direct the global design. Late in the year in 2004, I was approached by the search committee about the GDE Director’s job, but I was very reluctant to even consider it, due to my dedication to LIGO. Cleverly,

they asked me to at least come and talk to the search committee so they could benefit from my advice and ideas as to how the design phase should be done.

The rest is history! I agreed to come to talk to them and by thinking about how to do the design, I developed strong ideas as to how it should be done and presented them to the committee in a “give and take” interview in January. Sometime later, they decided to ask me to take on this job and after thinking about it very hard, I could hardly refuse. I gave them a plan, which was accepted that would allow me to continue at some level on LIGO, but I would give up my Caltech academic position to make enough time and flexibility to take on this task. Officially, I became GDE Director at the Linear Collider Workshop (LCWS05) at Stanford on March 18, 2004. So, that is officially the moment of birth of the GDE.

Clearly, I am in a very early stage of creating the GDE, so I can only outline for you a few key elements in how we are going to approach the design and more details will emerge in future articles.

The first decision I made was not to create a home laboratory for the GDE as had been outlined in the earlier plans. My reason is quite simple. If we want to move forward quickly and in the best way, we must involve in the GDE the key persons who have been developing the technologies and designs for the ILC. Recruiting and moving this set of people to a new site for what is still a fledgling project seemed unrealistic to me. My background is in large particle experiments and there we are very used to developing a design for a complex and difficult project with a dispersed collaboration. So, it is that model that I propose to follow.

The GDE members will for the most part, remain in their home laboratories and many will continue non-GDE work. My expectation is that to be effective in the GDE we need roughly half or more of the time of these key people and that is what I will be trying to obtain. So, the first important element in the GDE that I will be creating is to bring a set of key persons into the GDE from the existing laboratory ILC teams. I am getting suggestions as to whom we want to be in this core group and I will do my best to get a significant start on staffing this part of the GDE over the coming few months.

In addition to these core GDE members, there will be two targeted staff positions. The ILCSC recommended in their planning documents for the GDE that there be a “Regional Director” for each of the three regions. This person will be part of the GDE and will represent us to the agencies and the laboratories in each region to assure that the programs (especially the R&D programs) in those regions are well aligned with the goals and priorities of the GDE. The second person will be a senior engineering-cost person from each region, who will help us develop costing methodology that we can use in all three regions and will institute value engineering, trade studies and more generally give us the cost consciousness that will be crucial to developing an affordable proposal.

Finally, let me outline the schedule, as I see it now. The goal is to develop a complete consensus configuration by the end of 2005 that will serve as the baseline for doing a conceptual design by the end of 2006. This conceptual design will include the whole scope of the project, including an understanding of siting issues and site dependence, the detector scope and the performance and a reliable costing of the baseline concept. If we succeed at that ambitious task, we will then move into a detailed design phase aimed at producing a technical design report that will be completed 3-4 years from now.

Where does the ILC R&D and test program come into all of this? Once we have a baseline configuration for the ILC, we will know what alternatives we did not select that

might give better performance or cost that we want to pursue with the idea of possibly evolving the design later. In addition, we have a large number of R&D tasks that will be needed for demonstrations of our techniques, for understanding process for fabrication, etc.

I believe the ILC is the most exciting new large project on the horizon in the physical sciences. If we can bring the world community together behind a viable design for the machine and for a truly international laboratory, I believe we will be able to convince our governments to support us in fulfilling our dream. More later ...

## **2.2 The Challenges of the CLIC Technology – Experimental Program and First Results of the Test Facility CTF3**

Roberto Corsini, [CERN](#), Geneva, Switzerland  
mail to: [Roberto.Corsini@cern.ch](mailto:Roberto.Corsini@cern.ch)

### **2.2.1 Introduction**

The aim of the CLIC (Compact Linear Collider) Study is to investigate the feasibility of a high luminosity, multi-TeV linear e+e- collider. [1,2]. The CLIC design has been optimised for 3 TeV, but it is such that the collider can be built in stages, gradually increasing its energy without major modifications.

In order to limit the total length of the accelerator, CLIC makes use of normal conducting accelerating structures operating at a very high gradient (150 MV/m), and powered by 30 GHz RF pulses with a peak power of about 150 MW. Since conventional RF sources such as klystrons cannot provide pulses at this power and frequency, the CLIC scheme relies upon a two-beam-acceleration concept [3]. A high current electron beam, the so-called drive beam, runs parallel to the main beam and is decelerated to produce the RF power. Several drive beam pulses are actually generated in a centrally located area and then distributed along the main linac.

The generation of high-intensity drive beam pulses with the right time structure is one of the main challenges in CLIC.

Initially, a long pulse is accelerated using a low frequency (937 MHz) normal-conducting linac. Since in a linear collider the main beams are used only once per collision, the overall efficiency is paramount. In order to obtain a very good energy transfer to the drive beam, the drive linac is operated in the "full beam loading" condition, where the beam extracts almost all the power from the structures (see Figure 1). In this condition, an overall RF-power-to-beam efficiency of about 97 % is expected. This exceeds the efficiency that can be obtained in superconducting structures if one takes into account the cryogenic power needed for cooling.

Funnelling techniques in delay lines and combiner rings are then used to give the beam the desired bunch structure while increasing its intensity. In this process the electron bunches are interleaved by the use of transverse RF deflectors. The bunch spacing is thus reduced in stages from 64 cm to 2 cm, and the beam current is increased from 5.7 A to 180 A.

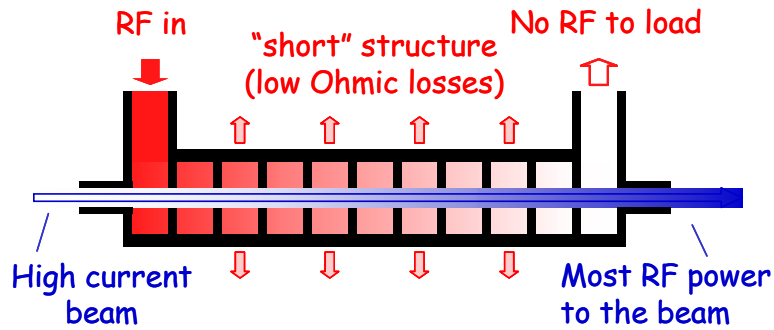


**Figure 1:** Principle of full beam loading acceleration: a high-current long beam pulse extracts most of the RF power from a short travelling wave structure.

It is generally accepted that CLIC technology is the only viable technology for multi-TeV colliders. However, several critical issues still need to be addressed in order to demonstrate its feasibility. In the past years, the International Technical Review Committee [4] has listed a number of crucial items for CLIC to prove feasibility (the so-called R1 items), and to arrive at a conceptual design (the R2 items).

The experimental program of the new CLIC Test Facility (CTF3) will concentrate on all the CLIC technology-related R1 and R2 issues, as opposed to issues that are common to all linear collider studies. The goal is to try to get an answer on the feasibility of the CLIC scheme before 2010. By then the first LHC results should be available and the energy required for a future linear collider would be better known.

CTF3 is presently being built and commissioned in several stages at CERN, by an international collaboration including BINP, CIEMAT, INFN-Frascati, LAL-Orsay, North Western University of Illinois, RAL, SLAC, Uppsala University and Finnish industry [5]. Many other institutes from around the globe have shown interest in joining the CTF3 collaboration. CTF3 uses the buildings of the former LEP pre-injector complex and makes maximum use of existing hardware. The present status and future plans of CTF3 are described in [6].

The main points that will be covered by the experimental program are:

1. Test of a prototype CLIC accelerating structure (including design features to damp higher order modes) at design gradient and pulse length (R1).
2. Validation of the drive beam generation scheme with a fully loaded linac (R1).
3. Design and test of an adequately damped power-extraction structure, which can be switched on and off (R1).
4. Validation of beam stability and losses in the drive beam decelerator, and design of a machine protection system.
5. Test of a relevant linac sub-unit with beam (R2).

### 2.2.2 Previous Experimental Results

In the past years, the CLIC collaboration has obtained many experimental results, which have guided and confirmed the technical choices undertaken by the study.

The feasibility of the two-beam acceleration concept was already demonstrated in the previous CLIC Test Facility, CTF2. In this facility, the energy of a single electron bunch was increased by 60 MeV using a string of 30 GHz accelerating cavities powered by a high intensity drive linac. However, the drive beam generation scheme of CTF2,

based on direct production from a photocathode gun, was intrinsically limited in total charge and in pulse length and cannot therefore be scaled up to the nominal CLIC parameters.

Nonetheless, CTF2 has been essential not only as a proof-of-principle but also as a test bed for CLIC components, including accelerating structures and other RF components. The last two years of the experimental program were in fact dedicated to RF conditioning and testing of accelerating structures after initial tests revealed damage to the copper irises at high field. New structure design options, aimed at reducing the peak surface field for a given average accelerating gradient, were explored. A big improvement in performance was obtained by employing irises made of arc-resistant materials like tungsten or molybdenum (see Figure 2). Eventually, a peak-accelerating gradient of 190 MV/m was obtained in CTF2 using molybdenum irises in 30 GHz copper structures [7]. The RF pulse length was however limited by the drive beam injector to 16 ns, well below the CLIC nominal value (70 ns at present). One of the first goals of CTF3 is to extend these investigations to longer pulse lengths, up to and beyond the nominal value.

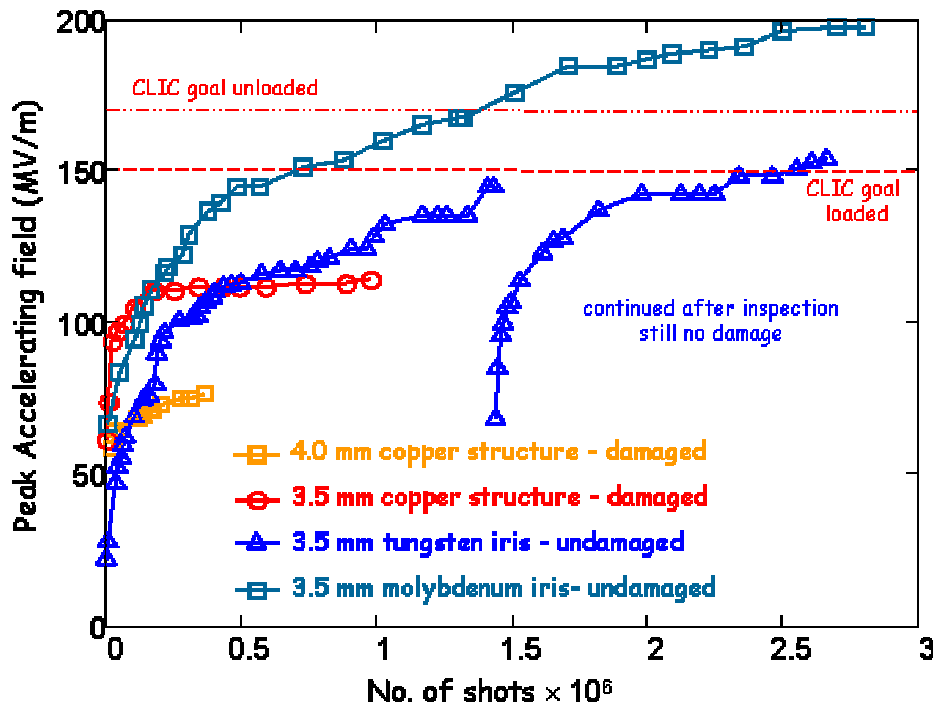


**Figure 2:** RF conditioning history of several accelerating structures, with irises made of different materials and with different apertures, tested with beam in CTF2.

An active pre-alignment system has been tested as well in CTF2, and held components in place during normal operation of the two-beam test accelerator within a window of  $\pm 2\text{-}3\ \mu\text{m}$ , a performance that meets the present CLIC requirement.

Experimental studies on vibration measurement and suppression were also performed in recent years [8]. In particular, a prototype CLIC quadrupole has been stabilized to the 0.5 nm level in a relatively noisy part of the CERN site using commercially available state-of-the-art equipment. Sub-nm stability is required in CLIC, where at collision the beam size is of the order of a nanometer.

An experimental demonstration of the bunch combination scheme was carried out in 2001 and 2002 using a modified layout of the former LEP Pre-Injector (LPI) complex, during the so-called preliminary phase of CTF3 [9]. The technical feasibility of manipulating the drive beam to increase current and bunch frequency was successfully demonstrated at low current (0.3 A). Up to five bunch trains were interleaved over five turns in a combiner ring to reach 1.5 A, without measurable losses (see figure 3). One of the aims of the new CTF3 programme is to demonstrate this combination process with long, high current pulses.

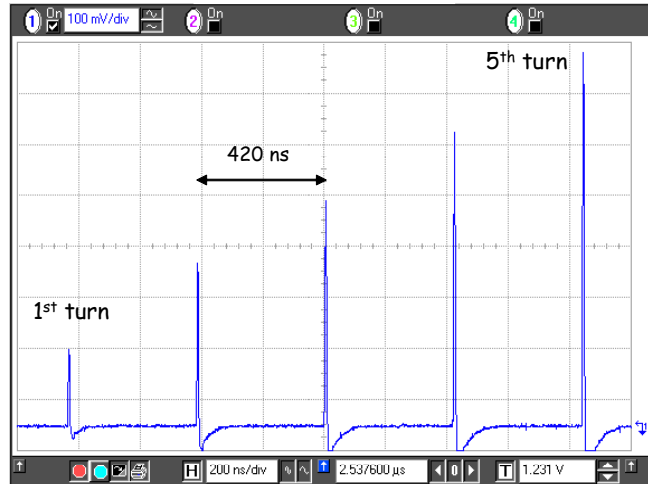


**Figure 3:** Oscilloscope trace from an intensity monitor in the CTF3 preliminary phase combiner ring, showing the increase in circulating beam current over five turns from 0.3 A to 1.5 A.

### 2.2.3 Status of the CTF3 complex

The CTF3 complex is designed to work at a lower beam current and a lower energy than foreseen for the CLIC drive beam (3.5 A instead of 5.7 A and 150 MeV instead of 2.4 GeV) [5].

In its final configuration (see figure 4) CTF3 will be composed of a 70 m long drive-beam linac followed by two rings, where the bunch manipulations will be carried out: a 42 m long delay loop and an 84 m circumference combiner ring. After the combination process the drive beam will have a current of 35 A, and will be transported to an experimental area to produce 30 GHz RF power in a high power test stand. In the same area a separate linac will provide a main beam for a representative CLIC two-beam module, and a test decelerator will be dedicated to drive beam stability studies. The installation also includes a second high power test stand (halfway along the linac) working at a lower beam current, this is needed to start RF component testing as early as possible.

In 2003 and 2004, the injector, linac, the dogleg 30 GHz power production line, and an end-of-linac chicane and instrumentation section have been installed and commissioned. The installation of the delay loop is under way and commissioning is

planned for the end of 2005. The combiner ring and the experimental area will be put in operation in 2006 and 2007.

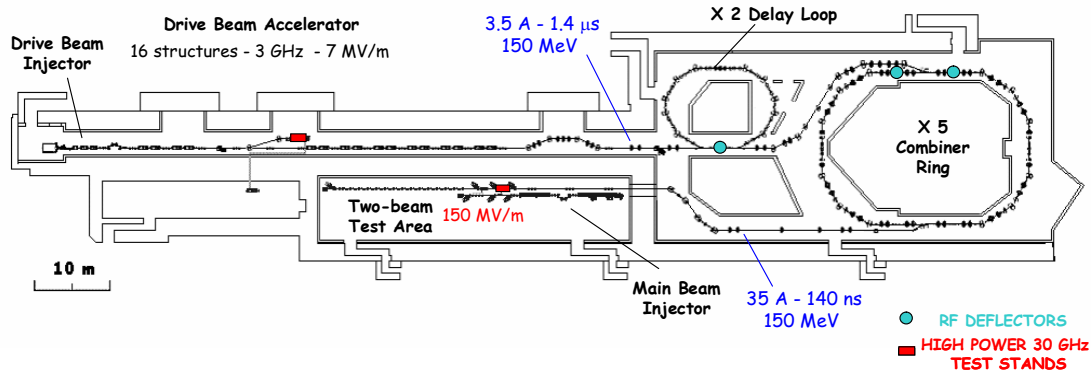


**Figure 4:** CTF3 layout.

### 2.2.3.1 Injector and linac

The drive beam injector was built by collaboration between SLAC (gun triode and beam dynamics design), LAL-Orsay (gun electronics, high-voltage equipment and pre-bunchers) and CERN. The  $1.5 \mu\text{s}$  long beam pulse is generated by a 140 kV thermionic gun. In 2003 and 2004 a 3 GHz bunching system was used, composed of a single-cell standing-wave pre-buncher and a graded- $\beta$  travelling-wave buncher. At the beginning of 2005 three sub-harmonic cavities (1.5 GHz) were added to the system. When they are powered, only one of every two 3 GHz buckets is populated. The cavities and their sources are wide-band systems to allow a fast switching of the bunch phase from odd to even 3 GHz buckets, this “coding” of different parts of the pulse being required for the subsequent combination process.

The bunching system provides beam energy of 5 MeV, and is followed by two travelling wave structures, which increase the energy to about 20 MeV. Solenoidal focusing is used all along the injector. A magnetic chicane with collimators is used to eliminate low energy beam tails and can be used to perform bunch compression.

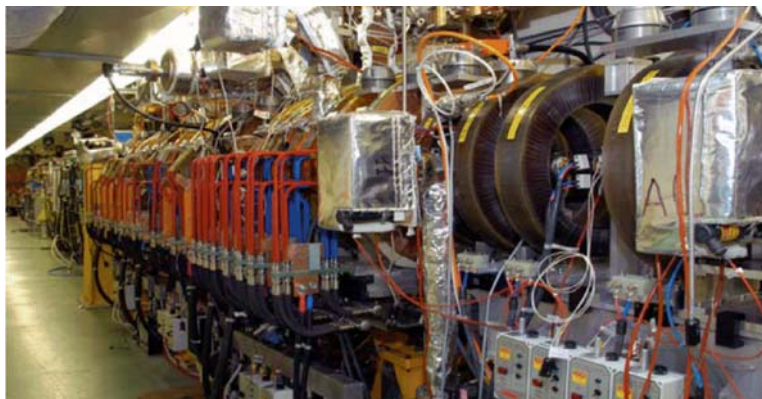


**Figure 5:** View of the CTF3 injector from the gun.

The CTF3 linac is composed of 11 modules. Each module is 4.5 m long and contains a quadrupole triplet. Eight of the modules include two travelling-wave structures each, while three modules are equipped with beam instrumentation equipment. The 3 GHz structures [10] work in the  $2\pi/3$  mode, have a length of 1.22 m and operate at a loaded gradient (nominal current) of 6.5 MV/m. In order to suppress the transverse Higher Order Modes (HOMs) the structures (called SICA, for Slotted Iris Constant Aperture) use four radial slots in the iris to couple out the HOMs to SiC loads. The mode selection is obtained through the field distribution, so that all dipole modes are damped. The Q-value of the first dipole is reduced below 20. A further reduction of the long-range wake-fields is achieved by detuning the HOM frequencies along the structure, using nose cones of variable geometry and different cell outer radii.

Simulations have shown that these techniques are needed to preserve the beam emittance during acceleration despite the high beam current and the long beam pulse. The RF power is supplied by klystrons with peak power ranging from 35 MW to 45 MW, which is compressed by a factor 2 to provide 1.5  $\mu$ s pulses of over 30 MW at each structure input. The pulse compression system uses a programmed phase ramp to obtain a rectangular pulse.

### 2.2.3.2 *The PETS beam line and the High Power Test Stand*

A dogleg beam line branches off nearly halfway along the drive linac. In this line, the drive beam can be sent to a special structure, called PETS (Power Extraction and Transfer Structure), where 30 GHz RF power is extracted from the beam and transported via a 17 m long low-loss waveguide to the test area in the former CTF2 building. This circular, over-moded waveguide with extremely low RF losses is an excellent development by IAP Nizhny Novgorod. This high power test stand will be used to condition and test CLIC prototype components such as accelerating structures.

### 2.2.3.3 *Chicane and end-of-linac diagnostics*

A four bending magnets chicane with variable momentum compaction factor is located at the end of the linac. This chicane is used to decrease or increase the bunch length. In this way, the bunch length can be optimized separately in the linac and in the rings. For operation with the nominal bunch charge, simulations have shown that longer bunches are needed in the delay loop and in the combiner ring to avoid coherent synchrotron radiation effects.



**Figure 6:** The bunch length manipulation chicane.

After the chicane, there is an instrumentation section that allows a series of beam measurements to be made. In particular, there is a 3 GHz RF transverse deflector which together with the optical transition radiation (OTR) screen and the following spectrometer enables bunch length measurements and direct observation of the longitudinal phase space. Both the chicane and the instrumentation section were built and installed by INFN-Frascati, who also has full responsibility for the delay loop.

#### 2.2.4 Commissioning and First Experimental Results

In 2003 the injector and the first three linac modules were installed. Beam commissioning started in June 2003. The design beam current and pulse length were reached rapidly, successfully demonstrating the operation under nominal working conditions of the structures with their novel-damping scheme.

During the following winter shutdown more modules were installed, bringing the total number of accelerating structures to 10. However, eight accelerating structures fed by four klystrons were still missing and were replaced by simple vacuum chambers, but all focusing magnets were already in place. The dogleg transport line, the 30 GHz power test stand, the bunch length manipulation chicane and the end-of-line instrumentation section were installed as well.

In 2004 the newly installed hardware was commissioned with beam and again the beam specifications were quickly met. A large part of the experimental run was dedicated to the first test of 30 GHz RF power production.

##### 2.2.4.1 *Injector and linac performances*

The gun provided a maximum current of 9 A at its design voltage of 140 keV. Above this value, a pulse-to-pulse current jitter started to appear. The pulse length can be varied between 200 ns and 1.5  $\mu$ s.

The bunching system showed a satisfying capture efficiency of about 75 %. The nominal current of 3.5 A was obtained after the momentum cleaning chicane for a gun current of about 5 A. The beam energy, measured in the end-of-line spectrometer, was 35 MeV. It was found that the nominal beam current could be largely exceeded and with 7.5 A from the gun, 5 A was transported to the final dump.

A variety of beam measurements were performed. Beam emittance and Twiss parameters were measured in several locations with the quadrupole scan technique using OTR aluminium screens and CCD cameras. A comparison of these measurements showed a good agreement with the optics model. The measured rms normalized emittance was close to the nominal value of  $100 \pi$  mm mrad in both planes. Bunch length was determined with an OTR screen and a streak camera, and by measuring the beam energy spread as a function of the RF phase. Typical measured values were about 4 ps rms for 3.5 A beam current. In 2004, bunch length measurements made using the RF deflector gave rms values between 2 ps to 7 ps depending on the setting of the collimators in the momentum cleaning chicane. These measurements are compatible with the design value of 5 ps.

Other activities during commissioning included development studies of a beam loss monitor system [11] and of beam halo measurements [12].

#### 2.2.4.2 Full Beam Loading Operation

The first important result obtained in CTF3 was the first proof of stable operation under full beam loading. The beam was remarkably stable and no sign of beam break-up was observed at high current. The energy spread during the initial beam transient (about 100 ns) could be easily reduced to a few percent by partial RF filling of the structures at beam injection.

The observation of the RF signals at the structures' output coupler (see figure 7) was particularly useful. It allowed for instance to easily set up the beam-to-RF phase by maximizing the beam loading and to determine the phase error between structures. The RF signals were also used to assess the RF-to-beam efficiency. This was done by measuring the RF power level at the structure input and output for a given beam current. The values obtained were then compared to both the measured beam energy gain and the calculations, and good agreement was obtained.

In the example of figure 7 the beam current was 4 A. The power at the structure input was 35 MW, and the power to the load was 0.4 MW with beam. The expected value of the resistive losses in the structure was 1.6 MW. The 33 MW of "missing power" agrees well with the beam energy gain in momentum ( $\sim 8.2$  MeV per structure). The RF-to-beam efficiency thus evaluated was 94 %.

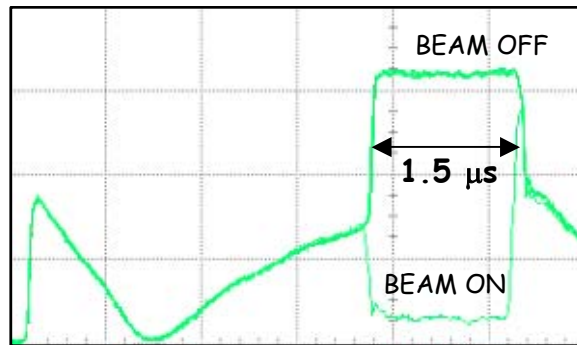


**Figure 7:** Oscilloscope trace showing the RF pulse at the output coupler of a structure. When the beam is on, it extracts more than 90 % of the energy contained in the useful part of the RF pulse (1.5  $\mu$ s). Virtually no power goes to the load.

#### 2.2.4.3 30 GHz power production

The commissioning of the dogleg beam line delivering the drive beam to the PETS was more arduous. The main limitation came as foreseen from the reduced aperture of the PETS. Due to the relatively low value of the beam current in the linac, the PETS coupling to the beam must be high; therefore the aperture (6.5 mm) is much smaller than the one planned for CLIC (of the order of 20 mm). This, together with the low beam energy, makes beam transport through the PETS a difficult task. Simulations have shown that even in the best conditions a few percent beam losses were to be expected. Indeed, especially for the higher power range, electron beam transport through the PETS was never 100 %, the best result obtained was about 90 % for a 3 A beam current.

The PETS itself had also to be conditioned as the 30 GHz power level during the run was increased, by increasing the gun current. A special operation mode in which the

3 GHz pulse compression system was operated at higher compression ratio and shorter pulse length was used to do this,. The highest 3 GHz power delivered to the structures in this case was about 60 MW, which is twice the nominal value. With this setting, drive beam pulses of up to 6 A and 200 ns were delivered to the PETS.

The 30 GHz power produced was in this case in good agreement with the expectations. Towards the end of the run, pulses with powers of about 75 MW and pulse duration above 70 ns were generated. More than 50 MW were delivered to an RF load in the ex-CTF2 test area using the over-moded waveguide. Such power levels and pulse lengths will be sufficient to test a prototype CLIC accelerating structure to the CLIC nominal gradient of 150 MV/m in the first run of 2005.

Somewhat better performances are expected next year, after the installation of two additional accelerating structures to increase the beam energy at the PETS location and the correction of some misalignments identified by beam-based observations during the first run.

#### 2.2.4.4 *Chicane and bunch length measurements*

A good beam transmission was rapidly obtained through the INFN chicane. Several optics measurements were performed. In particular emittance and Twiss parameters were measured at the beginning of the linac and after the chicane. Dispersion measurements were also performed in the chicane for several optics, corresponding to different momentum compaction values. In both cases, comparison with the MAD model showed good agreement.

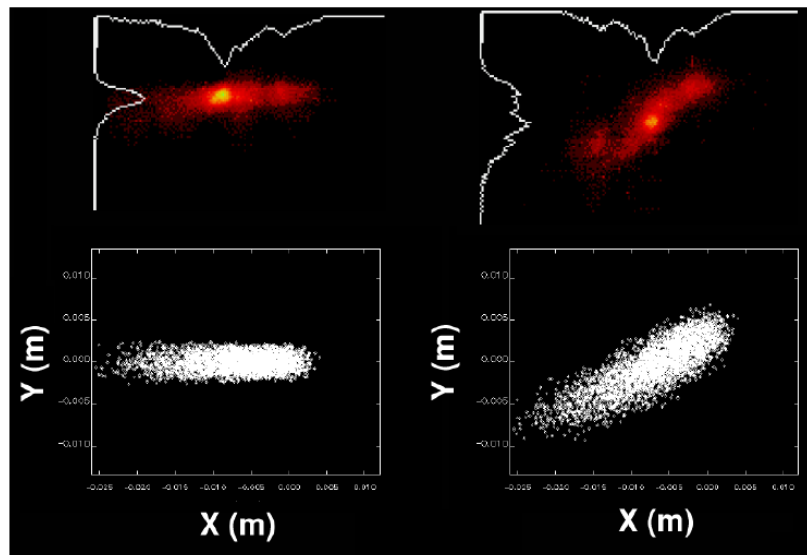


**Figure 8:** Measured (top) and simulated (bottom) transverse beam distributions with the RF deflector off (left) and on (right), for  $R_{56} = 0.1$  m. Horizontal dispersion at the location of the screen is responsible for the correlation visible in the images to the right (from C. Biscari, INFN/LNF).

A vertically deflecting RF structure was used after the chicane together with an OTR screen to make bunch length measurements. Initial measurements made with

different chicane settings showed bunch compression to less than 0.5 mm rms for an initial bunch length of 2 mm, this again is in good agreement with expectations.

In figure 8 images of the beam are compared to simulations and illustrate the change in vertical dimensions, proportional to the bunch length, obtained when the RF deflector is switched on. Since at the screen position the horizontal dispersion was non-zero, the horizontal axis is proportional to the beam momentum, and the tilt visible on the right images corresponds to a head-to-tail momentum variation in the bunch.

### 2.2.5 Conclusions and Outlook

The new CLIC Test Facility CTF3 has started to address some of the challenging issues that must be verified in order to establish the feasibility of the CLIC linear collider. In particular, a stable high beam current operation of the linac in fully loaded conditions has been already demonstrated. CTF3 has started its role as a 30 GHz power production facility, with the first accelerating structure tests coming on-line in 2005. Several beam dynamics topics have been tackled as well, with promising results especially for the bunch length manipulation and longitudinal phase-space gymnastics essential for the drive beam generation scheme. The project is proceeding as planned, alternating installation and commissioning periods. The next important step is the completion of the delay loop, which will be put in operation during 2005.

The CTF3 experimental program is very ambitious, and up to now it has been pursued thanks to the joint efforts of several institutes. It is clear that more resources will be needed to complete the program in the scheduled time. The intention expressed by other institutes to join the collaboration is therefore very important.

### 2.2.6 Acknowledgment

The results presented in this publication correspond to the work of many people. Many thanks go to all the members of the CTF3 collaboration involved in the design, installation and commissioning of the facility.

### 2.2.7 References

1. "A 3 TeV e+e- linear collider based on CLIC technology", CLIC Study Team, Editor G. Guignard, CERN 2000-008, 2000.
2. "The compact linear collider CLIC", I. Wilson, Physics Reports 404-404 (2004) 365-378.
3. "The CLIC RF power source", H. Braun et al., Editor R. Corsini, CERN 99-06, 1999.
4. "International linear collider technical review committee second report", Editor G. Loew, SLAC-R-606.
5. G. Geschonke and A. Ghigo Eds, "CTF3 Design Report", CERN/PS 2002-008 (RF).
6. R. Corsini, G. Geschonke, L. Rinolfi, F. Tecker (for the CTF3 Team), "Status of CTF3 at the end of 2004, Beam Commissioning Results and Plans for the Future", CARE/ELAN Doc-2004-026 and CLIC Note 622
7. W. Wuensch, C. Achard, S. Döbert, H. H. Braun, I. Syratchev, M. Taborelli, I. Wilson, "A Demonstration of High Gradient Acceleration", CERN-AB-2003-048-RF, CLIC Note 569, Proc. PAC 2003.
8. R. Assmann, W. Coosemans, G. Guignard, S. Redaelli, D. Schulte, I. Wilson, F. Zimmermann, "Colliding Nanobeams in CLIC with Magnets Stabilized to the Sub-nm Level", CERN-AB-2003-011 (ABP), CLIC Note 563, Proc. PAC 2003.

9. R. Corsini, A. Ferrari, L. Rinolfi, P. Royer, F. Tecker, “Experimental results on electron beam combination and bunch frequency multiplication”, Phys. Rev. ST Accel. Beams 7, 040101 (2004).
10. E. Jensen, “CTF3 Drive Beam Accelerating Structures”, Proc. LINAC 2002, 9-23 August 2002, Gyeongju (Kyongju), Korea, CERN/PS 2002-068 (RF) and CLIC Note 538.
11. T. Lefevre, H. Braun, R. Corsini, M. Velasco, M. Wood, “First Test of Beam Loss Monitoring on the CLIC Test Facility 3”, Proc. 11th Beam Instrumentation Workshop, 2004, Knoxville, USA.
12. T. Lefevre, H. Braun, E. Bravin, R. Corsini, A. L. Perrot, D. Schulte, “Beam Halo Monitoring on the CLIC Test Facility 3”, Proc. EPAC 2004.

## 3 Theme Section

### 3.1 Ion Sources for Synchrotron Injectors

Charles Hill, [CERN AB-ABP](#), Switzerland  
 mail to: [charles.hill@cern.ch](mailto:charles.hill@cern.ch)

#### 3.1.1 Introduction

One of the most important components of modern synchrotron complexes is the particle it accelerates. During the design of a particle accelerator, the origin and identity of the particle is often treated as a mathematical fiction instead of an entity that must be produced at the beginning of the acceleration process. In many cases the source of the particles must be made to fit around the design instead of being taken into consideration at an early stage.

Particles can be either protons or ions. Although this distinction is arbitrary the methods of production can be quite different and can contain some very interesting physics. Modern accelerator complexes, like CERN, which started off as proton laboratories, often include heavy ions in their panoply of particles.

#### 3.1.2 Ionisation

##### 3.1.2.1 *Plasma and ionisation*

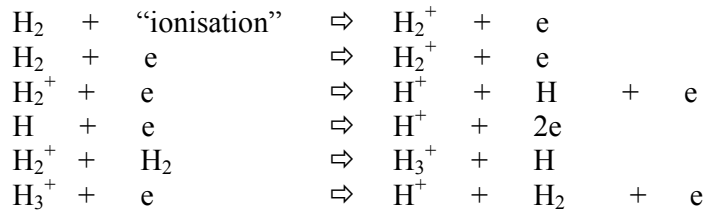
In any gaseous discharge, both negatively and positively charged particles exist in approximately equal proportions along with un-ionized neutrals and form a plasma. For a simple ion source, it is only necessary to extract the ion from the plasma and to accelerate it. However, a reasonable current with good beam qualities is usually needed and the objective of source design is to optimise these two parameters

Electron bombardment ionisation of the neutrals in the plasma is the most common method of increasing the plasma density. Energetic electrons passing close to, or colliding with, an electron orbiting an atom can give energy to that electron which moves to a higher, metastable, orbit. If the orbiting electron gains sufficient energy it can part company with the atom leaving it ionised. This energy of the incident electron

is the ionisation potential (when expressed in eV). As more and more electrons are removed from the ion, more energy is required to remove the next electron due to the increased binding between the remaining electrons and the positive nucleus. This ionisation potential is, however, only a threshold; ionisation efficiency increases with electron energy up to about three times the ionisation potential and falls off at higher energies.

### 3.1.2.2 Ionisation of hydrogen

It may seem that electron bombardment ionisation is a simple process. However, in reality, many processes are going on in competition in the plasma. The ion source must therefore enhance the production of the desired ion at the expense of other possible species. Even for a simple atom, like hydrogen, the processes in the plasma are believed to be the following:

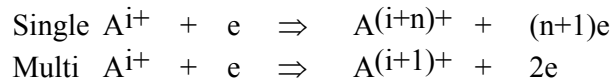


It is believed that the last two processes are important for the efficient production of protons.

There also exists a hydrogen ion consisting of a proton with two electrons (or a hydrogen atom with an extra electron). The binding energy of this electron is rather low (0.7 eV) and thus can be lost quite easily. These negative ions have become popular for charge exchange injection but due to the fact that the ion can be easily stripped to the neutral atom they were popular for fusion and weapon research. The production mechanism of these ions is poorly understood. A number of processes are involved which lead to different types of sources. These will be treated separately below.

### 3.1.2.3 Multiply charged ions

Electron bombardment ionisation can result in the removal of more than one electron from an atom or ion provided the bombarding electron has sufficient energy. There are two routes by which this can occur. In SINGLE-step ionisation, the incident electron must have energy of at least the sum of all the ionisation potentials of the removed electrons, whereas in MULTI-step ionisation it requires only the energy of each electron removed. The processes are as follows:



For example to go from lead 26+ to 27+, the threshold electron energy is 874 eV, whereas to go from 0+ to 27+ it is 9200 eV. The maximum charge state that can be attained is thus limited by the incident electron energy.

Multi-step ionisation is thus the only real route to high-charge-state ions but this process takes a time which depends on the plasma density and the ionisation cross

section, and must be shorter than the ion lifetime in the plasma. The energy dependence of the cross section means that the high energies required to produce high-charge states are not an advantage for the production of low-charged seed ions. Ions are lost from the plasma by losses to the walls and by electron capture from neutrals and plasma electrons.

### 3.1.3 Proton Sources

#### 3.1.3.1 Background

Protons are the most common particles accelerated up to high energies and are in general the easiest to produce. Many laboratories prefer to produce a particle known as H<sup>-</sup> in the ion source and inject these into the synchrotron from the linac using “charge exchange injection”. This involves injection through a foil to strip the H<sup>-</sup> to protons with the advantage that the filling of the synchrotron acceptance can be more easily controlled and with lower intensities, space charge problems can be reduced.

#### 3.1.3.2 Plasmatrons

Probably the most common type of ion source for hydrogen ion production is the Duoplasmatron. The current extracted from an ion source is dependent on the density of the plasma in the extraction region. Constricting the discharge, for example near the anode, not only increases the plasma density but also increases potential difference across the restriction that increases the energy of the primary ionising electrons (Unoplasmatron). Further compression and consequent further heating of the electrons can be achieved by adding a strong magnetic field around the constriction and, by controlling the primary plasma and magnetic compression, it is possible to optimise the yield of the desired ion.

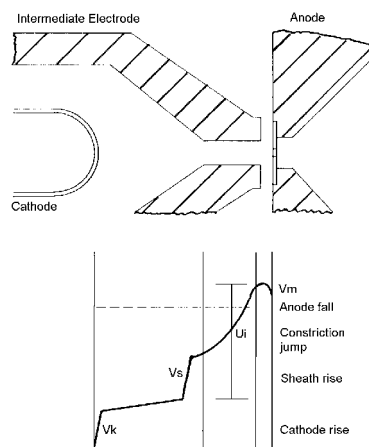


**Figure 1:** Idealised potential distribution in the duoplasmatron discharge

Figure 1 shows an idealised potential distribution in the constriction. The anode plasma is allowed to escape through a small aperture in the anode, and it is from this plasma that ions are extracted. Normally, the plasma streaming through the anode hole would be too dense to allow the extraction of ion beams with good optical properties so the plasma is allowed to expand into some form of expansion cup.

The CERN pulsed duoplasmatron [4,5], shown in Figure 2 has a water-cooled shaped iron plasma chamber with the constriction towards the anode. A solenoid surrounding the plasma chamber provides the field for magnetic compression in the constriction canal. The expansion cup is rather deep and contains an additional small solenoid to fine trim the plasma characteristics. Additionally, the cup contains a negatively biased electrode that can increase beam output probably by repelling electrons back into the streaming plasma and causing secondary ionisation near the anode.

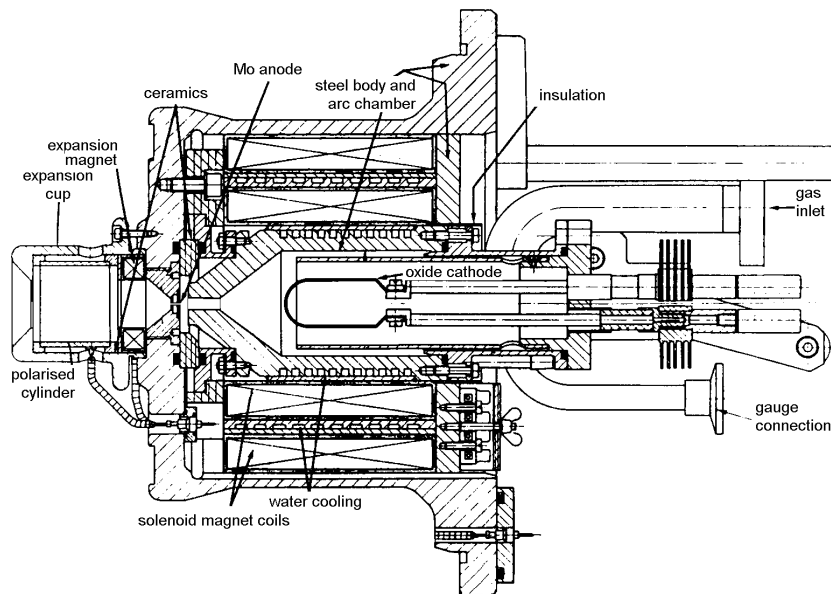


**Figure 2:** CERN standard duoplasmatron (with polarised expansion cup)

This source is routinely used at CERN to produce protons with beam pulse intensities of up to 500mA but has also been used to produce deuterons and alphas. The low energy and poor confinement of the primary ionising electrons in the anode plasma limits the performance to anything other than singly charged ions.

### 3.1.3.3 *Surface negative ion sources.*

Historically, negative hydrogen ion sources were modifications of existing proton sources such as duoplasmatrons with the ions extracted from the anode plasma off axis. Insertion of a floating electrode into the channel of the plasma chamber improved the yield of negative ions but the addition of caesium to the discharge dramatically increased the ion current (and electrons). The electron component of the beam from a negative ion source is due to the fact that the extraction cannot distinguish electrons from ions, and that electrons are abundant in the plasma. Electron – ion ratios can reach

1000:1 unless one accepts a high electron load in the preaccelerator, some means must be used to eliminate them at low energy.

The increase in source efficiency from the addition of caesium accelerated the development of higher intensity devices based on the cold cathode magnetron geometry. It transpired that it was more important to have a negatively biased caesiated (or low work function) surface in the discharge plasma than to have caesium in the discharge. Various miniature geometries have been developed using the cathode as the support for the caesium (Penning, magnetrons, planotrons) [16,17].

There is still no clear evidence as to what is happening inside a caesiated discharge. All or some of the following processes may be involved:

- 1) Dissociation of plasma produced caesium hydride
 
$$\text{Cs} + \text{H} \Rightarrow \text{CsH} \Rightarrow \text{Cs}^+ + \text{H}^-$$
- 2) Sputtering of lightly bound ions from the surface
- 3) Attachment of an electron after scattering from the surface

However, it is known that the surface coverage is important (about 0.7 monolayer) and that the energy of the incident ion must be low ( $>$  a few hundred eV). The importance of the coverage is such that as the duty cycle and the discharge power increases it becomes more and more difficult to maintain it. However, these sources can work in the steady-state mode and Figure 3 shows such a source as typically used at Fermilab and BNL. The magnetic field of the source can be used to deflect the electrons safely before acceleration.

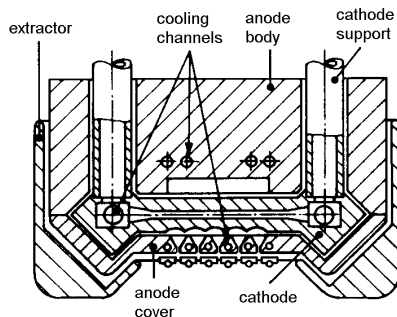


**Figure 3:** Cross section of a steady state magnetron negative ion source

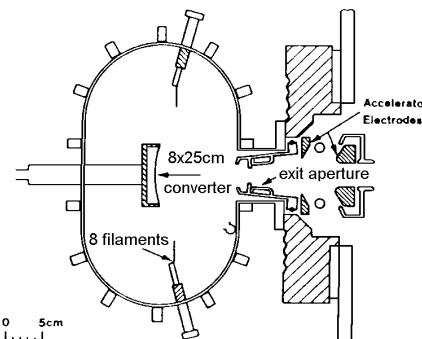


**Figure 4:** LBL surface production multipole negative ion source

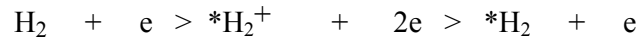
Unfortunately, these sources have a poor gas efficiency requiring large quantities of gas and hence large pumping systems or pulsed gas supplies. Some of these problems can be reduced if the plasma generation can be made independent of the conversion process. Fitting a negatively biased curved converter plate, with its centre of curvature in the extraction aperture, into a proton magnetic multipole (bucket) confinement source gave extractable negative ion currents whose intensity could be enhanced by caesium [18,7]. This gave all the advantages of the multipole source. Careful arrangement of the

electric and magnetic fields around the extraction aperture reduces the electron current to acceptable levels. A source that incorporated these features is shown in Figure 4.

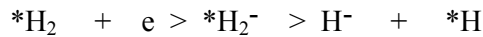
### 3.1.3.4 Volume negative ion sources

Measurements of the negative ions in large-volume, low-pressure hydrogen discharges indicated densities that were much larger than those predicted by theory [19]. Theoretical and experimental studies showed that dissociative attachment of electrons to highly excited molecules was enhanced relative to attachment to ground state molecules. The addition of a small dipole magnetic filter in the plasma volume of a standard multipole source, thus separating it into two regions, enhanced the  $H^-$  yield due to this process [20] whilst reducing the electron component. It is believed that the ion formation is a two-stage process:

- 1) In the production volume between cathode and filter, hot electrons (100 - 200eV) ionise and vibrationally excite hydrogen molecules,



- 2) Excited molecules and cold electrons (few eV) only diffuse past the filter. Dissociative attachment between molecules and electrons takes place in this volume,



Hot electrons that pass the filter would quickly strip the negative ion as the extra electron is only loosely bound.

Careful choice of the bias of the electrode that closes the front of the plasma volume, the addition of collars and the source operating pressure can reduce the electron component to very low values. The good gas efficiency of the multipole and the absence of caesium could make this type of source interesting for both fusion and accelerator use. A prototype source for an accelerator application [10,11] that uses microwave (ECR) heating of the plasma is shown in Figure 5. This is intended for a high duty cycle device. Again, the addition of caesium to the discharge has recently been shown to enhance the yield [7], however there are some worries that the migration of caesium might cause a deterioration of the performance of the highly stressed pre-injector or RFQ accelerator downstream of the source.

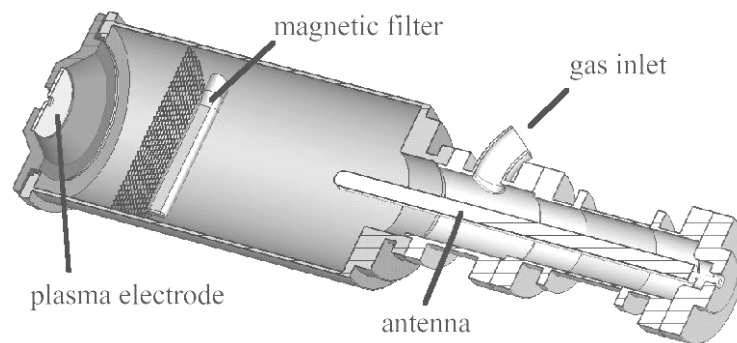


**Figure 5:** Prototype volume production, RF excited, negative hydrogen ion source

### 3.1.4 Multi charged ions

#### 3.1.4.1 *The Electron Cyclotron Resonance Source (ECRIS)*

Energetic electrons rotate in a magnetic field,  $B$ , with a Lamor frequency defined by the relation  $\omega = e.B/m$  or, in engineering units, 2.8GHz/kG. If a box containing plasma of some form is immersed in an arbitrary magnetic field there can exist a surface where the above relationship is true. If radio frequency power of this frequency is injected into the box, plasma electrons crossing this surface will, in general, be heated and can be used for further ionisation of the plasma. Thus the plasma density can increase up to a value that is believed to be limited when the plasma frequency, which is a function of the density, exceeds the RF frequency. With adequate confinement of the plasma and the use of microwave frequencies, high electron temperatures can be attained making this principle interesting for multi-charged ion production.

The ECR ion source [12] makes use of this effect using microwave frequencies. Longitudinal confinement is achieved by Helmholtz coils configured to give a “minimum B” field configuration and radial confinement by powerful permanent magnet multipoles (usually a hexapole). Plasma densities greater than  $10^{12} \text{ cm}^{-3}$  can be attained. This type of source is used routinely on heavy-ion cyclotrons and early versions used in the pulsed mode on synchrotrons for the production of  $\text{O}^{6+}$  and  $\text{S}^{12+}$  beams.

In the ECR plasma, there is one phenomenon that in recent years has made higher currents of highly charged ions available. Normally an ECRIS gives a better performance when used in the pulsed mode as compared to dc operation. However, it is possible to adjust a pulsed source in such a way that when the RF heating power is turned off, a large peak of highly charged ions appears. This effect, known as “Afterglow”, is believed to be due to a rapid loss of plasma electrons and the deconfinement of positive ions [13].

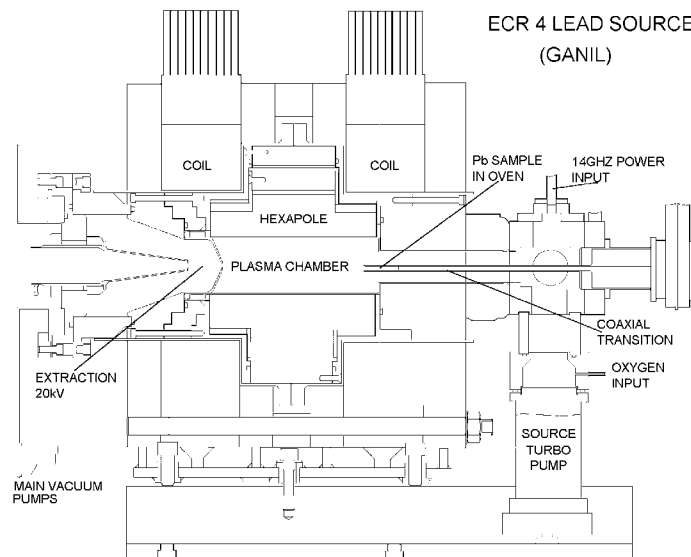


**Figure 6:** An ECRIS used for lead ions

Afterglow is used in a ‘‘CAPRICE’’ type ECR developed at GANIL (ECR4) for use at CERN [14]. This source is a steel bodied source with minimum B coils and a permanent magnet hexapole. Figure 6 is a schematic of this source. In normal operation it has given pulsed beam currents of  $80\mu\text{A}$  of  $\text{Pb } 27+$  suitable for synchrotron use.

Recent work on ECRIS using a superconducting ECRIS with adjustable fields has improved knowledge of the scaling laws in these sources [15]. This has led to the development of a source known as GTS-LHC [16], which incorporates these refinements and is expected to give improved performance as compared to ECR4. This source was built for the ‘‘Ions for LHC’’ project and is currently in installation.

### 3.1.4.2 Electron Beam Ion Source (EBIS)

In the Electron Beam Ion Source (EBIS), a fast, dense, electron beam interacts with cold ions trapped in an electrostatic well. Ions are confined radially by the potential well in the electron beam, and axially by electrostatic mirrors. Ions accumulated in the trap can be expelled by lowering the potential of one end of the trap. As the interaction time between hot electrons and ions depends on the electron energy and the source length, for highly charged ions this time is necessarily short. Thus high density, and hence high current density, electron beams are required. In practice a current density of the order of  $1000\text{A}/\text{cm}^2$  is needed. As normal thermionic cathodes are usually limited to less than  $100\text{A}/\text{cm}^2$  some form of beam compression is needed, and to maintain this beam against space charge forces the source is normally immersed in a solenoidal magnetic field. Correct configuration of the solenoid field will also give the compression. [17,18]

A schematic of an EBIS is shown in Figure 7. In this mode of operation, ions, including metallics, from a traditional source can be injected into the trap and further ionised by the electron beam [19]. In view of the trap nature of the source, the ionisation process can be allowed to continue for a relatively long time making this source interesting for high-charge ions (even up to fully stripped) for slow cycling accelerators. Care is needed with the very high current densities involved -- in most cases the electron beam is blown up in the collector (anode) and the energy in the beam recovered if this is felt to be worthwhile. A disadvantage of the trap is a pre-defined capacity of charge accumulation, which includes rest gas, and some problems in expelling all ions at extraction

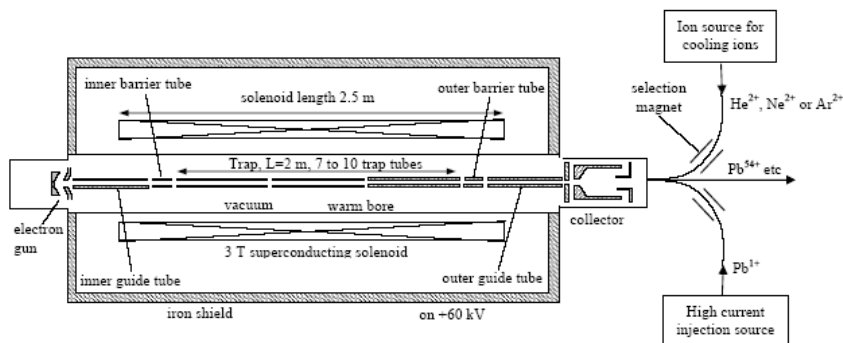


**Figure 7:** Conceptual confined flow EBIS with external injection

### 3.1.5 Final Remarks

This note is intended to be a short and simple introduction to the vast field of plasma Ion Sources. It is neither complete nor too deep as, in many cases, the physics processes occurring in these plasmas are both extremely complicated and dynamic. However, this physics is what makes Ion Sources so fascinating to their specialists. Now, whenever the beam disappearance is blamed on the pre-injector, there may be some understanding of what is going on inside these devices.

### 3.1.6 References

1. B. Vosicki et al., The Duoplasmatron Source for the CERN-PS Linac, Proc. Linear Accelerator Conference, Los Alamos, 1966 (LA-3609, 1966)
2. M. Hone, The Duoplasmatron Ion Source for the New CERN Linac Preinjector, CERN/PS/LR 79-37 (1979)
3. M. Kobayashi et al., Studies of the Hollow Discharge Duoplasmatron as a source of H-Ions, Rev. Sci. Inst., 47, 1425 (1976)
4. K. Prelec, Negative Hydrogen Ion Sources, BNL-33354 (1983)
5. Yu. Belchenko et al., Ion Sources at the Novosibirsk Institute of Nuclear Physics, Proc. Int. Conf. on Ion Sources, Berkeley, 1989, Rev. Sci. Inst., 61, 378 (1990)
6. K. Ehlers, K. Leung, Characteristics of a Self-extraction Negative Ion Source, 3rd. Int. Symp. Production and Neutralisation of Negative Ions and Beams, Brookhaven, 1983, AIP Conf. Proc. 111 (1984)
7. K.N. Leung, Multicusp Ion Sources, Proc. 5th. Int. Conf. Ion Sources, Beijing, 1983, Rev. Sci. Inst., 65, 1165 (1984)
8. M. Bacal et al., H<sup>-</sup> and D<sup>-</sup> Production in Plasmas, 3rd. Int. Symp. Production and Neutralisation of Negative Ions and Beams, Brookhaven, 1983, AIP Conf. Proc. 111 (1984)
9. K. Leung et al., Extraction of Volume Produced H<sup>-</sup> Ions from a Multicusp Source, Rev. Sci. Inst., 54, 56, (1983)
10. C. Hill et al., H-Source Development at CERN, 10<sup>th</sup> Int. Symp. Production and Neutralisation of Negative Ions and Beams, Kiev, Ukraine, Sept 2003, to be published.
11. Work supported under the EU Framework 5 programme through contract HPRI-CT-2001-50021, "HP- NIS"
12. R. Geller et al., Status of the Multiply Charged Heavy-ion Source MINIMAFIOS, Rev. Sci. Inst., 56, 1505 (1985)
13. G. Melin et al., Some Particular Aspects of the Physics of the ECR Sources for Multicharged Ions, Proc. Int. Conf. on Ion Sources, Berkeley, 1989, Rev. Sci. Inst., 61, 236 (1990)
14. M.P. Bourgarel et al., First Results of the 14.5GHz GANIL ECR Ion Source with the CW and the Pulsed Operation Mode, 2nd EPAC, Nice, 1, 645 (1990)
15. Work supported under the EU Framework 5 programme through contract HPRI-CT-1999-50014, "Innovative ECRIS"
16. C.E. Hill et al., GTS-LHC: A New Source For The LHC Ion Injector Chain, Proc. 16<sup>th</sup> Int. Conf. on ECR Ion Sources, Berkeley, USA, Sept, 2004, to be published (<http://leitner.lbl.gov/ecris04/preprints.htm>)
17. J. Arianer, C. Goldstein, The Orsay Electron Beam Ion Source, Int. Conf. Heavy Ion Sources, Gatlinburg, 1976, IEEE Trans. Nucl. Sci NS-23, 979 (1976)
18. R. Schmeider, Physics of the EBIS and its Ions, NATO Workshop on Physics of Highly Ionised Atoms, Cargese, 1988, Plenum Press (1989)

19. F. Wenander, An EBIS as heavy Ion Source for the LHC Pre-injector, 8<sup>th</sup> Int. Symp. On Electron Beam Ion Sources and Traps and their Applications, EBIS-T 2000, Upton, NY, Nov 2000 - pages 48-58

### Further Reading

1. The Linac, Accelerator Conference Proceedings (JACOW) (bi-annual)
2. The International Ion source Conference Proceedings (Rev. Sci. Instr.) (bi-annual)
3. Negative Ion Workshop Series (currently random)
4. ECRIS Workshop Series (currently bi-annual)
5. T. Green, Intense Ion Beams, Rep. Prog. Phys., 37, 1257 (1974)
6. A. Forrester, Large Ion Beams, Fundamentals of Generation and Propagation, Wiley (1988)
7. I. Brown, The Physics and Technology of Ion Sources, Wiley (1989)
8. CERN Accelerator Schools, General Series

## 3.2 R&D of RFQ Drift-Tube Proton Linacs in IHEP-Protvino

Yu.A. Budanov, A.P. Maltsev, V.A. Teplyakov  
IHEP, Protvino, Moscow Reg., 142281, Russia  
mail to: [budanov51@mail.ru](mailto:budanov51@mail.ru)

### 3.2.1 Introduction

The concept itself of focusing with an RF field is well known by now due to worldwide application of RFQs [1]. The first RFQ was commissioned in IHEP-Protvino in 1972 [2]. Since then, many publications dealt with this type of focusing. Still, RF focusing may be used to accelerate ions up to much higher energies, as compared to those accessible with a conventional RFQ. To this end, drift tubes are employed, and such accelerators are thus referred to as RFQ Drift-Tube Linacs, the RFQ-DTL.

It is with advent of the first ion linear accelerators that numerous attempts were undertaken to use components of high-frequency electric field to focus beams as well. Stability of a particle motion in a linear accelerator can be attained via choosing a dedicated geometry for accelerating gaps such as to force transverse components of accelerating field to exert the RF quadrupole focusing effect. Primary feasibility studies for this kind of focusing were, mostly, theoretical and foresaw either a weak focusing effect, or an unacceptably low accelerating rate. In 1959, Vladimirovsky proposed how to use the RF focusing in an Alvarez structure [3]. Quadrupole components were to be driven in between drift tubes with by means of a finger-electrode array in an accelerating gap [3]. Naturally, electric breakdown sustainability is thus noticeably reduced. It turns out impossible to achieve a high voltage across accelerating gap inherent in a conventional Alvarez structure.

This problem can be alleviated by a four-fold increase of a number of accelerating gaps per  $\beta\lambda$ . First, it was proposed to use *H*-wave resonator to accelerate at  $\beta\lambda/2$ -mode. Second, the accelerating  $\beta\lambda/2$ -cell was broken into two parts (a double gap) by inserting a spacer electrode biased to an intermediate potential. This scheme was put forward by Teplyakov [4].

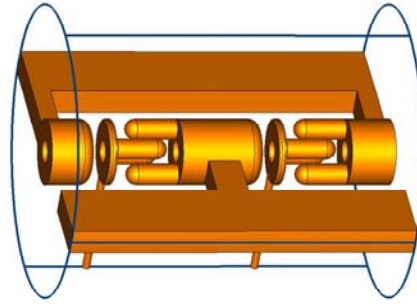


**Figure 1:** Channel of an RFQ-DTL, length  $\beta\lambda$ .

Among numerous ways of implementing this idea, an option exists free of focusing electrodes in the first half of a double gap (an accelerating gap), RF field focusing fields being driven in the second half (a quadrupole gap). Accelerating and focusing channel (of length  $\beta\lambda$ ) of such a double-gap scheme is shown in Fig. 1.

In the scheme just specified, a competitive rate of proton acceleration extends to 30–40 MeV, and ample focusing is ensured throughout. Higher values of shunt impedance are also considered as an advantage of the layout. At small  $\beta$ , the impedance exceeds significantly that of the Alvarez structure.

### 3.2.2 Acceleration and focusing in RFQ-DTL

Fig. 2 sketches an accelerating cell with one spacer electrode. It is this structure that is employed in the first sections of operational URAL-30 and URAL-30M linacs of IHEP-Protvino.

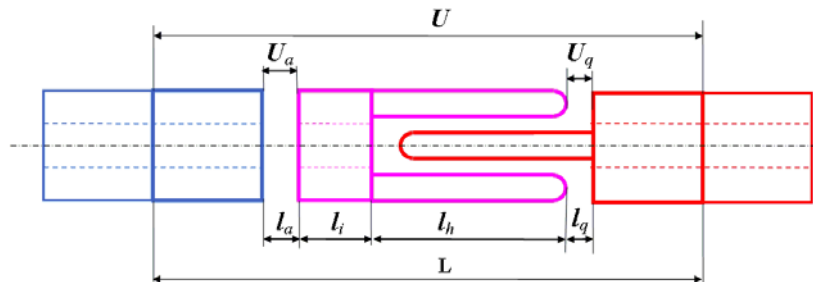


**Figure 2:** Schematic layout of an accelerating cell.

It is possible to estimate acceleration rate in an RFQ-DTL with a well-known equation yielding of energy gain per one period of acceleration,  $\Delta W = e\theta U \cos \varphi_s$ . Acceleration efficiency  $\theta$  takes into account effect of two accelerating gaps that are shown in Fig. 2. It is a specific feature of an RFQ-DTL worth further commenting.

An approach to calculate accelerating and focusing parameters is reported in [5] for a double-gap version. Generally, number of gaps in an accelerating cell can exceed two. A technique to estimate  $\theta$  and frequency of transverse oscillations  $\mu$  is described in [6]. In short, the notion of gap complex efficiency  $\tilde{\theta}$  is introduced [6], which

incorporates the efficiency  $\theta$  itself and coordinate  $z_s$  of gap electrical centre. For an arbitrary gap, the absolute value of  $\tilde{\theta}$  is equal to  $\theta$  while phase of  $\tilde{\theta}$  equals  $k_1 z_s$  ( $k_1 = 2\pi/\beta\lambda$ ):

$$\tilde{\theta} = \theta \exp(ik_1 z_s). \quad (1)$$

Then,  $\tilde{\theta}$  of acceleration cell made of  $J$  accelerating gaps is

$$\tilde{\theta} = \sum_{j=1}^J \varepsilon_j \tilde{\theta}_j, \quad \varepsilon_j = u_j / u, \quad (2)$$

where  $\tilde{\theta}_j = \theta_j \exp(ik_1 z_s^j)$  is complex efficiency of gap  $j$ ,  $u_j$  is voltage across gap  $j$ ,  $u$  is net voltage per cell. Efficiency  $\theta_a$  of a single axially symmetric gap is well known, while for a single quadrupole gap its efficiency  $\theta_q$  is derived in [6],

$$\theta_a = \frac{2 \sin k_1 \frac{l_a}{2}}{k_1 l_a I_0(k_1 a)}, \quad \theta_q = \frac{2 \sin k_1 \frac{l_q}{2} \cos k_1 \frac{l_h}{2}}{k_1 l_q I_0(k_1 a)}. \quad (3)$$

Expressions (2), (3) prove to be useful since they allow for getting factor  $\theta$  for an arbitrary multielectrode structure proceeding from “elementary” components  $\theta_a$  and  $\theta_q$  (3) via (2). Say, for a cell shown in Fig. 2

$$\theta_{aq} = \sqrt{\varepsilon_a^2 \theta_a^2 + \varepsilon_q^2 \theta_q^2 + 2\varepsilon_a \varepsilon_q \theta_a \theta_q \cos k_1 \left( l_i + \frac{l_a + l_h + l_q}{2} \right)}, \quad (4)$$

where  $\varepsilon_a = u_a / u$ ,  $\varepsilon_q = u_q / u$ . In accelerator URAL-30, value of  $\theta$  varies from 0.7 to 0.9. Fig. 3 sketches various types of acceleration cells, the first option being used in the last section of URAL-30.

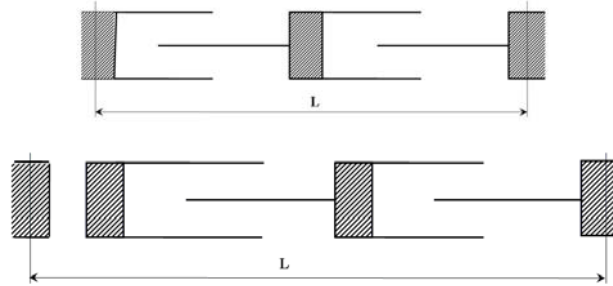


**Figure 3:** Examples RFQ-DTL layouts with one and two spacer electrodes.

RF quadrupole field provides focusing. The major analytical results are reported in [5], [6] for FD and for FFDD focusing patterns. Both these variants are employed in accelerators URAL-30 and URAL-30M. The particular type of focusing is set with a proper orientation of quadrupole electrodes. The layout of electrodes for various patterns of focusing is shown in Fig. 4.

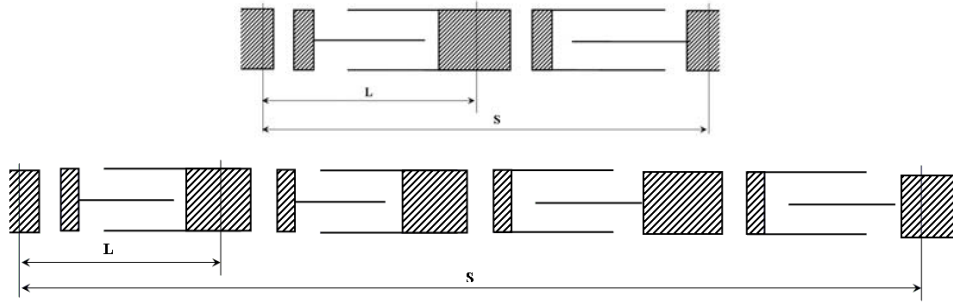


**Figure 4:** Arranging FD and FFDD focusing patterns.

### 3.2.3 Operational RFQ-DTL Facilities

In 1968, the first experimental model of a linac based on the RFQ principle was assembled [7]. The URAL-30 proton linac was commissioned in 1977. It applies a through front-to-end RFQ-focusing up to the top energy of 30 MeV. For a few years to follow, diverse and instructive experimental studies of the machine were performed, and a sound practical experience acquired. Since 1985 till now, this facility routinely operates as an injector to booster proton synchrotron of IHEP.

By now, many parts and subsystems of URAL-30 no longer comply with up-to-date requirements and thus call for replacement. A-few-year-long scientific research efforts and computer simulations allowed launching design of an upgraded machine.

This accelerator, URAL-30M, is currently being manufactured in IHEP. For the time being, a conventional RFQ and two of four RFQ-DTL sections (up to 15 MeV) are assembled and subjected to pre-commissioning tests. Others are being fabricated.

In this machine, measures are foreseen to facilitate a better section-to-section matching of beam. The particular attention is paid to interface between RFQ and RFQ-DTL. To this end, accelerating rate at exit from RFQ approaches that at entry to RFQ-DTL. A more regular transverse focusing pattern is foreseen — FD periodicity is applied in both, RFQ and RFQ-DTL sections. On the contrary, the RFQ-DTL section of URAL-30 relied on the FFDD layout.

To ensure the improved stability of operation, maximum E-field on the surface tips of electrodes is lowered down to  $\leq 350$  kV/cm. Voltage jumps in between sections are reduced noticeably. Vane-to-vane voltage  $U$  is now ramped along the cavity length, downstream of beam motion. This allows compensating for a descent in accelerating rate  $\propto 1/\beta$  inherent in an invariable-voltage option (e.g., that of URAL-30).

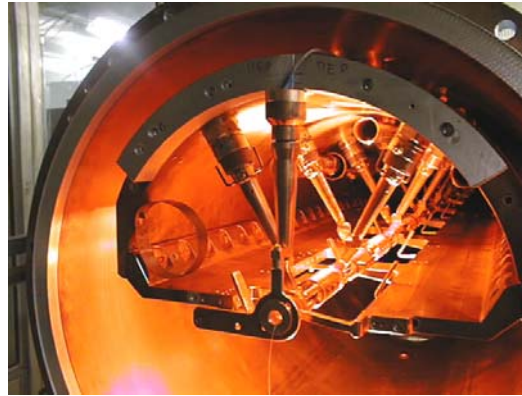


**Figure 5:** Open view of *SH*-cavity.

The accelerating structure itself diverges essentially from that of URAL-30. Both, cavity and tanks are manufactured of a copper-plated aluminum alloy. Electrodes are tooled of bulk OFC copper. An old-fashioned H-cavity is used only in the first section of URAL-30M. Other sections employ the so-called sector *H*-cavity (an *SH*-cavity), see Fig. 5. These exhibit a higher shunt impedance and enable much an easier assembly of the electrodes. The latter procedure is not a trivial task since it should yield the prescribed partition of overall voltage  $U$  in between accelerating ( $U_A$ ) and focusing ( $U_Q$ ) gaps. To this end, support stems of intermediate (spacer) electrodes must be installed at a well-controlled angle with respect to the vertical plane of the cavity symmetry. The design goal is to provide constant voltage  $U_Q$  across quadrupole gaps, while keeping the voltage across accelerating gaps ramped along beam path,  $U_A \propto \beta$ . Contrary to URAL-30, URAL-30M has lengths of accelerating gaps varying along the cavity section.

At the moment, IHEP is getting involved into R&D and manufacture of a prototype first section for 40 MeV RFQ-DTL at 352.2 MHz — the intended RFQ-DTL option for the warm front-end part of the CERN SPL project [8].

The RFQ-DTL in question can also be used for acceleration of heavy ions in a proper range of  $\beta$ .

The concept of RFQ-DTL is far from having exhausted itself. Further activity in this direction looks well promising.

### 3.2.4 References

1. I.M. Kapchinsky, V.A. Teplyakov. *Pribory & Tekhnika Experimenta*, 1970, v.2, p. 19; *Pribory & Tekhnika Experimenta*, 1970, v. 4, p. 17.
2. N.I. Golosay et al. *Atomic Energy*, 1975, v. 39(2), p. 123.
3. V.V. Vladimirovsky. *Pribory & Tekhnika Experimenta*, 1959, v.3, p.36.
4. V.A. Teplyakov. *Pribory & Tekhnika Experimenta*, 1964, v.6, p.24.
5. A.P. Maltsev, C.M. Ermakov, V.A. Teplyakov. *Atomic Energy*, 1967, v.23(3), p.195.
6. Yu.A. Budanov. *Sov. Physics JTP*, 1991, v.61, p.162.
7. A.P. Maltsev, V.B. Stepanov, V.A. Teplyakov. Preprint IHEP 69–2, Serpukhov, 1969.
8. ISTC Project # 2889, <http://tech-db.istc.ru/istc/db/projects.nsf/all-projects/2889>.

### 3.3 Beam Halo in High Intensity Proton/H<sup>-</sup> Linear Accelerators

Frank Gerigk

[RAL, ASTeC, Intense Beams Group](#), Chilton, Didcot, OX11 0QX, UK

mail to: [Frank.gerigk@rl.ac.uk](mailto:Frank.gerigk@rl.ac.uk)

#### 3.3.1 Introduction

High intensity linear accelerators form the basis for a large number of future science facilities such as spallation neutron sources, neutrino or beta-beam facilities, accelerator driven systems (transmutation, energy amplifier), and radioactive ion beam facilities. Common to all these projects is the requirement to keep uncontrolled beam losses below a level of 1 W/m, which is generally regarded as the limit for hands-on maintenance. Aiming at average beam powers in the MW range, these machines have to control losses with a precision of  $10^{-6} - 10^{-7}$ /m in order to avoid performance limitations due to machine activation. Hence an understanding of all processes leading to the development of a low-density beam halo surrounding the beam core is essential.

The first project attempting to establish MW beam power with a proton linac was the LANSCE [1] machine at Los Alamos (0.8 GeV). Commissioned in 1972 it took more than 10 years to establish a proton beam with 16.5 mA peak current and  $\sim 1$  MW average beam power. For short pulse spallation sources or neutrino factories the task becomes even more challenging due to the need for H<sup>-</sup> acceleration. There, the requirement for short (ns) intense bunches necessitates an accumulator/compressor ring system with multi-turn charge-exchange H<sup>-</sup> injection from the preceding linac. Accelerating H<sup>-</sup>, however, adds a number of problems to an already challenging high-intensity linac design: a) ion sources with the required duty cycles and beam currents are still under development, b) generally the output distributions of H<sup>-</sup> sources contain more halo particles than those of proton sources, c) low-loss multi-turn ring injection demands a low-energy beam chopper which introduces a major source for emittance growth and halo development, d) ionisation of H<sup>-</sup> due to rest-gas in the beam pipe produces additional losses.

The combined design effort for a number of high-intensity linac projects (APT [2], SNS [3], JPARC [4], CONCERT [5], TRASCO [6], ESS [7], SPL [8], etc) and the imperative for low-loss operation made considerable contributions to our current understanding of beam halo formation. This article summarises the some of most relevant results for high-power proton/H<sup>-</sup> linacs and aims to provide an introduction of the basic halo mechanics. It will outline recent developments in the field and will close with ongoing efforts to validate the theory experimentally.

#### 3.3.2 Halo Mechanisms in Linacs

The most important mechanism for halo development is based on parametric 2:1 resonances between the oscillations of a mismatched beam core and the movements of single particles. The course of events that expels these particles into a low-density halo is explained in the following with a simple 1D particle-core model and its consequences are then outlined using the 3D mismatch modes of bunched beams.

Apart from parametric resonances a number of additional effects contribute to beam halo formation but they can either be avoided by following simple design rules or they

are of minor importance in linear accelerators. Among them are: a) resonances between the beam envelopes and the focusing structure which can yield rapid rms emittance increase and beam halo but which are usually avoided by keeping the zero current tunes (phase advances) in all three planes below  $90^\circ$  per focusing period, b) intrabeam scattering which is generally considered to be of minor importance [9, 10], c) space charge coupling resonances [11] which can yield emittance exchange between the planes but which, by themselves, do not contribute to the development of beam halo [12].

### 3.3.3 The Particle-Core Model

#### 3.3.3.1 Basic equations

The particle-core model describes the basic principle of single particles being driven out of the beam core by means of parametric resonances [13, 14]. Here, one particle interacts with a beam that is represented by a charged volume. In the simplest 1D case one considers an azimuthally symmetric continuous beam with a uniform charge density. For the sake of simplicity the external focusing forces of the usually periodic lattice are averaged and replaced by a uniform focusing channel. Following the model outlined in [15] the transverse equation of motion for the core envelope radius  $r_c$  as a function of the axial coordinate  $s$  can be written as

$$r_c'' + k_0^2 r_c - \frac{\varepsilon^2}{r_c^3} - \frac{K}{r_c} = 0, \quad (1)$$

with  $k_0$  representing the averaged transverse focusing forces,  $\varepsilon$  being the total unnormalised beam emittance, and  $K$  being a space charge constant containing mass, axial velocity, charge, and the number of particles. The depressed tune per unit length is defined as  $k^2 = k_0^2 - (2K/r_0^2)$ . In case of a matched beam the core envelope remains constant at

$$r_c^2 = r_0^2 = \frac{\varepsilon}{k_0} \left( u + \sqrt{1 + u^2} \right) \text{ with } u = \frac{K}{2\varepsilon k_0}. \quad (2)$$

Assuming the beam core to be an infinitely long cylinder of charge, the equation of motion for a single particle moving through the space charge field of the beam ( $F_{sc}$ ) can be written as

$$x'' + k_0^2 x - F_{sc} = 0 \text{ with } F_{sc} = \begin{cases} Kx/r_c^2 & |x| < r_c, \\ K/x & |x| \geq r_c. \end{cases} \quad (3)$$

Applying Gauss' Law one finds a linear dependence of the space charge force on the particle radius inside the beam boundaries, while outside the core the forces become nonlinear and no longer depend on the actual size of the charged cylinder.

### 3.3.3.2 Initial mismatch

Using Eq.(1-3) one can study the effect of initial mismatch on the beam core and the single particle. Without mismatch the core envelope remains constant and the single particle oscillates with constant amplitudes in the space charge field of the core. Introducing an initial mismatch, the core starts to oscillate with a certain eigenfrequency and thus modulates the space charge forces seen by the single particle. As a consequence thereof the single particle amplitude starts to oscillate around its equilibrium as shown in Fig. 1.

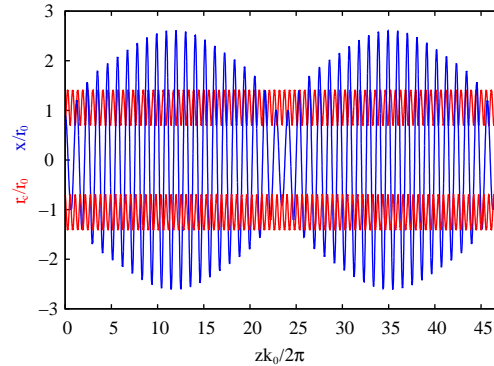


**Figure 1:** Particle trajectories and core envelopes for initial mismatch in a 1D uniform focusing channel with:  $k/k_0=0.8$ ,  $r_c/r_0=0.8$ ,  $x(0)=0.9 r_0$ .

Fig. 1 shows clearly that the oscillation frequency of the core is twice as fast as for the single particle, hinting at the existence of a parametric 2:1 resonance. The single particle gains in amplitude until it is  $180^\circ$  out of phase with the core oscillation and subsequently loses in amplitude until the phase difference is once more reduced to  $0^\circ$ . Since the model assumes a constant emittance there is no energy transfer between the core and the single particle oscillations and the process carries on indefinitely. The resonant nature of the process suggests that only particles within a certain range of the 2:1 resonance frequencies will be affected by the core oscillations. This can be visualised by plotting once per oscillation period the phase space position of single particles that start with different initial radii. Fig. 2 shows such a stroboscopic plot for tune depressions of 0.8/0.6 (left/right) and a 20% core mismatch.

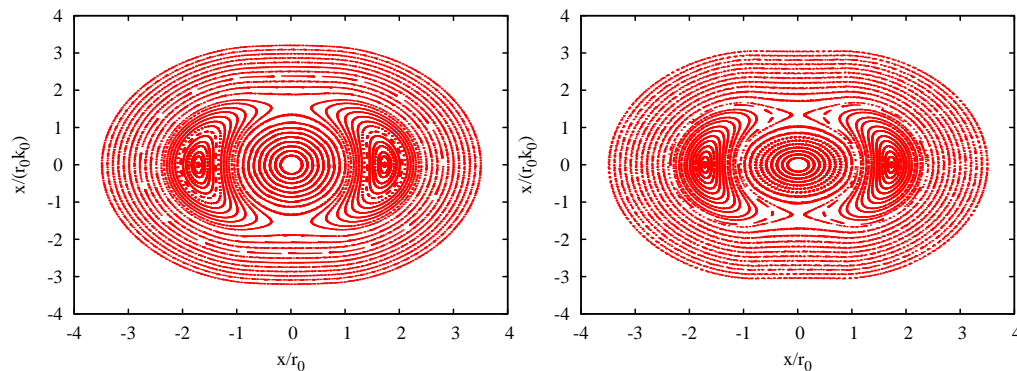


**Figure 2:** Stroboscopic plot for initial mismatch in a 1D uniform focusing channel with: *left:*  $k/k_0 = 0.8$ , *right:*  $k/k_0=0.6$ , *both:*  $r_c/r_0 = 0.8$ ,  $0.2 < x(0)/r_0 < 3.5$ .

One can see that particles with small ( $< 0.5 r_0$ ) and large ( $> 2.3 r_0$ ) initial radii are basically unaffected, while the particles in between are caught in resonances and now oscillate around certain fixed points in phase space. For increasing space charge forces the resonant regions increase in size and more particles become affected by the mismatch oscillations. In other words: stronger space charge forces provide a larger spread of single particle tunes and in consequence they increase the probability for single particles to get expelled by a parametric resonance. However, as shown in [15], the fixed point-core distance and the maximum halo radius are only sensitive to the strength of the initial mismatch but not to the strength of the tune depression. An important outcome of the particle-core studies, which is also confirmed by 3D particle tracking, is that the maximum radius for halo particles due to initial mismatch appears to be limited. The simple 1D model predicts this limit at  $\approx 7$  rms radii, while more elaborate 3D models predict more than 10 rms radii for certain focusing regimes [16].

### 3.3.4 3D Mismatch Modes

In a 3D bunched beam there are three degrees of freedom for the oscillations of the beam core and hence one can expect three *bunched beam eigenmodes* or *mismatch modes*. Starting from the 3D envelope equations with space charge<sup>1</sup>

$$\begin{aligned} a_x'' + a_x \kappa_x(s) - \frac{K_3[1-f(s)]}{2a_y b} - \frac{\epsilon_x^2}{a_x^3} &= 0, \\ a_y'' + a_y \kappa_y(s) - \frac{K_3[1-f(s)]}{2a_x b} - \frac{\epsilon_y^2}{a_y^3} &= 0, \\ b'' + b \kappa_z(s) - \frac{K_3 f(s)}{a_x a_y} - \frac{\epsilon_z^2}{b^3} &= 0. \end{aligned} \quad (4)$$

one can use the smooth approximation together with a perturbation of the matched solution [ $a(s) = a_m(s) + \Delta a(s)$ ] to derive the eigensolutions for these modes [17, 18]. In this approach the transverse  $s$ -dependent focusing forces  $\kappa(s)$  are averaged and the dependence of the form factor  $f(s)$  on the aspect ratio of the bunch is ignored. The three modes are named according to their properties as:

- **Fast mode** or **high-frequency mode** or **breathing mode**: the beam core expands and contracts in all three planes simultaneously but with different amplitudes in the transverse and longitudinal planes. It has the highest oscillation frequency of all three modes and is usually the most ‘harmful’ mode in terms of halo development.
- **Quadrupolar mode**: the beam core oscillates only in the transverse planes with  $180^\circ$  phase difference between  $x$  and  $y$ . It oscillates twice as fast as the core particles and will therefore always form parametric resonances with these particles.
- **Slow mode** or **low-frequency mode**: the transverse/longitudinal beam envelopes oscillate with different amplitudes and with a  $180^\circ$  phase difference between transverse and longitudinal oscillations.

<sup>1</sup>  $K_3$  representing the 3D space charge constant

The eigensolutions for the three modes can be written as

**quadrupolar mode:**

$$\frac{\Delta a_x}{a_x} = A_m \cos\left(\sigma_{env,Q} \cdot \frac{s}{L_p} + \phi\right), \quad \frac{\Delta a_y}{a_y} = -A_m \cos\left(\sigma_{env,Q} \cdot \frac{s}{L_p} + \phi\right), \quad \frac{\Delta b}{b} = 0, \quad (5)$$

**fast/slow mode:**

$$\frac{\Delta a_{x,y}}{a_{x,y}} = A_m \cos\left(\sigma_{env,F/S} \cdot \frac{s}{L_p} + \phi\right), \quad \frac{\Delta b}{b} = \frac{A_m}{g_{F/S}} \cos\left(\sigma_{env,F/S} \cdot \frac{s}{L_p} + \phi\right), \quad (6)$$

with  $A_m$  denoting the amplitude mismatch. The amplitude factors  $g_F (>0)$  and  $g_S (<0)$  as well as the tunes of the eigenmodes  $\sigma_{env,Q/F/S}$  can be expressed as functions of the zero- and full-current tunes of the lattice. Using the analytic approximations of [17] Fig. 3 shows an example for the excitation of the fast mode for beams with 6D waterbag and Gaussian distributions.

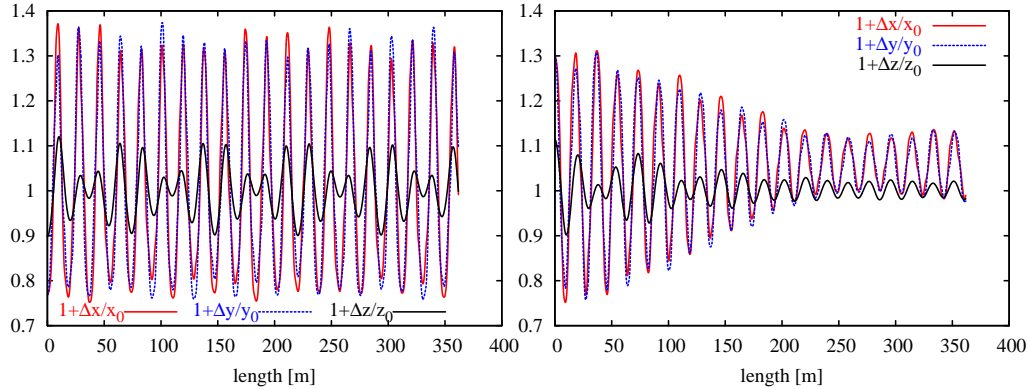


**Figure 3:** Core oscillations for a 6D waterbag/Gaussian (left/right) beam due to the excitation of the fast mode with 30% initial mismatch. (IMPACT [19] simulation with  $10^6$  particles.)

Although the excitation is not perfect (e.g. the longitudinal amplitudes are changing considerably from period to period) it is clearly visible that the oscillations in all 3 planes are in phase. In case of the waterbag distribution the oscillations seem to carry on undisturbed while for the Gaussian distribution the amplitudes decrease to a certain minimum and then stay there. The damping of the oscillations of the Gaussian beam can be explained by the transformation of the “free energy” which is stored in the mismatch oscillations into beam halo [20]. This means that the halo development compensates the initial mismatch. The fact that this process takes place much faster in case of the Gaussian distribution is likely to be caused by the presence of the “Gaussian tails” and of more “initial noise” when compared to the homogenous 6D waterbag. Realistic linac distributions are typically somewhere “in between”, meaning that simulations with Gaussian distributions usually give a good “worst case” estimate. Even though the fast mode mismatch usually yields the most dramatic effect it is worth considering several different types of input mismatch to study the sensitivity of a particular lattice to errors.

A simpler approach without using specific eigenmodes is suggested in [21], where an analytic estimate for rms emittance growth due to mismatch is derived from the “free

energy” considerations. The averaged rms emittance growth is calculated as a consequence of an averaged mismatch in x, y, and z and is estimated to follow

$$\frac{1}{3} \left( \frac{\Delta \varepsilon_x}{\varepsilon_x} + \frac{\Delta \varepsilon_y}{\varepsilon_y} + \frac{\Delta \varepsilon_z}{\varepsilon_z} \right) \approx \alpha (M_{rms} - 1)^2, \quad (7)$$

where  $\alpha$  is a weak function of the tune depression and can be approximated as  $\alpha \approx 2.5$ . The rms mismatch factor  $M_{rms}$  is given by

$$(M_{rms} - 1)^2 = \frac{1}{3} \sum_{i=x,y,z} (M_i - 1)^2. \quad (8)$$

How the emittance growth is distributed to the different planes depends on the resonances, which are excited by the mismatch. The maximum halo radii accompanying the emittance growth approximately follow the predictions from the 1D [15] and 3D [16] particle-core models and are found between 7 and 10 multiples of the rms radius.

It is worth mentioning that end-to-end linac simulations often exceed the predictions for rms emittance growth and maximum halo radii given by the “free energy” approach and the particle-core model. The theoretical models do, however, provide a guideline for minimum growth values that could be achieved with a “perfect” linac design.

### 3.3.5 Simulations & Experiments

3D particle tracking for multi-MW linacs poses significant challenges in terms of processing power. A realistic representation of all lattice elements and large particle numbers ( $> 10^7$ ) are needed to resolve losses in the order of 1 W/m. Furthermore, the calculation of statistical machine errors requires a large number of simulations to allow accurate predictions of beam loss versus machine tolerances.

In the LEDA beam halo experiment [22] a first attempt was made to verify theoretical predictions for halo development with experiments. The results support the picture of the particle-core model and the observed emittance growth is consistent with the predictions from the “free energy” model [20]. The experiment also triggered the development of a dedicated halo monitor allowing density measurements to levels as low as  $10^{-5}$  of the core densities. However, several open questions remain after LEDA:

- a) The timescale for emittance growth seemed to be much faster in the experiment than in theoretical predictions and the question remains if a longer transport line would yield further emittance growth.
- b) The predictions for emittance growth and halo development did not take into account the influence of statistical errors or machine misalignment.
- c) The input/output distributions of the RFQ could not be measured, making it difficult to reproduce the experimental results with 3D simulations [23].

In spring 2006 and 2007 two 7-day code/machine benchmarking experiments are authorised to take place at GSI using the UNILAC DTL section. The set-up will allow transverse and longitudinal emittance and beam distribution measurements at the entrance and exit of the DTL for various currents and phase advance settings. In preparation for the experiment several codes have been compared using the UNILAC DTL lattice [24]. For the linac itself improved diagnostics systems are being installed to allow high-resolution measurements for the different settings of the linac.

### 3.3.6 Recent Developments

Recent studies show that the presence of noise [25] or statistical machine errors [26] can drive the particles of a matched beam beyond the maximum amplitudes predicted by the particle-core model for beams with initial mismatch. Due to the continuous feeding of “mismatch energy” into a high-intensity beam it is found that statistical errors yield continuously increasing halo radii, eventually resulting in beam loss at the apertures of the beam pipe. For mismatched beams it is found [26] that the presence of noise enhances the halo development triggered by mismatch alone. The process of expelling particles can be simulated by adding noise or statistical errors to the focusing terms of the particle-core model, and one can show that the underlying mechanism is again based on a parametric 2:1 resonance [26]. Even though statistical machine errors are not the dominating source of beam halo, they certainly contribute to its development and they do explain particle loss even in accelerators with large apertures.

Another area of halo development that is usually neglected is the low energy part of proton or especially H- accelerators: ion source and LEBT. Both parts are difficult to simulate and only recently did the linac community start new efforts to track particles in LEBTs including the transient behaviour of space charge compensation as well as scattering and ionisation [28].

### 3.3.7 Summary

Parametric resonances are generally considered to be the major source of halo development in high intensity linacs. The mechanics of expelling particles to large amplitude radii can be understood with a simple particle-core model and studied in depth by exciting the 3 mismatch eigenmodes in tracking simulations for the lattice in question. Generally one can say that the best strategy for a low-loss linac design is to remove or minimise all possible sources of mismatch. This means: a) to minimise the number of transitions between different focusing structures, and to avoid all sudden changes in the focusing lattice, b) to make all transitions as smooth as possible, i.e. to maintain a smooth variation of the tunes across lattice changes, c) to minimise statistical errors, which are nothing else than “distributed” mismatch, d) to use substantial effort on the front-end design (LEBT, RFQ, MEBT), because once a beam is mismatched the only way to damp the core oscillations and to return to an equilibrium is the development of beam halo. This also means that halo scraping can only help to control the effects of mismatch but it is certainly not a tool to correct the mismatch itself, nor will it prevent further halo formation.

### 3.3.8 References

1. Los Alamos Neutron Science Center, <http://lansce.lanl.gov>.
2. J. David Schneider, “APT accelerator technology”, in *Proceedings of the 1996 Linear Accelerator Conference*.
3. Spallation Neutron Source, Oakridge, <http://www.sns.gov>.
4. Japan Proton Accelerator Research Complex, <http://j-parc.jp>.
5. Jean-Michel Lagniel, “High-power proton linac for a multi-user facility”, in *Proceedings of the 2000 European Particle Accelerator Conference*.
6. D. Barni et al., “Status of the high current proton accelerator for the TRASCO program”, in *Proceedings of the 2002 European Particle Accelerator Conference*.

7. ESS Accelerator Team, "The ESS project", vol. 3, technical report, ISBN 3-89336-303-3, (2002).
8. The SPL Study Group, "Conceptual design of the SPL, a high-power superconducting H-linac at CERN", M. Vretenar et.al., CERN 2000-012.
9. R.L. Gluckstern and A.V. Fedotov, "Coulomb scattering within a spherical beam bunch in a high current linear accelerator", in *Proceedings of the 1999 Particle Accelerator Conference*.
10. N. Pichoff, "Intrabeam scattering on halo formation", in *Proceedings of the 1999 Particle Accelerator Conference*.
11. I. Hofmann, "Stability of anisotropic beams with space charge", in *Physical Review E*, **57**, 4713, (1998).
12. F. Gerigk and I. Hofmann, "Beam dynamics of non-equipartitioned beams in the case of the SPL project at CERN", in *Proceedings of the 2001 Particle Accelerator Conference*.
13. J. O'Connell, T.P. Wangler, R. Mills, and K.R. Crandall, "Beam halo formation from space-charge dominated beams in uniform focusing channels", in *Proceedings of the 1993 Particle Accelerator Conference*, (IEEE Report No. CH 3279-7, 1993), pp. 61-64.
14. R. Gluckstern, "Analytic model for halo formation in high current ion linacs", *Phys. Rev. Lett.* **73**, 1247 (1994).
15. T.P. Wangler, K.R. Crandall, R.D. Ryne, and T.S. Wang, "Particle-core model for transverse dynamics of beam halo", *Phys. Rev. ST Accel. Beams* **1**, 084201 (1998).
16. J. Qiang and R.D. Ryne, "Beam halo studies using a three-dimensional particle-core model", *Phys. Rev. ST Accel. Beams* **3**, 064201 (2000).
17. A. Letchford, K. Bongardt, and M. Pabst, "Halo formation of bunched beams in periodic focusing systems", in *Proceedings of the 1999 Particle Accelerator Conference*.
18. N. Pichoff, "Envelope modes of a mismatched bunched beam", technical report DAPNIA/SEA 98/441.
19. J. Qiang, R.D. Ryne, S. Habib, and V. Decyk, "An object-oriented parallel particle-in-cell code for beam dynamics simulations in linear accelerators", *Journ. Comp. Phys.* **163**, 1 (2000).
20. M. Reiser, "Free energy and emittance growth in nonstationary charged particle beams", *J. Appl. Phys.* **70**, 1919 (1991).
21. I. Hofmann et.al., "Review of beam dynamics and space charge resonances in high intensity linacs", in *Proceedings of the 2002 European Particle Accelerator Conference*.
22. T.P. Wangler et.al., "Experimental study of proton-beam halo induced by beam mismatch in LEDA", in *Proceedings of the 2001 Particle Accelerator Conference*.
23. J. Qiang et.al., "Macroparticle simulation studies of a proton beam halo experiment", *Phys. Rev. ST Accel. Beams*, **5**, 124201 (2002).
24. A. Franchi et.al., "Benchmarking linac codes for the HIPPI project", in *Proceedings of the ICFA-HB2004 workshop*. [http://www-linux.gsi.de/~franchi/HIPPI/code\\_benchmarking.html](http://www-linux.gsi.de/~franchi/HIPPI/code_benchmarking.html)
25. C.L. Bohn and I.V. Sideris, "Fluctuations do matter: large noise-enhanced halos in charged-particle beams", *Phys. Rev. Lett.* **91**, 26 (2003).
26. F. Gerigk, "Beam halo in high-intensity hadron accelerators caused by statistical gradient errors", *Phys. Rev. ST Accel. Beams* **7**, 064202 (2004).
27. I.V. Sideris and C.L. Bohn, "Production of enhanced beam halos via collective modes and colored noise", *Phys. Rev. ST Accel. Beams* **7**, 104202 (2004).
28. A.B. Ismail, R. Duperrier, S. Lin, and D. Uriot, "CEA developments for HIPPI", talk at HIPPI04, [http://hippi04.web.cern.ch/hippi04/Final\\_talks/WP5/WP5\\_CEA\\_RDuperrier.pdf](http://hippi04.web.cern.ch/hippi04/Final_talks/WP5/WP5_CEA_RDuperrier.pdf)

### 3.4 Recent Advances on the Multi-Turn Extraction Using Stable Islands of Transverse Phase Space

Massimo Giovannozzi on behalf of the Study Group of PS multi-turn island extraction  
[CERN](http://cern.ch), AB Department, 1211 Geneva 23  
 mail to: [Massimo.Giovannozzi@cern.ch](mailto:Massimo.Giovannozzi@cern.ch)

#### 3.4.1 Introduction

Since the year 2001, intense efforts were dedicated to the study of a novel technique to perform multi-turn extraction from a circular particle accelerator. A report on Beam Dynamics Newsletter was already published [1], discussing the principle of the novel technique, which relies on the use of nonlinear magnetic fields (sextupolar and octupolar) to generate stable islands in the horizontal transverse phase space. By means of an appropriate tune variation, a specific resonance is crossed, the fourth-order in the case under study, and the beam is split by trapping inside the stable islands moving from the origin of the phase space towards higher amplitudes. A good model consists in choosing a simple FODO cell with a sextupole and an octupole located at the same longitudinal position, both represented in the single-kick approximation [2]. For the application under study, only the horizontal plane is relevant. Hence, the dynamics of such a system is generated by a 2D one-turn transfer map, which can be computed and it turns out to be a polynomial map of the form:

$$\begin{pmatrix} x_{n+1} \\ x'_{n+1} \end{pmatrix} = R(\omega_n) \begin{pmatrix} x_n \\ x'_n + x_n^2 + \kappa x_n^3 \end{pmatrix}, \quad (1)$$

where the co-ordinates  $(x, x')$  are dimension-less normalised co-ordinates [2],  $R(\omega)$  represents a rotation matrix of an angle  $\omega = 2\pi\nu$  and  $\kappa$  depends on the ratio between the strength of the sextupole and the octupole with a weight given by the value of the optical beta-function at the location of the nonlinear magnetic elements [3,4], namely

$$\kappa = \frac{2}{3} \frac{K_3}{K_2^2} \frac{1}{\beta_x} \quad (X, X') = \lambda(x, x') \quad \lambda = \frac{1}{2} K_2 \beta_x^{3/2}, \quad (2)$$

where  $(X, X')$ ,  $(x, x')$  stand for normalised Courant-Snyder co-ordinates and dimension-less normalised co-ordinates, respectively. It is important to stress that the angle  $\omega$  is indeed a function of the turn number. In all the plots shown in this article, as well in the numerical and analytical computations reported here, the special dimension-less normalised co-ordinates are used.

An example of the change of the phase space topology during the resonance crossing is shown in Fig. 1.

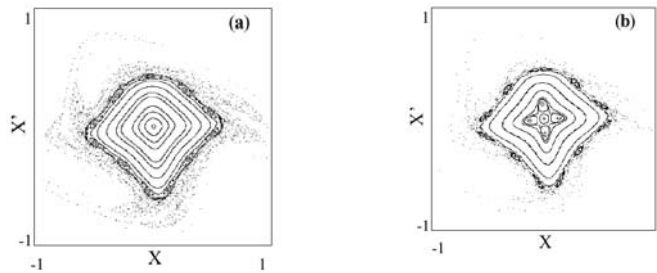


**Figure 1:** Topology of the normalised phase space during resonance crossing.

The evolution of the beam distribution during the resonance crossing is shown in Fig. 2.

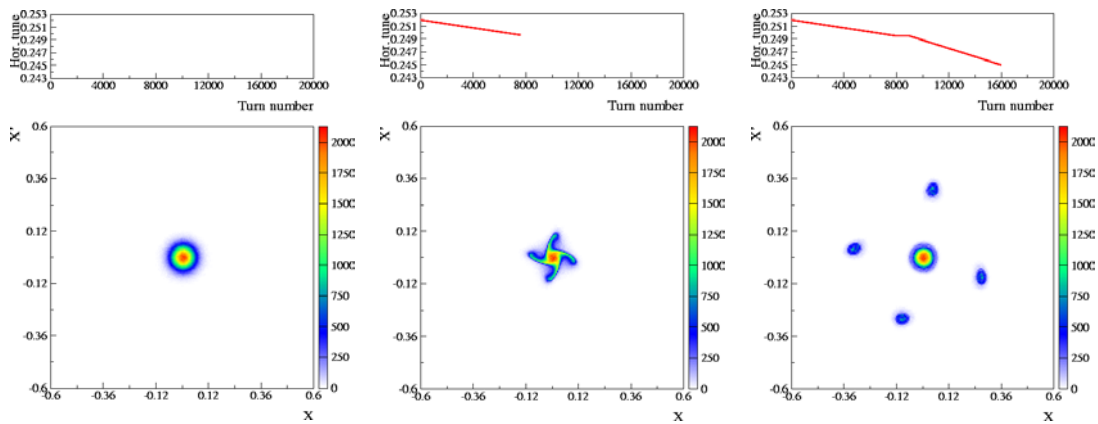


**Figure 2:** Evolution of the beam distribution during resonance crossing: the initial state is represented by a bi-Gaussian beam (left), at resonance-crossing some particles are trapped inside the moving islands (centre), at the end of the process, the particles trapped in the islands are moved towards higher amplitudes (right).

When the tune is changed the islands move through the phase space region where the charged particles sit and some are trapped inside the islands. At some stage a complete separation between the beamlets and the central core occurs and the distance between the beamlets can be increased at will by simply acting on the tune. It is worthwhile stressing that the beam after trapping has a peculiar structure, i.e. it is made by two disconnected parts: the beamlets, which are indeed one single structure closing-up after four machine turns (see Fig. 3), and the central core.

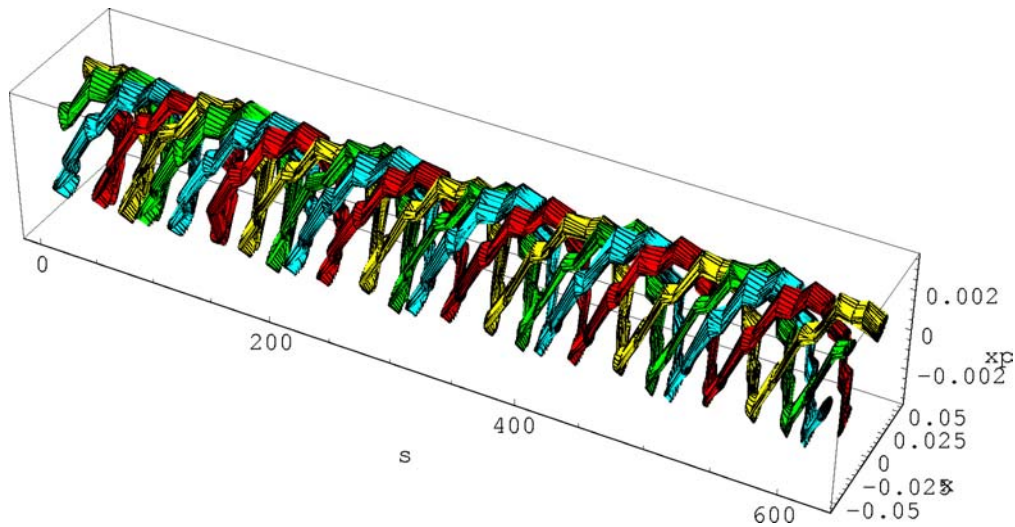


**Figure 3:** 3D view of the beamlets along the circumference of the CERN-Proton Synchrotron (PS) machine. The fifth beamlet, i.e. the beam core, is not shown here.

The islands' phase at two key PS sections, namely the extraction septum location and the one where the wire scanner to measure the horizontal beam profile is installed, is shown in Fig. 4.

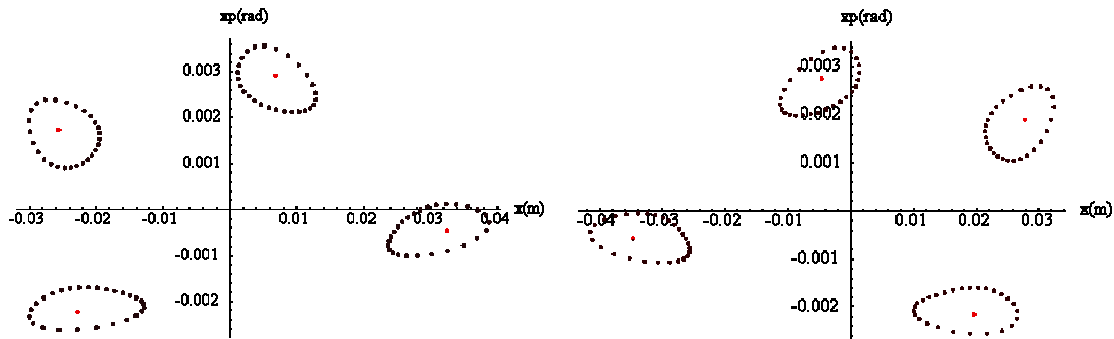


**Figure 4 :** Shape of the stable islands at two straight sections of the PS machine, namely the extraction section (left) and the section where the wire scanner used for profile measurements (see next Sections) is located (right).

The idea behind this process is that such a beam splitting in the transverse phase space can be used to perform multi-turn extraction. In fact, once the various beamlets are separated, the whole structure can be pushed towards an extraction septum by means of a closed slow bump. Then, kicker magnets generate a fast closed bump and one island jumps beyond the septum blade so that the beamlets are extracted out of the machine in four turns. The fifth beamlet, i.e. the beam core, is extracted using a classical single-turn extraction.

The choice of the resonance to be crossed is completely arbitrary: the use of a fourth-order resonance is dictated by the CERN-specific application. The extraction mode from the Proton Synchrotron (PS) to the Super Proton Synchrotron (SPS)

foreseen to deliver the high-intensity proton beam for the planned CERN Neutrino to Gran Sasso (CNGS) experiments [5] is the so-called Continuous Transfer (CT) [6]. The beam is sliced onto an electrostatic septum and it is transferred to the SPS in five turns. The main drawback of such an extraction technique is the high losses in the septum, generating serious problems for the hands-on maintenance of the device. Furthermore, the extracted slices feature different shapes in phase space, thus inducing betatron mismatch at injection in the receiving machine and, eventually, emittance blow-up [7,8]. These points represent serious obstacles for the planned intensity upgrade for the CNGS beam [9].

The goal for this study is to achieve beam splitting with virtually no losses of a beam made by eight bunches, accelerated to 14 GeV/c, with about  $5\text{-}6 \times 10^{12}$  protons/bunch.

### 3.4.2 Further Developments

#### 3.4.2.1 Analysis of the Capture Process for the Fourth-Order Resonance

Following the first encouraging results [10, 11] a series of studies were launched to analyse in more details the capture and trapping process in view of improving the control of the parameters of the beamlets. This goal was tackled using two complementary approaches: a numerical and an analytical one. In the first case, the simple model described in Eq. (1) was used to perform numerical simulations by varying a number of key parameters such as the functional dependence of the linear tune on the number of turns, the strength of the nonlinear elements, and the parameters of the initial distribution, e.g. form of the distribution – Gaussian or uniform – and its emittance. As far as the tune-dependence on the number of turns is concerned, two models were used, i.e. a linear dependence or a polynomial one. No major differences were found for the two options and in all the simulations reported in this paper a linear dependence is used.

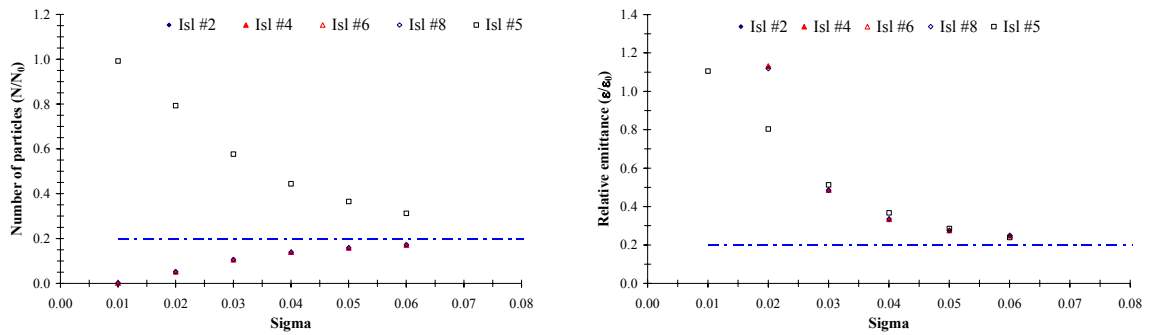


**Figure 5:** Results of numerical simulations to evaluate the intensity trapped in each island vs. the sigma of the initial bi-Gaussian distribution (left) and the emittance of each beamlet vs. the sigma of the initial bi-Gaussian distribution (right). The dot-dashed line represents the goal of perfect splitting, i.e. equal intensity and emittance among the five resulting beamlets.

In Fig. 5 an example of the simulation results is reported. In the real application of this method, it is important to have a uniform sharing of initial intensity and emittance among the five beamlets after the trapping process. Hence, ideally one aims at having 20 % of the initial intensity in each beamlet as well as 20 % of the initial emittance. In the simulations discussed here, the fraction of trapped particles and the emittance of each beamlet are computed as a function of the sigma of the initial Gaussian distribution. All the other parameters are kept fixed for this study. The different markers refer to the five beamlet (the one marked *Is/#5* is indeed the central core).

It is apparent that increasing the sigma of the initial beam distribution has a positive impact on both intensity and emittance sharing. This is a consequence of the fact that the islands have a small size near the origin, hence they tend to capture fewer particles in the region with the highest density. Therefore, increasing the sigma means increasing the particle's density at larger amplitude, where the islands are bigger. An important point is that the ideal value of 20 % sharing among the beamlets seems to be within reach by properly tuning the appropriate parameters.

On the theoretical side intense efforts were devoted in computing the islands parameters, e.g. width, position, and secondary frequency, as a function of the linear tune and the strength of the nonlinear elements (sextupoles and octupoles) [12]. This was achieved by using the normal forms approach [2].

Analytical formulae linking the islands parameters, see Figure 6, to the linear tune  $\omega$ , the detuning term  $\Omega_2$ , the resonant term  $u_{0,3}$ , the strength of the nonlinear elements  $\kappa$ , and the distance from the resonance  $\varepsilon$  are reported in the following. The distance of the fixed point from the origin,  $\rho_+$ , and the maximum distance between separatrices,  $\Delta$ , can be expressed as:

$$\rho_+ = -\frac{\varepsilon}{\Omega_2 + 2\varepsilon|u_{0,3}|}, \quad \Delta = 4\sqrt{\left|\frac{\varepsilon}{\Omega_2}\right| \cdot |u_{0,3}| \rho_+^2} \quad \text{where}$$

$$u_{0,3} = \frac{i}{16} e^{i\omega} \left( \cot \frac{\omega}{2} - \cot \frac{3\omega}{2} - 2k \right) \quad \Omega_2 = -\frac{1}{16} \left( 3\cot \frac{\omega}{2} + \cot \frac{3\omega}{2} \right) - \frac{3}{8} \kappa.$$

The island surface and the secondary frequency are respectively

$$\Sigma = 16\sqrt{\left|\frac{\varepsilon}{\Omega_2}\right| \cdot |u_{0,3}| \rho_+^2} \quad \omega_{\text{sec}} = 4\sqrt{|\Omega_2 \varepsilon| \cdot |u_{0,3}| \rho_+^2}$$

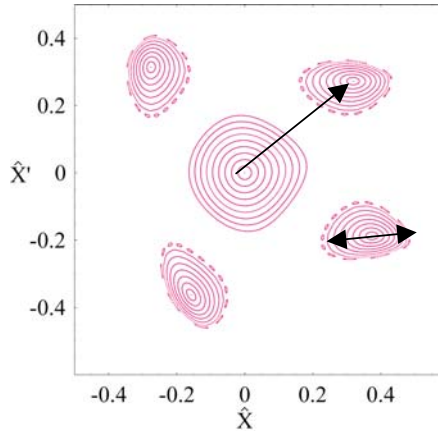


**Figure 6:** Example of islands and their characteristic parameters

The knowledge of the analytical dependence of the islands' size of the tune and on the strength of the nonlinear elements allows finding a way to move the beamlets while keeping the surface constant. In Fig. 7 an example is shown. To achieve the optimal control it is now necessary to vary the strength of the sextupoles and octupoles at the end of the capture process just before the transport towards higher amplitudes starts (left).

In the centre part, the islands' surface is shown and it is clearly kept constant once the fractional part of the linear tune is higher than 0.256. Correspondingly (right) the islands centre continues moving, even though at a lower speed, when the surface is kept constant. It is planned to test these results by means of numerical simulations to evaluate the impact on the properties of the generated beamlets.

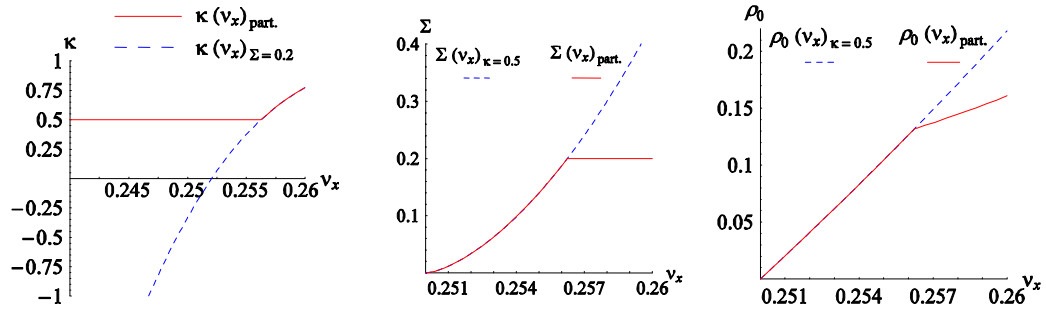


**Figure 7:** Example of control of the islands' size while moving them towards higher amplitudes. The solid line represents a solution with constant island surface, while the dashed line corresponds to a constant value of the strength of the nonlinearities.

### 3.4.2.2 Extension to Other Resonances

Indeed, a rather straightforward extension of the proposed method to perform multi-turn extraction from a circular accelerator consists in crossing a different resonance, hence generating a different number of beamlets at the end of the splitting process [13]. The most natural alternative to the fourth-order resonance is to use third-order one. This has also another important consequence. In fact, the fourth-order is a stable resonance, which means that particles sitting near the origin of phase space will not be trapped by the moving islands. Therefore, for a stable resonance of order  $n$ ,  $n+1$  beamlets will be generated. On the other hand, when the resonance is unstable, particles will be pushed away from the origin and will fill the islands. Thus, for an unstable resonance of order  $n$ ,  $n$  beamlets will be generated.

The results of numerical simulations performed using an initial Gaussian distribution and crossing the third order resonance are shown in Fig. 8.

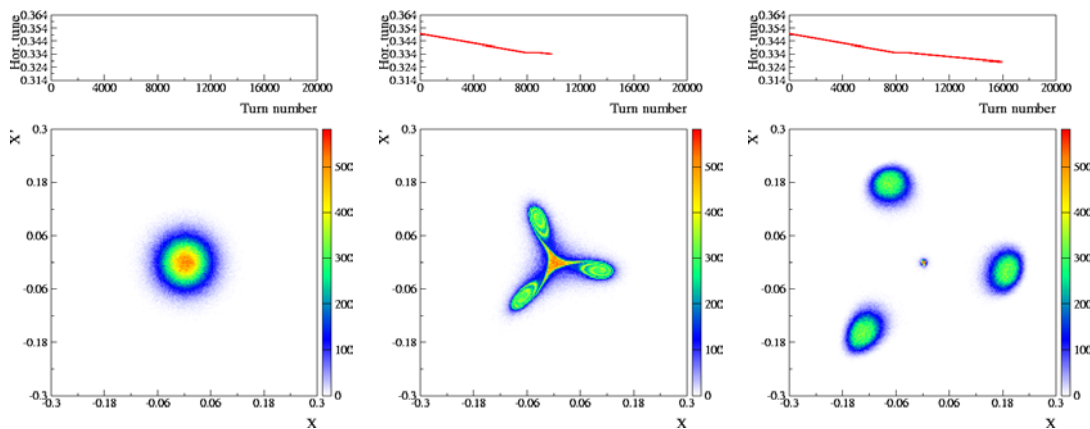


**Figure 8:** Evolution of the beam distribution during resonance crossing: the initial state is represented by a Gaussian beam (left), at resonance-crossing some particles are trapped inside the moving islands (centre), at the end of the process, the particles trapped in the islands are moved towards higher amplitudes (right).

Contrary to the previous case, almost no particle is left at the origin. Furthermore, another interesting side effect is that the potential difference in term of particle sharing and emittance between the central and the other beamlets is not present in this case.

Of course, the method can be generalised to other resonances: two examples are shown in Fig. 9.

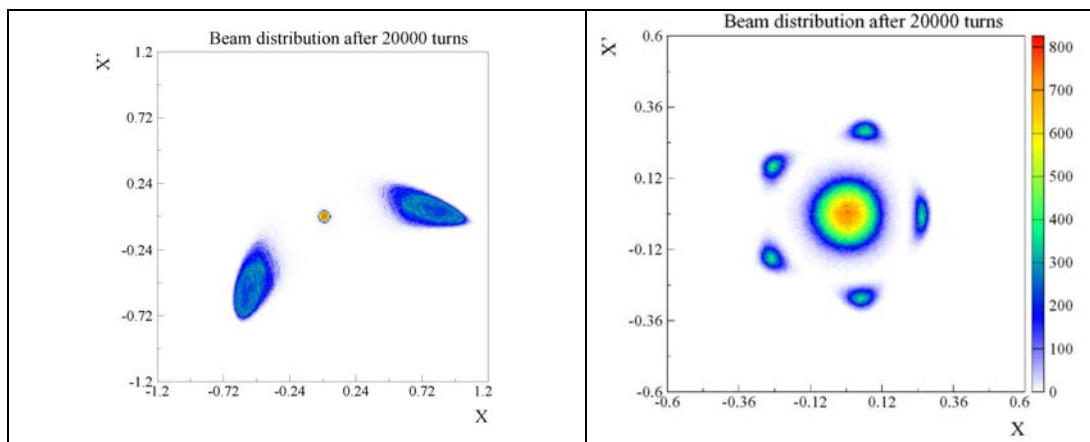


**Figure 9:** Final stage of the splitting process after crossing the half-integer resonance (left) and the fifth-order resonance (right).

It is worthwhile stressing that when the resonance order is increased, the islands' size tends to become smaller, thus implying that there will be fewer and fewer particles trapped in the islands. Furthermore, there will be less room for locating the blade of an extraction septum without intercepting any particle.

### 3.4.2.3 Multi-Turn Injection Using Stable Islands

The most recent development is the application of the proposed technique to multi-turn injection [14]. This is a sort of natural consequence of the time-reversal property of the phenomena under consideration. However, there are interesting implications, which might be relevant for situations where the space charge forces are dominant. In Fig. 10 an example of multi-turn injection based on the use of stable islands in the transverse phase space is shown.

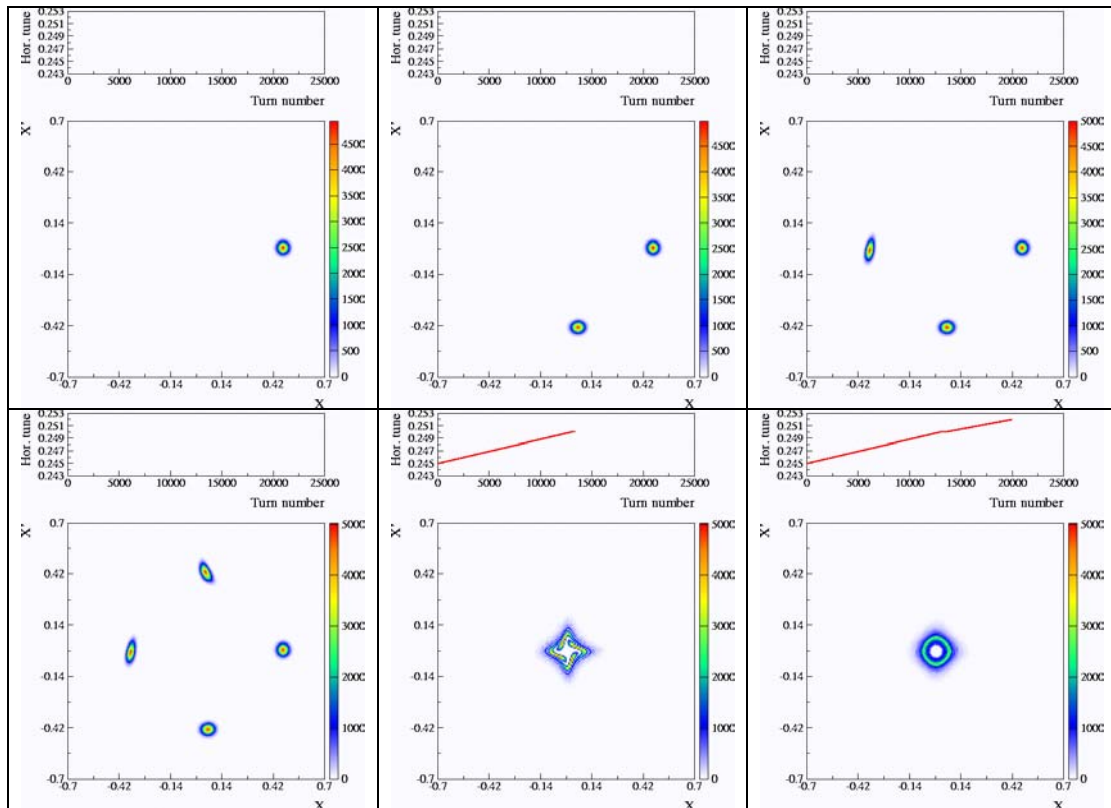


**Figure 10:** Multi-turn injection by means of trapping in stable islands of transverse phase space. Four turns are injected and the beamlets merged by crossing the fourth-order resonance. As a result a hollow beam in the transverse phase space is generated.

In the case presented here, the fourth-order resonance is used: four turns are injected into the outermost island, which should be beyond the injection septum blade. Then, the tune is changed to merge the four beamlets back into one single structure. The fact that the islands have a size approaching zero near the origin implies that the beamlets will not be merged into a perfect Gaussian beam, but the final result is, instead, a hollow beam. Of course, this could be extremely important for high-intensity beams, as the hollow structure in the transverse phase space allows reducing the tune spread. It is important to stress that the simulations presented here do not take into account the Coulomb interaction between the particles, hence the observation made should be confirmed by more detailed simulations taking into account also space charge effects. Another important point is that a fifth turn could also be injected: in this case instead of

a hollow beam the final distribution would be the superposition of a hollow one plus a Gaussian at the centre: this opens up the possibility of performing a sort of painting in the transverse phase space.

### 3.4.3 Experimental Results

#### 3.4.3.1 Overall Measurement Strategy

In parallel with the computational and theoretical analysis of the problem, an intense experimental campaign was launched since the end of year 2001 [15-18] on the CERN PS. This entailed the development of new measurement systems, such as the turn-by-turn orbit measurement system [19, 20], as well as the installation of sextupoles and octupoles to generate the stable islands.

The magnetic elements and the beam instrumentation used in the experimental campaign are shown in Fig. 11. The tune is changed by means of two families of focusing and defocusing quadrupoles, normally used to tune the machine. Sextupoles and octupoles are used to generate the stable islands; the extraction kicker is used to displace the beam and induce betatron oscillations for phase space measurements; a wire scanner [wire] is used to measure the horizontal beam profile; two pickups are used to record the betatron oscillations.

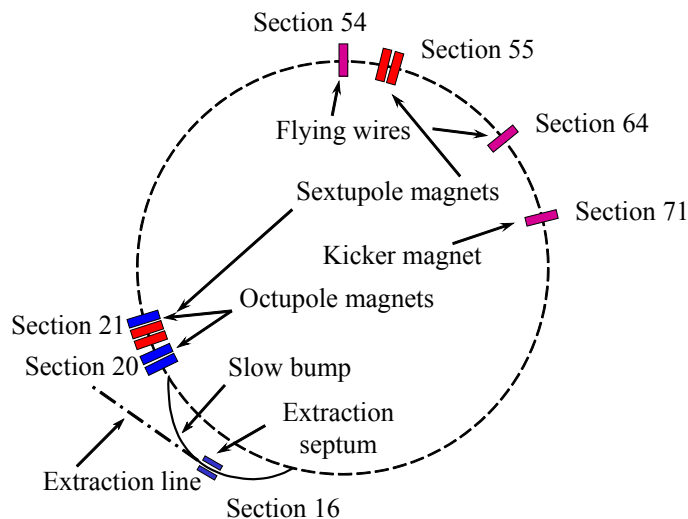


**Figure 11:** Schematic layout of the PS machine with the elements used for the experimental study of the novel multi-turn extraction.

The overall strategy for the experimental campaign was based on three stages:

1. Measurement of the phase space topology. This is performed by displacing a low-intensity, single-bunch, pencil beam, by means of the extraction kicker. The betatron oscillations measured by two pickups are then recorded on a turn-by-turn basis and analysed to detect the presence of stable islands. Normally the position signal features a decoherence, due to beam filamentation induced by

nonlinear effects and chromaticity. Whenever the beam is displaced inside one island, natural decoherence is almost completely suppressed. An example of the measurement results is shown in Fig. 12 [4]. The position signal as a function of turn number is shown in the upper part: no sign of decoherence is visible. Damped oscillations are visible in the first part of the time-series. These indicate that the beam is rotating around the island's centre. From the first part of the time-series it is possible to measure the so-called secondary frequency [2] or island tune [21]. Furthermore, it is possible to scan over the amplitude inside the island to evaluate a sort of detuning curve [4]. The result of such a type of measurement is shown in the lower left part. Finally, the information from the two pickups is combined to reconstruct the transverse phase space topology (lower right). A clear signature of the presence of four islands is visible.

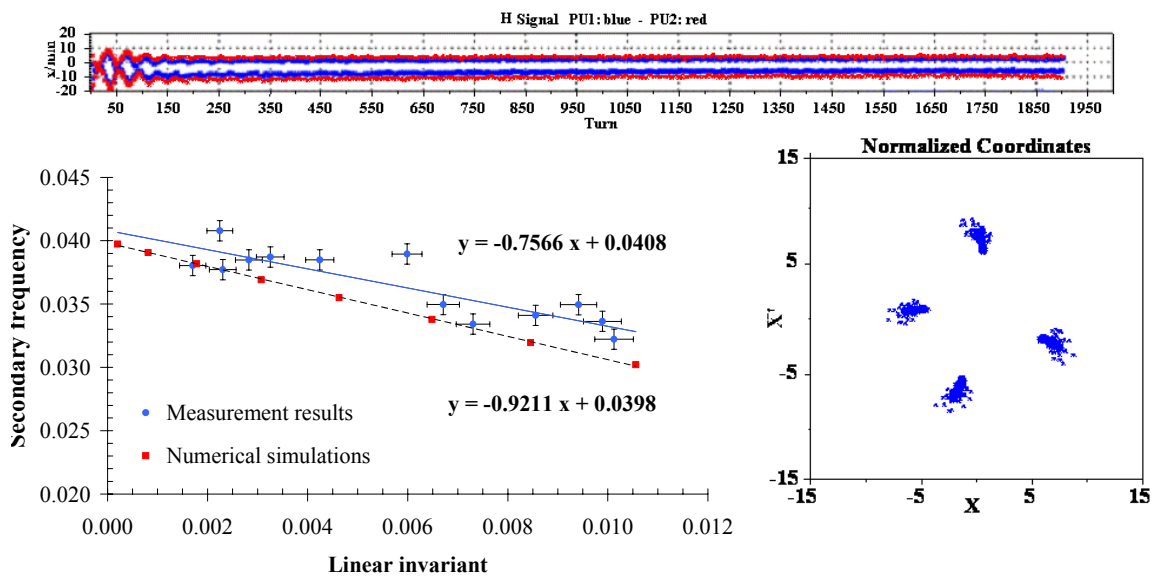


**Figure 12:** Results of the phase space measurements in presence of stable islands generated by means of sextupoles and octupoles. The beam position vs. the number of turn is shown in the upper part, while the reconstructed phase space is shown in the lower right part. The secondary frequency vs. the amplitude inside the island is shown in the lower left part.

2. Trapping measurement with a low-intensity beam. The key measurement, i.e. the verification of the splitting due to resonance crossing is usually performed first with a low-intensity, single-bunch beam. This has the advantage of suppressing any possible effect due to Coulomb interaction between the protons in the bunch. Furthermore, a special care is devoted at the level of the PS-Booster ring, the PS injector, when generating this special beam. In fact, as already mentioned, the larger the horizontal emittance of the initial beam, the more efficient the trapping is. Therefore, the beam is artificially blown-up in the horizontal plane, while keeping the vertical emittance as small as possible. Ideally, the horizontal emittance should have as much as possible a value similar to that of the high-intensity beam, while the vertical one should be similar to that of the pencil beam used for the phase space measurement. The first requirement allows reproducing conditions achieved

when operation with an intense beam, while the second one allows reducing the nonlinear horizontal/vertical coupling, thus facilitating the setting-up during the first attempts. During this stage of the measurements the key instrument is the wire scanner [22]. It allows recording the horizontal beam profile, thus showing the details of the splitting. Examples of profile measurements can be seen in Figs. 13, 14, 16, and 17. The raw data are fitted using five Gaussian distributions whose parameters, mean, sigma, integral, are assumed to reflect the properties of the beamlets.

3. Trapping measurement with a high-intensity beam. This represents the most important test for this novel approach. The best result achieved is shown in Fig. 13, where the intensity as a function of time is shown (left) together with the measured horizontal beam profile at the end of the capture process (right). The injected intensity is slightly above  $6 \times 10^{12}$  protons and small losses are visible up to transition crossing (second vertical red line). Then, the intensity stays remarkably constant up to extraction, which is performed by means of a kicker in a single turn after having merged back the beamlets in order to reduce the beam size in the horizontal plane to match the septum acceptance. In the right part of Fig. 13 the beam profile after the splitting is shown. A number of peaks are visible; in particular the central one features rather large tails. Indeed, the left tail is due to the projection of the beamlet behind (see Fig. 2, right). Another important point is that the left-most beamlet is very well separated and the region between it and the central core is depleted. This feature is crucial for having small or no losses at all at extraction, as it guarantees no interaction between the extraction septum blade and the beam.

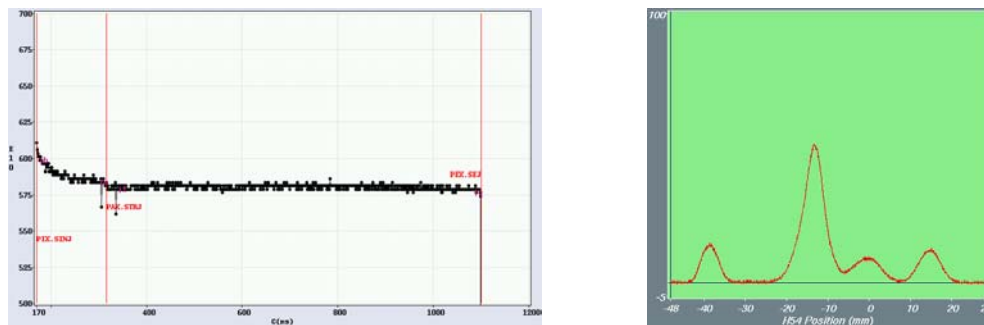


**Figure 13:** Best result achieved with a high-intensity beam, whose intensity as a function of time (left) and horizontal beam profile at the end of the capture process (right) is shown. The fact that the profile is not centred at zero is due to an instrumental offset of the wire position.

A final test was performed to increase the fraction of particles trapped inside the islands. For this study, a special setting of the octupoles was programmed: instead of keeping their strength constant all over the resonance-crossing phase, the current was suddenly increased just before resonance crossing and then gradually reduced. This should generate large islands at small amplitudes, thus trapping more particles from the region where the density is high, and then keeping almost constant the island's size. The

results are shown in Fig. 14, where the current as a function of time for both the sextupoles and the octupoles are shown (left) as well as the measured horizontal beam profile (right).

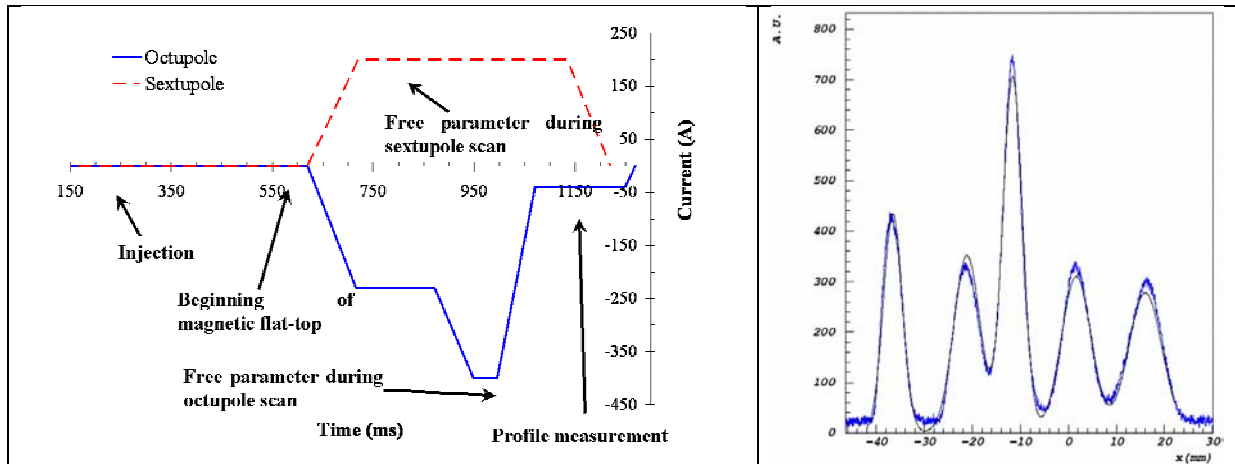


**Figure 14:** Current as a function of time for the sextupoles and octupoles as used in the special test to increase the fraction of particles trapped in the beamlets (left). The resulting horizontal beam profile after splitting is also shown (right). The fact that the profile is not centred at zero is due to an instrumental offset of the wire position.

Under these new conditions it was indeed possible to increase the fraction of particles inside the islands, achieving a value of 18% against a previous value of about 13%. It is worthwhile mentioning that for the optimal performance of the SPS machine, the allowed fraction of particles inside each beamlets is limited to  $(20 \pm 5) \%$ : if this holds for the central core the limit for the other beamlets is instead  $(20 \pm 1) \%$ . However, the price to pay was the presence of slightly higher losses during resonance crossing up to the level of 2-3% of the total beam intensity.

As a final result the beam distribution as measured in the transfer line downstream the extraction point from the PS machine is shown in Fig. 15. An Optical Transition Radiation (OTR) [23] is used to record the two-dimensional beam distribution in physical space.

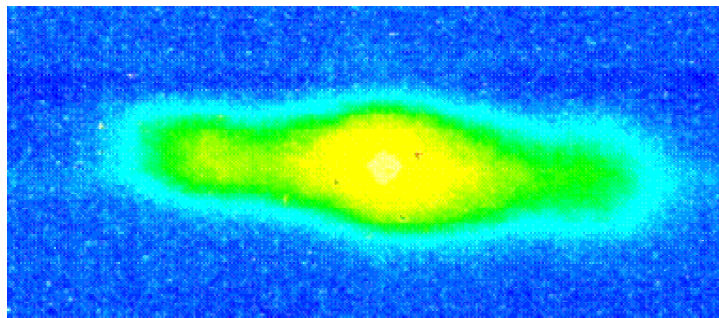


**Figure 15 :** Two-dimensional beam distribution in physical space of the split beam in the transfer line downstream of the PS extraction point.

The peculiar shape of the beam distribution is clearly visible: the two lateral peaks represent the projection in the physical space of the beamlets.

The main parameters of the single-bunch beams used in the experimental campaign are summarised in Table 1.

**Table 1:** Parameters of the three single-bunch beams used for the experimental tests of the novel multi-turn extraction. The emittance is the normalised, one sigma value.

Parameter	Intensity (protons/b)	$\varepsilon^*_H(\sigma)$ ( $\mu\text{m}$ )	$\varepsilon^*_V(\sigma)$ ( $\mu\text{m}$ )	$\Delta p/p(\sigma)$ $10^{-3}$
Low-intensity, pencil beam	$5 \times 10^{11}$	2.3	1.3	0.25
Low-intensity, large horizontal emittance	$5 \times 10^{11}$	6.2	1.6	0.25
High-intensity beam	$6 \times 10^{12}$	9.4	6.4	0.60

#### 3.4.3.2 *Special Measurements*

In addition to the measurements performed to establish the feasibility of the proposed method, a number of detailed measurements were performed to study the dependence of the beamlets parameters, such as fraction of captured particles, position, width, on the nonlinear parameters and, what is even more important, on the way the resonance is crossed. Although in the numerical simulations the influence of a polynomial dependence on the turn number of the linear tune was tested, in the real experiments only a linear tune variation was tested. However, the influence on the resonance crossing speed was assessed.

During such a test the resonance was crossed twice with the aim of bringing back the beamlets towards the centre core. In case the resonance crossing is slow enough, one could argue that it should be possible to end up in a state not too different from the initial one. The crossing speed was the same in both directions and after the first resonance crossing, the tune was kept constant for a period of 20 ms or 180 ms (see Fig. 16 upper part for a sketch of the measurement principle). The horizontal beam profile was measured at three different moments: before the first resonance crossing, after the first resonance crossing when the tune was constant and the beam split, after the second resonance crossing. The crossing speed is changed and the profiles for many values of the crossing speed recorded.

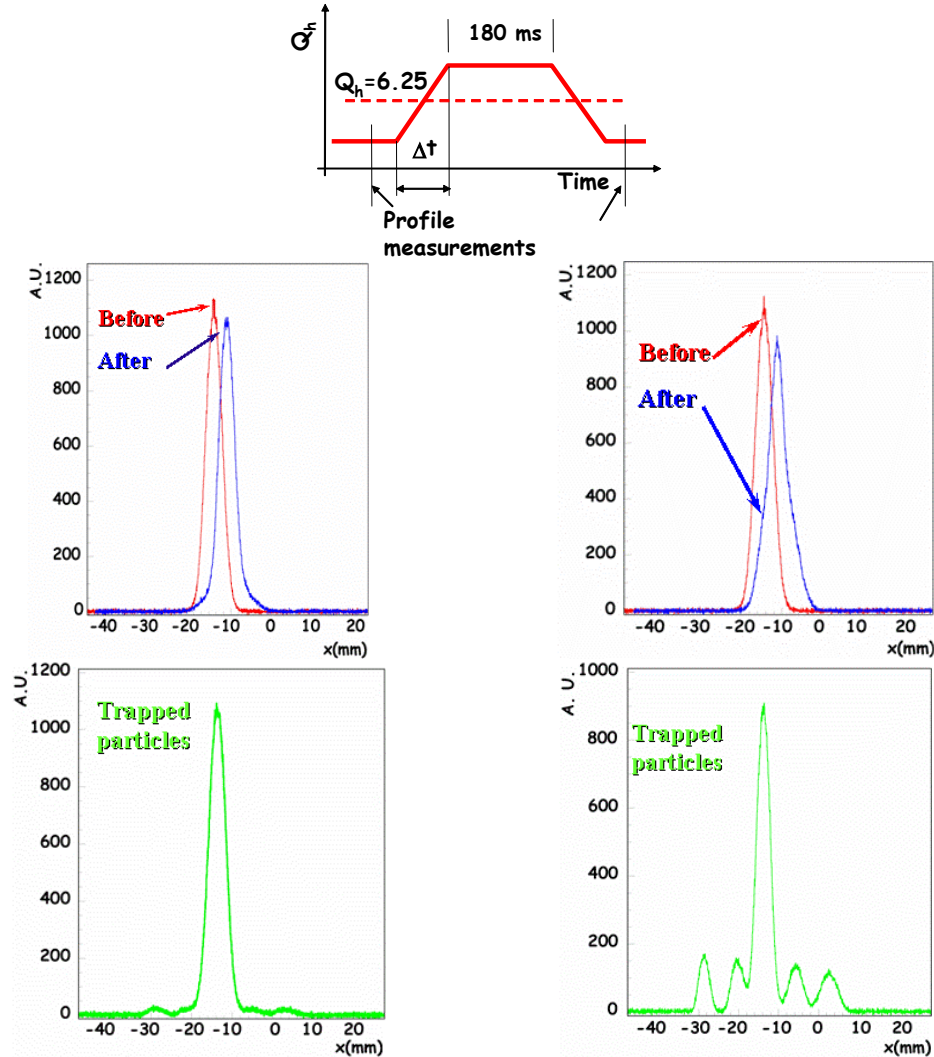


**Figure 16:** Results of the dependence of the beamlets parameters on the resonance crossing speed. The sketch of the measurement principle is shown in the upper part. The horizontal profiles for a fast crossing (5 ms) are shown in the left part, corresponding to the three moments, while the profiles on the right correspond to a slow crossing (90 ms). The fact that the profiles are not centred at zero is due to an instrumental offset of the wire position.

When a fast crossing occurs, almost no particles are trapped inside the moving islands and the final profile resembles very much the initial one. On the other hand, when a slow crossing occurs, many more particles are trapped inside the islands, but the final beam profile is no more Gaussian and differs from the initial one. The hypothesis is that the tails are generated by the beamlets when they are put back into the central core. As long as the crossing time is longer than 30-40 ms the fraction of particles trapped inside the beamlets stays constant and the final profile features non-Gaussian tails. The situation does not change quantitatively in case the period when the tune is kept constant is reduced drastically: the process seems to be always non-reversible.

The influence of the octupole strength on the number of particles captured in the islands is the last example of detailed measurement presented in this paper. The maximum negative current corresponding to the second plateau shown in Fig. 14 (left) is changed. The influence of the octupole is twofold: it changes the islands' size and it varies the detuning with amplitude, thus moving the islands' centres. In Fig. 17 the results are shown.

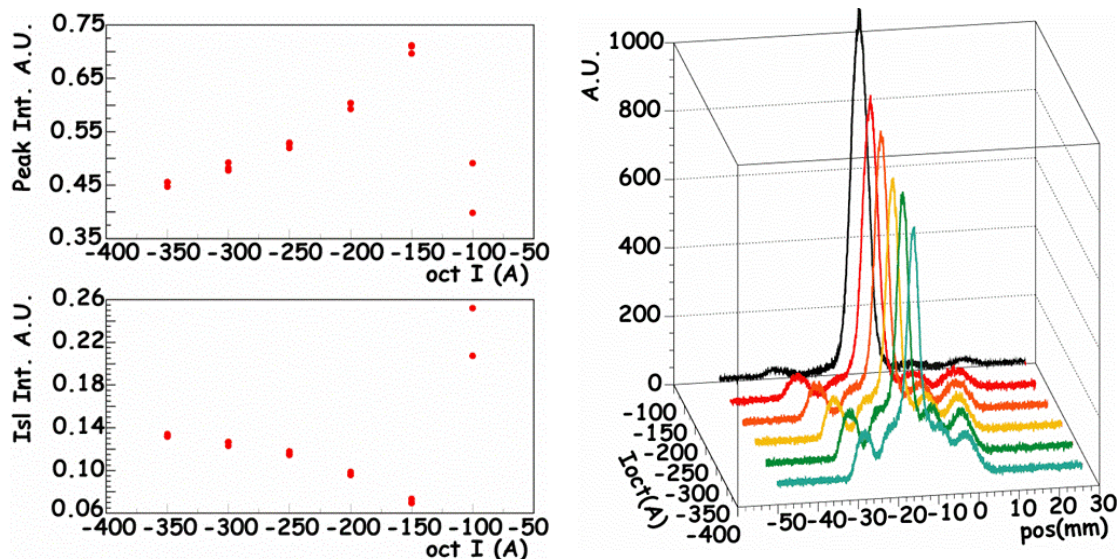


**Figure 17:** Results of the influence of the octupolar strength on the fraction of particles trapped in the beamlets (upper left) with respect to the intensity in the central core (lower left). A series of horizontal beam profiles measured for different values of the octupolar strength are also shown (right part).

The increase of the number of particles trapped when the strength of the octupole is reduced is clearly visible (upper left). At the same time, the fraction of particles remaining in the central core is reduced (lower left). Two points are clearly outliers: the fit procedure failed for those two cases because of the too low intensity captured in the islands. The horizontal beam profile measured at the end of the splitting process is shown in Fig. 17 (right). The impact of the octupole on the fraction of particles trapped, as well as on the position of the beamlets is clearly visible.

### 3.4.4 Towards an Operational Version of the Multi-Turn Extraction

The experimental campaign was completed by the end of the year 2004. During the long shutdown of the PS machine, which will be re-started in Spring 2006, the analysis of the required modifications to implement the proposed multi-turn extraction will take place. The main modifications to the PS ring will involve a new layout of the slow bump used to approach the beam to the extraction magnetic septum and a new fast, closed-bump around the extraction septum. As far as the fast closed-bump is concerned, it will be generated by means of kicker magnets, which will have to be built in the next years. A crucial issue is the available aperture, as the situation is particularly critical in the extraction region. Due to the very principle of the novel multi-turn extraction, once

the beam is split, there will be five beamlets circulating in the ring with different closed-orbits (see Fig. 18, where the trajectory for the four beamlets are shown).

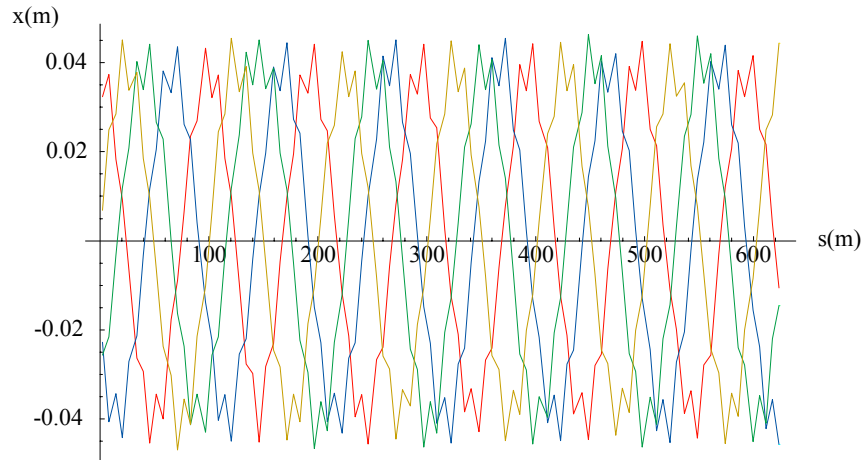


**Figure18 :** Closed-orbit for the four beamlets along the circumference of the PS machine. The closed-orbit of the central core is the origin of phase space.

The closed bumps, both the slow and the fast one, will affect differently the closed-orbits of the five beamlets and the aperture should be large enough to accommodate all beamlets simultaneously without losses.

A Study Group was set-up since 2003 [24] with the mandate to study both the theoretical, experimental, and implementation aspects of the proposed multi-turn extraction. The activity of the Study Group was prolonged in 2004 and the conclusions will be published in Spring 2005.

The details of the installation schedule are not known, yet. However, tests with beam will be resumed in 2006 to study how to reduce the losses observed during resonance crossing when the fraction of particles captured inside the beamlets is increased. By 2007 the new layout of the slow bump should be operational, while the fast bump should be installed and commissioned in 2008 at the latest. Therefore, the commissioning of the proposed multi-turn extraction will take place in 2008. During that year, it is foreseen to leave in operation the hardware related with the present CT extraction, to allow delivering beam to the CNGS experiments, while commissioning the novel multi-turn extraction. Finally, upon completion of this crucial stage, the CT will be decommissioned and the novel multi-turn extraction will be the only mean to deliver beam to the CNGS experiments.

### 3.4.5 References

1. R. Capi, M. Giovannozzi, "Studies of Multi-Turn Extraction at CERN-PS via particle trapping in Islands of phase space", Beam Dynamics Newsletter 25, September 2001.
2. A. Bazzani, G. Servizi, E. Todesco, G. Turchetti, "A normal form approach to the theory of nonlinear betatronic motion", CERN Yellow Report, 94-02, 1994.
3. R. Capi, M. Giovannozzi, "Multi-turn extraction and injection by means of adiabatic capture in stable islands of phase space", Phys. Rev. Spec. Top. Accel. Beams 7, 024001, 2003.

4. M. Giovannozzi, P. Scaramuzzi, "Nonlinear Dynamics Studies at the CERN Proton Synchrotron: Precise Measurements of Islands Parameters for the Novel Multi-Turn Extraction", proceedings 9th European Particle Accelerator Conference, Luzern, Switzerland, p. 1861, 2004.
5. K. Elsener (Ed.), *et al.*, "The CERN Neutrino Beam to Gran Sasso (Conceptual Technical Design)", CERN 98-02, 1998.
6. C. Bovet, D. Fiander, L. Henny, A. Krusche, G. Plass, "The Fast Shaving Ejection for Beam Transfer from the CPS to the CERN 300 GeV Machine", proceedings of the 1973 Particle Accelerator Conference, p.438, 1973.
7. R. Cappi, M. Giovannozzi, "Computation of betatron mismatch and emittance blow-up for multi-turn extraction", CERN-PS-2002-083-AE; December 2002.
8. R. Cappi, M. Giovannozzi, "Multiturn Extraction: Performance Analysis of Old and New Approaches", Nucl. Instrum. & Methods A 519, p. 442, 2004.
9. R. Cappi (Ed.), *et al.*, "Increasing proton intensity of PS and SPS", CERN-PS (AE) 2001-041, 2001.
10. R. Cappi, M. Giovannozzi, "Novel Method for Multi-turn Extraction: trapping charged Particles in Islands of Phase Space", Phys. Rev. Lett. 88, 104801, 2002.
11. R. Cappi, M. Giovannozzi, "Adiabatic Capture of Charged Particles in Islands of Phase Space: a New Method for Multiturn Extraction", proceedings 8th European Particle Accelerator Conference, Paris, France, p. 1250, 2002.
12. P. Scaramuzzi, "Studio di una nuova tecnica per estrarre fasci di particelle cariche da un acceleratore circolare usando risonanze stabili dello spazio delle fasi trasversale", Diploma Thesis University of Milan, November 2004.
13. R. Cappi, M. Giovannozzi, "Adiabatic Capture of Charged Particles in Stable Islands : A Novel Approach to Multi-Turn Extraction", proceedings 2003 Particle Accelerator Conference, Portland, Oregon, p. 2910, 2003.
14. M. Giovannozzi, J. Morel, "A Novel Technique for Multiturn Injection in a Circular Accelerator Using Stable Islands in Transverse Phase Space", in preparation.
15. R. Cappi, M. Giovannozzi, M. Martini, E. Métral, G. Métral, A. S. Müller, R. Steerenberg, "Adiabatic Beam Trapping in Stable Islands of Transverse Phase Space : Measurement Results at CERN Proton Synchrotron", proceedings 2003 Particle Accelerator Conference, Portland, Oregon, p. 388, 2003.
16. M. Giovannozzi, R. Cappi, S. Gilardoni, M. Martini, E. Métral, A. S. Müller, A. Sakumi, R. Steerenberg, "Multiturn Extraction Based on Trapping in Stable Islands at CERN PS: Recent Measurement Advances", proceedings 9th European Particle Accelerator Conference, Luzern, Switzerland, p. 173, 2004.
17. M. Giovannozzi, R. Cappi, S. Gilardoni, M. Martini, E. Métral, A. S. Müller, P. Scaramuzzi, R. Steerenberg, "Multiturn extraction based on trapping in stable islands", CERN-AB-2004-095; October 2004.
18. R. Cappi, S. Gilardoni, M. Giovannozzi, M. Martini, E. Métral, A. S. Müller, R. Steerenberg, "Final Results from the Novel Multi-Turn Extraction Studies at CERN Proton Synchrotron", in preparation.
19. M. E. Angoletta, A. S. Müller, "A multiturn measurement system for the CERN PS", proceedings of the 8th European Particle Accelerator Conference , Paris, France , p. 1948, 2002.
20. M. E. Angoletta, M. Giovannozzi, M. Martini, E. Métral, G. Métral, A. S. Müller, R. Steerenberg, "Analysis of Multi-Turn Beam Position Measurements in the CERN PS", proceedings of the 8th European Particle Accelerator Conference , Paris, France , p. 1273, 2002.
21. T. Satogata, *et al.*, "Driven Response of a Trapped Particle Beam", Phys. Rev. Lett. 68, 1838, 1992.
22. C. Steinbach, M. Van Rooij, "A Scanning Wire Beam Profile Monitor", IEEE Trans. Nucl. Sci. 32, p. 1920, 1985.

23. C. Bovet, R. Jung, “A New Diagnostic for Betatron Phase Space Matching at Injection into a Circular Accelerator”, LHC Project Report 3, June 1996.
24. M. Giovannozzi (Ed.), *et al.*, “Report of the Study Group on the New Multi-Turn Extraction in the PS Machine”, CERN-AB-2004-003-ABP; January 2004.

### 3.5 Beam Tests of a Stochastic Slow Extraction in the U70

S. Ivanov and O. Lebedev, IHEP–Protvino  
 mail to: [ivanov\\_s@mx.ihep.su](mailto:ivanov_s@mx.ihep.su)

#### 3.5.1 Introduction

During the recent (November–December, 2004) machine run of U70 (a 70 GeV proton synchrotron of IHEP, Protvino, Moscow Region) feasibility beam tests of an advanced, stochastic slow extraction (SSE) scheme were accomplished successfully.

S. van der Meer of CERN has pioneered the SSE concept in 1978, [1]. The underlying idea was to substitute a headway relative motion of entire beam towards a transverse extraction resonance (or vice versa) with a diffusive mechanism of beam transport. R. Cappi, W. Hardt and Ch. Steinbach next subjected this principle to a successful proof in the CERN PS machine where 9 s long good-quality spills of 24 GeV protons were demonstrated [2]. Subsequently, a very slow noise extraction of antiprotons from the LEAR storage ring was made operational, spill duration exceeding a few hours [3].

As is well understood since after, the SSE scheme enables to attain a two-fold goal of (i) yielding much a longer spill and (ii) ensuring far a better spill quality, i.e. getting a lower AC-to-DC ratio in snapshot of a spill. The SSE is less prone to adverse effect of unavoidable ripples in magnetic optics that deteriorate a spill. As such, it might turn topical for the ageing U70 machine.

#### 3.5.2 Specifics of the scheme

The SSE at U70 is far from being a one-to-one clone of the initially proposed scheme [1] and its implementation in [2, 3].

Conventionally, the SSE scheme is applied to a coasting, azimuthally uniform beam that has a trivial appearance of longitudinal phase-plane trajectories. On the contrary, due to technical constraints inherent in U70, the waiting beam there is neither bunched nor azimuthally uniform. Prior to ejection, it circulates in a close outer and highly non-linear vicinity of empty 200 MHz RF buckets imposed by an auxiliary (dilution) cavity. This very cavity is also employed as an actuator to inject a controlled base-band low-pass phase noise around the non-random 200 MHz carrier ever present.

Schematic picture of extraction is sketched with a Steinbach diagram (see Fig. 1). To a great extent, it is self-explanatory. Core 7–9 of the beam to be ejected is debunched from 6 MHz (the main RF) in the lower half-plane ( $\varphi$ ,  $(p-p_0)/p_0$ ), below the lower branch 6 of an empty RF bucket 2–6. A spacer layer 6–7 is left to preclude a premature extraction and allow for a room to accommodate a thin wedge-like tail of beam distribution towards a sink 6 during extraction. Momentum image of operating stop-band 3–4 of horizontal extraction resonance  $3Q_x = 29$  is wholly overlapped with the upper half-bucket 2–5.

Essentially, one would recognize in Fig. 1 a steady-state extraction of  $2\pi$ -long 200 MHz bunches that are continuously re-filled by one-way diffusion from the outer beam stack 7–9. This technique to feed the resonance looks a lot like a reversed halation process in a bunched beam (stack in a coasting halo region, diffusion proceeding towards a reference particle 5).

Terminal route 6–4 of a journey towards resonance ends up via conventional synchrotron oscillations. These are very fast as compared to diffusion transport. Local velocity of entering the resonance is therefore increased noticeably. It gets commensurable to impact velocity under a phase displacement technique occasionally used for extraction with a beam being squeezed through gaps between buckets. The RF buckets themselves constitute a trap around extraction resonance that heavily (and favorably so) mixes protons prior to ejection. The entire region 2–6 of longitudinal phase-plane that is strongly affected with a non-random component of the 200 MHz voltage is fully engaged in servicing the extraction.

More beam dynamics details and calculations on this subject can be found in [4].

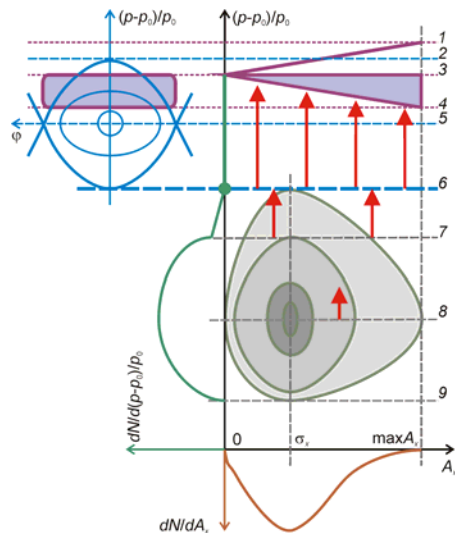


**Figure 1:** Steinbach diagram of SSE from U70 where 2–6 is an empty RF bucket with a reference particle 5; 3–4 is an image of extraction stop-band; 6–9 is waiting beam stack kept around a lower orbit 8 and having a thin noise-diluted tail 6–7.

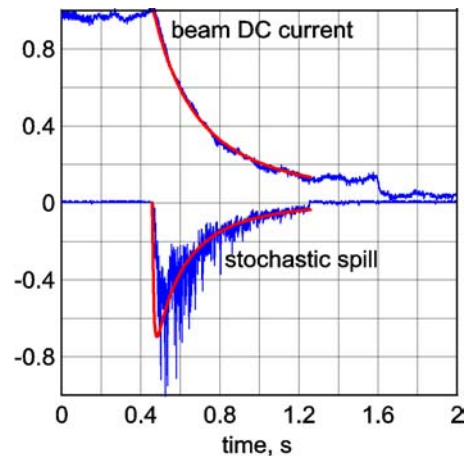


**Figure 2:** Recorded (ragged rays) and calculated (smooth line) snapshot of a stochastic spill from U70 under a time-invariant noise power spectrum.

### 3.5.3 Beam observations

Beam observations were performed on a 60 GeV ejection plateau of U70. All the magnetic optics was fed in a sustained regime with DC currents. Fractional momentum spread of beam  $\Delta p/p_0 = \pm 1 \cdot 10^{-3}$  at base. Horizontal chromaticity ( $dQ_x/d(p-p_0)/p_0$ ) is set equal to  $-15$ . Amplitude of RF 200 MHz is 480 kV. A flat low-pass spectrum of phase noise extends from DC to  $\pm 4.2$  kHz (at  $-3$  dB level). For the time being, only non-flat natural stochastic spills, imposed by noises with spectra invariant through time of spill,

were recorded. A typical level of noise at beam is estimated as  $P_0 = 10^{-5}$  rad<sup>2</sup>/Hz, and less. Ragged (blue) oscillograms in Fig. 2 show a sample of recorded stochastic spill from U70. Smooth (red) curves in Fig. 2 plot the relevant calculated signals [4] fitted to observations. About 88% of beam is extracted in 0.8 s. Time of spill was found to be readily extendable to 1.9 s. It was a top time allowed for by existing power supplies feeding the sextupole lenses which drive the extraction resonance  $3Q_x = 29$ . Spectrum of AC ripple is free of the mains harmonic interferences altogether. This ripple appears due to persistent interferences in magnetic optics and, supposedly, due to leakage of (a rather excessive) operational noise through a beam-transfer function. No measures to settle the spill ripple with feedbacks were taken until now.

### 3.5.4 Further prospects

The design goal [4] is to get flat-topped spills lasting for 2–3 s and longer so as to make a full profit on generic advantages of the SSE. Flattening spill patterns will be forced via a proper ramping of noise power  $P_0$  during extraction, its cut-off frequency being kept intact.

Feasibility of SSE from U70 in line with [4] is now confirmed with beam observations. This scheme promises yielding smoother and longer spills, which would hopefully upgrade functionality of the machine.

### 3.5.5 References

1. S. van der Meer, “Stochastic Extraction, a Low-Ripple Version of Resonant Extraction”, CERN/PS/AA Note 78–6, Geneva, March 1978.
2. R. Cappi, W. Hardt, and Ch. Steinbach, “Ultraslow Extraction with Good Quality Factor”, in Proc. of 11th Int. Conf. on High Energy Accelerators, Geneva, July 1980, pp. 335–340.
3. G. Molinari and H. Mulder, “The Improved Ultra Slow Extraction Noise System at LEAR”, in Proc. of the 4th EPAC–94, London, July 1994, vol. 3, pp. 2376–2378.
4. S. Ivanov and O. Lebedev “A Feasibility Study for Stochastic Slow Extraction of Beam from U70 Synchrotron”, Preprint IHEP 2004–22, Protvino, May 2004; also “A Stochastic Slow Extraction Scheme for U70 Synchrotron”, Report THUPCII06 to RUPAC-2004, Dubna, October 2004.

## 3.6 IDRA: design study of a protontherapy facility

Riccardo Zennaro, [TERA Foundation](#)  
mail to: [Riccardo.Zennaro@cern.ch](mailto:Riccardo.Zennaro@cern.ch)

### 3.6.1 Introduction

Hadron therapy is an emerging radiotherapy technique that has developed worldwide in the last 10 years, but its origins are in 1946, when Robert Wilson [1] remarked that the narrow Bragg peak, which characterises the energy loss of a mono-energetic proton beam or other ions in matter, could allow a very accurate dose delivery to a target. A comparison between protons and X rays, which are largely used in conventional radiotherapy, shows the evident advantages offered by protons in terms of dose distribution accuracy; see Figure 1.

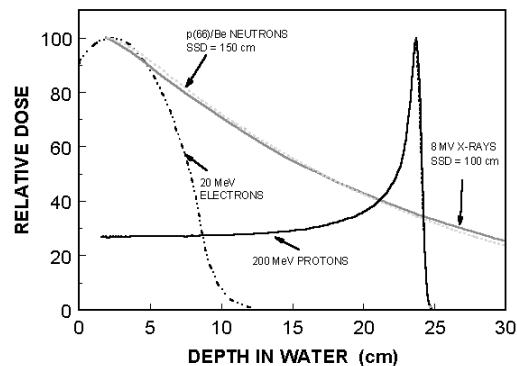


**Figure 1:** Comparison between photons and protons in water.

Since the depth of the peak inside a target is related to the energy of the beam, it is possible to irradiate thick cancer targets by superposition of different Bragg peaks; this is the so-called *spread out Bragg peak* (SOBP) technique, obtained by reducing progressively the beam energy; see Figure 2. This dose distribution is much more indicated for therapy than the one of X rays, which presents a roughly exponential absorption in matter.

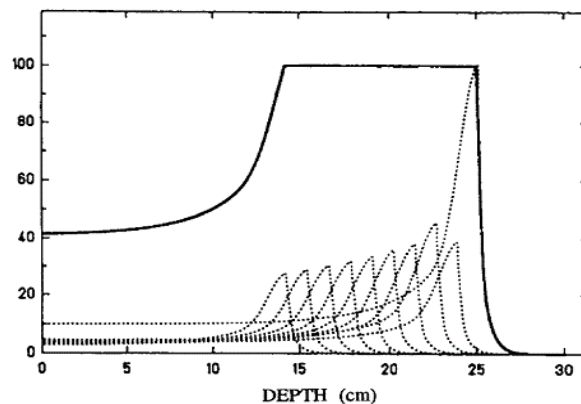


**Figure 2:** SOBP composed of doses delivered at different energies (dotted Lines).

At the end of 2004 about 40000 patients were treated with protons and more than 2000 with carbon ions [2]. Protons have practically the same biological effects as photons but a much better dose conformation. Carbon ions present even a larger *Radiobiological Effectiveness* (RBE) and are better suited in the case of radio resistant tumours that cannot be treated successfully with neither X rays nor protons [3].

Today there are *three* dedicated hospital-based centres for deep protontherapy in the United States, *four* in Japan and *one* in China opened at the end of 2004. Two of the four Japanese centres can also treat patients with carbon ions. Several other hospital-based centres for protons are under construction in United States, Germany, China and South Korea. In 2007, two European centres both for protons and carbon ions will start to treat the first patients. The first, designed by GSI, will be in Heidelberg (Germany), the second is the CNAO (in Italian: “Centro Nazionale di Adroterapia Oncologica”),

whose ground-braking ceremony took place on March 5, 2005, in Pavia (Italy). The “spiritus movens” for the CNAO was the Italian Foundation TERA (<http://www.tera.it>), active since 1992 in promoting the use of hadrons for therapy.

Since the beginning, TERA has developed in parallel with the CNAO, a programme of compact proton accelerators [4]. A particular effort has been dedicated to the study of a high frequency proton linac.

In fact, as a result of the requirements of compactness of the linac and due to the very low beam current for the therapy, a high frequency is a natural choice. Of course a high frequency implies a small beam iris, but this is not a problem since the current needed for protontherapy is of only few nanoamperes.

In 1994, the design of a 3GHz *side coupled linac* (SCL)[4] was proposed in the framework of studies of compact accelerators. The SCL was the terminating part of a chain of linear accelerators. In [4] it was also presented the “booster option”, namely an SCL used to boost the energy of a beam pre-accelerated by a cyclotron; thus the name LIBO (LInac BOoster). The combination of a cyclotron and LIBO has later been called *Cyclinac* (CYClotron plus LINAC) and it has become the heart of IDRA, a complete medical facility.

### 3.6.2 IDRA

#### 3.6.2.1 IDRA overview

IDRA (in Italian: “Istituto per la Diagnostica e la Radioterapia Avanzate”) is a multipurpose facility for the production of radiopharmaceuticals for diagnostic and therapy, and high-energy protons for the radiotherapy of superficial and deep-seated tumours; see Figure 3.

The heart of IDRA is a proton Cyclinac, i.e. the combination of a high current 30 MeV commercial cyclotron and a linear accelerator that boosts the proton beam produced by the cyclotron up to 210 MeV for the treatment of deep-seated tumours (the Bragg peak of a 210 MeV proton beam is at a depth of about 30 cm in water).

The large current of the cyclotron is used to produce radiopharmaceuticals that are employed for several diagnostic purposes, for instance:  $^{18}\text{F}$  fluorine-D-glucose (FDG) is used for diagnostics combined with *Positron Emission Tomography* (PET).

The large current beam can also be used for epithermal neutron production for *Boron Neutron Capture Therapy* (BNCT) for the treatment of brain glioblastomas, of melanoma of the skin and for *Boron Neutron Capture Synovectomy* (BNCS), a promising treatment technique for rheumatoid arthritis.

One of the multiple beam lines of the cyclotron is dedicated to inject the beam into LIBO-30, which provides a further acceleration of a small portion of the beam up to the energy required for proton therapy.

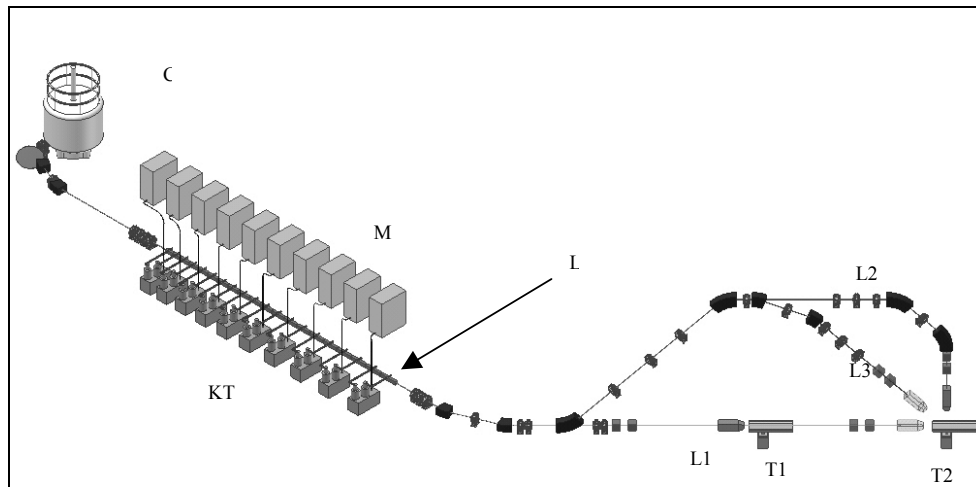


**Figure 3:** 3D-view of IDRA; the beam extracted from the cyclotron (C) is injected into LIBO-30 (L) and, post-accelerated, three extraction lines (L1, L2, L3) distribute it to two treatment rooms (T1, T2). On top of the linac, but in a different gallery, 10 solid-state modulators designed by TERA (M) feed 10 double klystron high voltage oil tanks (KT); the RF power generated by the 20 klystrons is then delivered to the 20 modules of LIBO-30 (L) via wave-guides.

### 3.6.2.2 LIBO: the LInac BOster

The idea of LIBO goes back to 1993, when compact medical proton linear accelerators were studied [4, chapter 9].

In this design, a 200 MeV SCL was the last part of a linear structure consisting of *radio frequency quadrupole* (RFQ), followed by a novel structure called *side coupled drift tube linac*, (SCDTL) (L.Picardi et al, patented by ENEA, [5]), and hence terminated with the SCL [6] working at 3 GHz. Such a high frequency is unusual for protons but is largely used in hospitals by thousands of commercial electron linacs for conventional radiotherapy. Therefore the choice of the 3 GHz implies not only compactness of the linac but has also a wide market of klystrons.

The initial idea of LIBO was based on a 30 MeV cyclotron followed by a linac, to boost the low energy beam to 200 MeV or more [6].

After a LIBO design was based on the characteristics of the 62 MeV cyclotron of the Clatterbridge centre for oncology in UK [7]. The SCL, composed of nine modules, was called, for this reason, LIBO-62.

In 1998 in the framework of a scientific collaboration between TERA Foundation, CERN, INFN and the University of Milan, INFN and the University of Naples, it was decided to build and test a prototype corresponding to the first module of LIBO-62 [8]. The prototype (see Figure 4) was built in CERN [9]. In 2000 it was power tested in the LIL gallery [10]. The tests were really successful and the prototype could reach an accelerating gradient of 28.5 MV/m, much larger than the designed one, 15.8 MV/m.

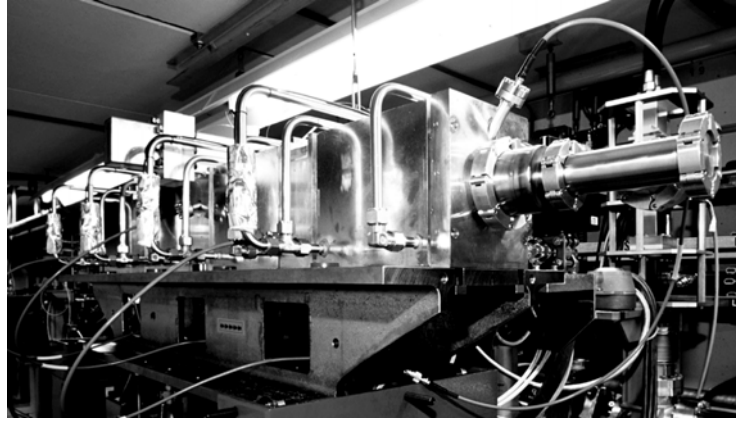


**Figure 4:** The LIBO prototype.

In 2001, the prototype was installed in the INFN Laboratorio nazionale del Sud (LNS) to be tested with a proton beam generated by the CS cyclotron. The results of the acceleration tests were in accordance with the predictions [11, 8].

Meanwhile, a new design of LIBO, going back to an energy of only 30 MeV, has been developed. This gives the possibility to use a higher number of commercial cyclotrons, which can also produce a large beam current, necessary for radioisotopes production.

In the present design, LIBO-30 is a modular side-coupled linear accelerator (SCL) composed of 20 modules. Each module is composed of two accelerating sections denominated “tanks”, which are connected via an RF bridge, which houses also a permanent magnetic quadrupole. An additional permanent magnetic quadrupole is installed at the output of each module, forming thus a FODO lattice. Each tank is composed of 14 accelerating cells that provide the beam acceleration and 13 coupling cells that provide the correct power flow through the module. The shape of the cells and the RF parameters were determined with Superfish. The effective shunt impedance ( $ZT^2$ ) varies from a minimum of 22 M $\Omega$ /m in the first module to the maximum of 67 M $\Omega$ /m in the last one. Computations show also that the value of  $ZT^2$  is roughly proportional to the length of the relative module; this is valid especially in the central and last part of the linac. This behaviour permits to inject the same power in the 20 modules with only minor variations of the axial electric field  $E_z$  that increases from 16.7 MV/m in the first module up to 19.0 MV/m from the eleventh module to the end. Thanks to the large accelerating field, LIBO-30 is only 16.4 m long with an effective gradient of almost 11 MV/m.

The relative low value of the synchronous phase ( $-15^\circ$ ) goes in the direction to minimize the total length and to reduce the defocusing effects of the RF field. The drawback is the low acceptance in phase; in our case this does not represent a problem due to the low current required for the therapy. The normalized beam acceptance is:

$$A_n = \pi\beta\gamma R^2/\beta^+ = 3.5 \pi \text{ mm mrad}$$

where  $R$  is beam hole radius (4 mm),  $\beta^+$  is the largest of the two transverse Twiss parameters in the middle of the first PMQ (1.15 m), and  $\beta\gamma$  the relativistic factor at the injection (0.255).

Figure 5 shows the first module, which is under construction.

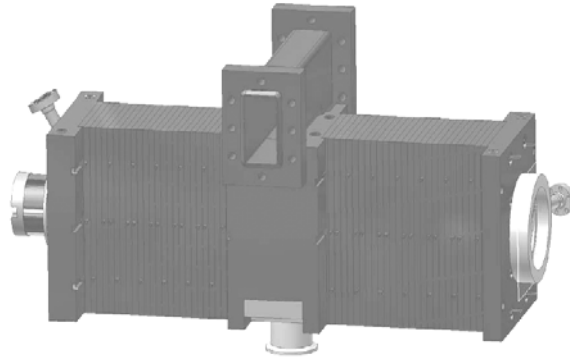


**Figure 5:** The first module of LIBO-30; the wave-guide brazed on top of the central bridge-coupler feeds the two tanks.

The main parameters of the linac are presented in table 1.

**Table 1:** Main LIBO-30 parameters

Frequency:	2998 MHz
Beam energy range:	30-210 MeV
Number of modules:	20
Accelerating electric field on axis:	16.7-19.0 MV/m
Average accelerating gradient:	10.9 MV/m
Synchronous phase:	-15°
Total length:	16.39 m
Total peak power in the linac:	60.8 MW
Effective shunt impedance ( $ZT^2$ ):	22-67 MΩ/m
Pulse length:	5 μs
Repetition rate:	200 Hz
Duty cycle:	0.1%
Total average power in the linac:	60.8 kW
Number of accelerating cells per tank:	14
Number of PMQs:	41
PMQ gradient:	170-130 T/m
Number of klystrons:	20
Number of modulators:	10
Beam hole radius:	4 mm
Maximum required average beam current:	5 nA
Transverse normalized beam acceptance:	3.5 π mm mrad
Transverse geometrical beam acceptance:	13.7 π mm mrad
Trapped beam in the longitudinal plane:	10.2%

### 3.6.2.3 Beam energy modulation

One of the main characteristics of LIBO is the possibility of varying continuously the energy of the accelerated beam in order to irradiate tumors at different depths. For this reason, the 20 modules are fed individually by a dedicated klystron, of which the

RF power amplitude and phase can be independently adjusted. By switching off one or more klystrons and by varying the amplitude or phase of the RF power in the last module switched on, the beam energy is adjusted to the required value.

The energy can be varied continuously in the range 120 – 210 MeV. It is also possible to extract a 66 MeV beam, obtained with only the first 6 klystrons switched on, for eye melanoma treatment.

The two solutions to vary the beam energy by adjusting the RF amplitude or phase in the klystron have been studied and compared; each solution has some advantages and drawbacks. The modulation of the phase of a klystron is easy and fast, by acting on the low-level phase circuits of the RF driver. The drawback is the increase in the beam energy spread. On the contrary, the change of the RF power amplitude results in a smaller increase in the beam energy spread but it moves the operation of the klystron out of the saturation region, which may give rise to power instabilities. To avoid this problem, the RF amplitude modulation should be provided by varying the klystron voltage, but this is more complicated and requires frequent changes of the modulator and klystron operational settings.

Radiotherapy for delimited tumours requires a distal fall-off of the dose limited to 2mm [12]. The range  $R$  in tissue at beam energies  $E$  which interest us is given by the approximate formula [13]:

$$R = 0.00176 \left( \frac{E}{\text{MeV}} \right)^{1.82} \quad [\text{cm, in water}].$$

Consequently, the distal fall-off  $\Delta R$  due to energy-spread  $\Delta E$  is given by the equation:

$$\frac{\Delta R}{R} = 1.82 \frac{\Delta E}{E}$$

Figure 6 compares the energy spread resulting from using the amplitude and phase variation techniques in the entire range 120-210 MeV; both cases, however, satisfy the requirement of a distal dose fall off of 2 mm.

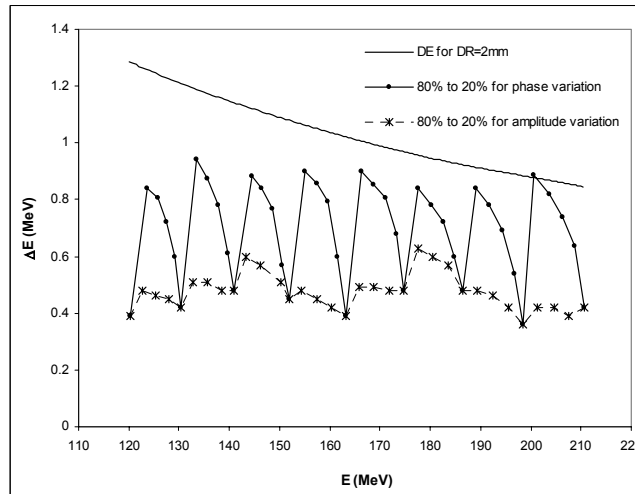


**Figure 6:** Energy spread due to phase modulation and amplitude modulation. The energy spread is defined considering the distribution in energy of the accelerated beam and by keeping the distance in energy between 80% to 20% of the beam in such distribution.

### 3.6.2.4 LIBO-30 transverse beam optics

The possibility to continuously vary continuously the energy of the accelerated beam has serious constraints on the design of the transverse optics. In particular, the requirement to extract a beam of only 66 MeV needed a careful study.

A solution based on a dedicated 66 MeV beam line after the sixth module has not been considered. This design would require an additional space between the sixth and the seventh module to install a switching dipole, thus causing important debunching effects on the beam to be accelerated in the higher energy modules. Therefore it has been decided to transport also the partially accelerated beam for eye melanoma therapy along the whole structure, but with modules 7-20 switched off. The use of permanent quadrupole magnets does not make it possible to adjust the FODO optics as a function of the variable rigidity of the beam. The gradients of the 41 permanent quadrupoles had to be therefore chosen so as to adequately transport both the 66 MeV and the 210 MeV beam.

The choice of the transverse betatron phase advance per focusing period,  $\sigma_t$ , determines the transverse acceptance of the linac; it is known that  $\sigma_t=76.3^\circ$  is the condition to maximize the acceptance [14].

Since the geometrical emittance decreases with  $\beta\gamma$ , it is possible to diminish significantly the phase advance  $\sigma_t$ , by keeping constant, or only slightly reducing, the maximum beam dimensions in both transverse planes along the linac; see plot 1 of Figure 7.

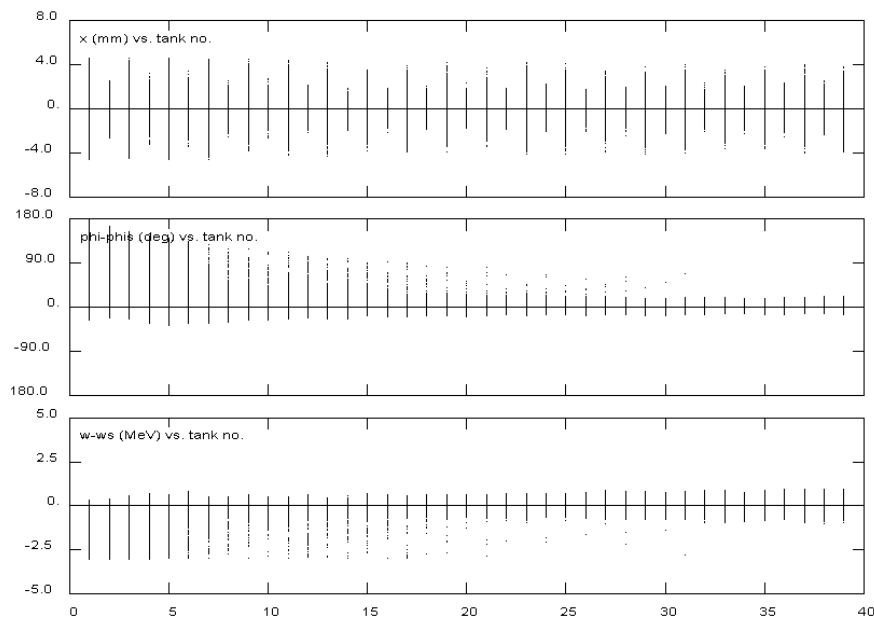


**Figure 7:** The beam evaluated in the middle of the PMQs in the case of full acceleration to 210 MeV. From top to bottom: beam transverse beam profile, phase width and energy spread along the linac.

This solution, based on a large variation of  $\sigma_t$ , gives the largest acceptance, avoids losses of the fully accelerated beam and allows the transport of the 66 MeV beam through the whole linac, thanks to the relatively low gradients of the quadrupoles in the

central and terminating part of the linac. To satisfy this condition, it has been decided to start with  $\sigma_r=74^\circ$  at the injection, to have a large acceptance, and gradually reduce it to only  $44^\circ$  for the 210 MeV beam at the extraction; see Figure 8.

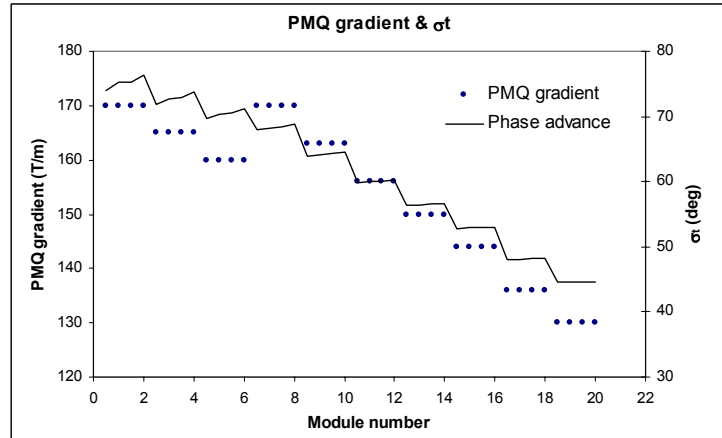


**Figure 8:** PMQ gradient and transverse phase advance per focusing period.

### 3.6.2.5 Beam injection in LIBO and multi-particle computations

The multi-particle computations have been done with LINAC [15]; no space-charge effects have been considered since the current during the pulse is of the order of few microamperes.

The input beam has been considered as continuous, since the RF frequency of the cyclotron, which is normally of the order of 30-70 MHz, is much lower than the LIBO frequency, 3 GHz, and completely uncorrelated. The use of a buncher has not been considered mainly for three reasons. The first is compactness; a buncher requires a certain drift to have an effect. The second is the relatively high energy of the input beam; at 30 MeV a buncher is not very efficient. The third reason is the absence of a real need to bunch the beam since the required beam current for the treatment is of only few nanoamperes and a commercial 30 MeV cyclotron can provide a large current (hundreds of microamperes).

To reduce beam losses and radiation damage in LIBO, the cyclotron source has to be pulsed at the linac repetition rate (200Hz), with a pulse duration just exceeding the linac pulse (5  $\mu$ s).

For safety reasons, a chopper in the injection line prevents the injection of the beam in the LIBO gallery when it is not required.

For all these reasons, beam losses do not represent a major problem in terms of activation due to the low current injected in the linac.

With a synchronous phase of  $-15^\circ$ , the trapped beam in the stationary bucket is roughly 11%. Plot 2 and plot 3 of Figure 7 show the effects of the longitudinal capture.

The beam that is not captured in the stationary bucket is mainly lost along the linac; see Figure 9; only a small portion is extracted at a much lower energy.

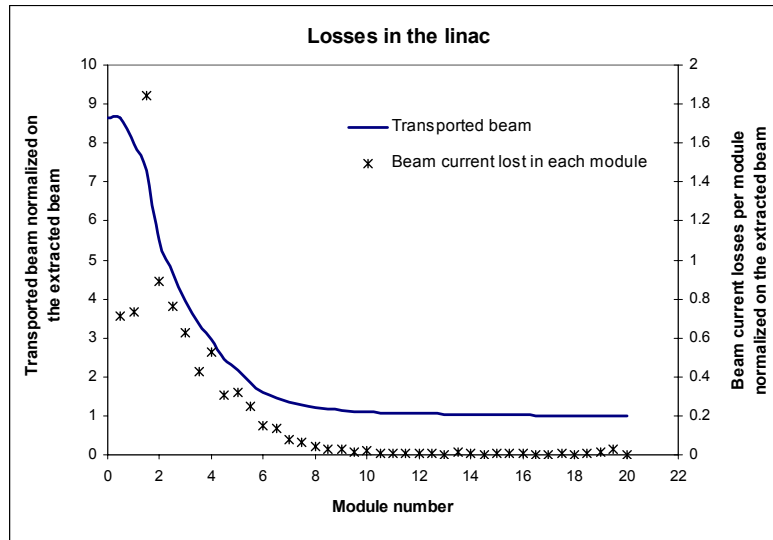


**Figure 9:** The beam losses in LIBO for the case of full acceleration to 210 MeV. For the 66 MeV beam the results are identical.

Computations based on LINAC show that in the case of the 210 MeV beam, only 6.7% of the extracted beam is not fully accelerated and 90% of this beam has an energy lower than 100 MeV; see Figure 10. In the case of the 66 MeV beam, the situation is even better and the extracted beam can be considered completely accelerated. The worst case is the 120 MeV beam; 7.3% of the extracted beam is not fully accelerated, of this 90% has an energy lower than 96 MeV; see Figure 10.

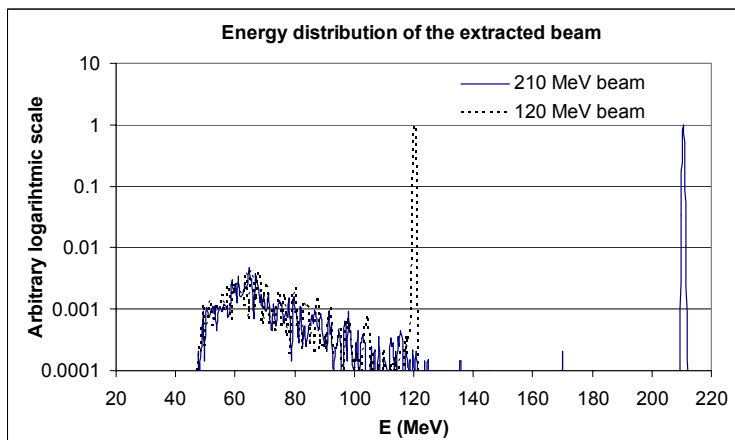


**Figure 10:** Energy distribution of the extracted beam in logarithmic scale.

However, the large difference in energy makes it very easy to select the good beam by using a chromatic system placed downstream of LIBO in the common part of the extraction lines.

LIBO-30 transverse normalized beam acceptance is  $3.5 \pi$  mm mrad (see table 1) which is somewhat smaller than the emittances of commercial 30 MeV cyclotrons. To avoid further losses in the linac, the beam is appropriately collimated and four quadrupoles allow matching into LIBO-30.

### 3.6.3 Acknowledgment

The author would like to express his sincere appreciation to the TERA group and all the members of the LIBO collaboration.

The origin of the work presented in this paper, is the construction of the LIBO prototype, which was possible because of the contribution of Carlo De Martinis (University and INFN of Milan), Vittorio Vaccaro (University and INFN of Naples) and their colleagues. CERN, and especially the PS and ETT divisions, gave fundamental technical support for the construction of the prototype and for the power test. In particular, Maurizio Vretenar, Balazs Szeless and Ettore Rosso played key roles in the production of the prototype.

A particular thank-you goes to the Chairman of TERA Foundation, Ugo Amaldi, who was the initiator of all our activities, concerning hadrontherapy, stimulating the work of his colleagues and especially encouraging new ideas.

It must be remarked that the successful results of the prototype, and the development of LIBO, from the beginning to the present design, would not have been possible without the expertise of Mario Weiss, TERA, who was the project leader of the LIBO prototype. To him goes my sincere gratitude also for reading and commenting on the manuscript.

I am very grateful to the Monzino Foundation (Milan) for the continuous and generous support given to TERA activities.

### 3.6.4 References

1. R.R. Wilson, *Radiology* 47 (1946) 487.
2. PTCOG, number 35, January 2005 pp. 11.
3. G. Kraft, *Strahlenther. Onkol.* 166 (1990) 10; G. Kraft, *Prog. Part. Nucl. Phys.* 45 (2000) 473.
4. U. Amaldi, M. Grandolfo, L. Picardi (Editors) *The RITA network and the design of compact proton accelerators*, INFN-Laboratori Nazionali di Frascati, 1996.
5. L. Picardi, *Eur. Phys. J. AP* 20, 61-68 (2002).
6. U. Amaldi, B. Larsson (Editors) *Hadrontherapy in oncology*, Proceedings of the First International Symposium on Hadrontherapy, Como October 1993, pp.53-58.
7. A. Clarke, et al., *Assessing the suitability of a medical cyclotron as an injector for an energy upgrade*, Proceedings of the European Particle Acceleration Conference on EPAC, Stockholm, 1998, pp. 2374-2376.
8. U. Amaldi et al. / *Nuclear Instrumentation and Methods in Physics Research A* 521 (2004) 512-529.
9. P. Berra et al., *Study, construction and test of a 3 GHz proton linac-booster (LIBO) for cancer therapy*, Proceeding of the European Particle Acceleration Conference on EPAC, Wien, 2000, pp. 2495-2497.
10. B. Szeless, et al., *Successful high power test of a proton linac booster (LIBO) prototype for hadrontherapy*, Proceedings of the Particle Acceleration Conference on PAC, Chicago, 2001, pp.624-644.
11. C. De Martinis, et al., *Beam tests on a proton linac booster for hadrontherapy*, Proceedings of the European Particle Acceleration Conference on EPAC, Paris, 2002, pp. 2727-2729.
12. U. Amaldi and M. Silari (editors), *The Tera Project and the Centre for the Oncological Hadrontherapy*, second edition (1995), Vol.2, pp. 278.
13. U. Amaldi, personal communication.
14. K. L. Brown, *First and second order charged particle optics*, SLAC-PUB-3381, July 1984.
15. LINAC, multi-particles code developed by K. R. Crandall (USA).

## 4 Activity Reports

### 4.1 The RAL Front End Test Stand

M A Clarke-Gayther<sup>a</sup>, D C Faircloth<sup>a</sup>, D J S Findlay<sup>a</sup>, F Gerigk<sup>a</sup>, P F Harrison<sup>b</sup>,  
 A P Letchford<sup>a</sup>, K R Long<sup>c</sup>

<sup>a</sup> ISIS Accelerator Division, Rutherford Appleton Laboratory, Oxon. OX11 0QX, UK

<sup>b</sup> Department of Physics, University of Warwick, Coventry, CV4 7AL, UK

<sup>c</sup> Department of Physics, Imperial College, London, SW7 2BW, UK

mail to: [A.Letchford@rl.ac.uk](mailto:A.Letchford@rl.ac.uk),

#### 4.1.1 Introduction

High power proton accelerators (HPPAs), which is to say those with beam powers in the megawatt range, have many possible applications including drivers for spallation neutron sources, neutrino factories, waste transmuters, energy amplifiers and tritium production facilities. These applications typically propose beam powers of 5 MW or more compared to the highest beam powers achieved from proton accelerators in routine operation of 0.16 MW and 0.75 MW, for the pulsed ISIS machine at RAL [1] and the CW SINQ machine at PSI [2] respectively. Therefore, in the case of pulsed machines, an increase in beam power by a factor of  $\sim 30$  is envisaged. This factor is far from trivial to achieve even though beam power of  $\sim 1$  MW is scheduled to become available in the next few years at SNS [3] and J-PARC [4].

It is generally accepted that the quality of the beam through the accelerator facility can be strongly influenced by the beam quality at the very beginning or front end of the linac. Some idea of the required quality can be gained by noting that the informal universal standard for unplanned beam loss along a proton accelerator is  $1 \text{ Wm}^{-1}$  if reasonably practical maintenance is to be possible. Since even for a 1 MW beam this represents a fractional loss of 1 part in  $10^6$  per metre, it is clear that high quality beams are essential.

In order to contribute to the development of HPPAs, a front-end test stand is being constructed at the Rutherford Appleton Laboratory (RAL) in the UK in collaboration between RAL, Imperial College London and the University of Warwick. The aim of the RAL front end test stand is to demonstrate that low energy beams of sufficiently high quality can be produced and is not primarily aimed at one particular application; instead it is intended to allow generic experiments exploring a variety of beam current and pulse distribution regimes.

#### 4.1.2 The Front End Test Stand

The RAL front end test stand has five main components: a 60 mA  $\text{H}^-$  ion source, a low energy beam transport (LEBT) to match the beam from the ion source into a Radio Frequency Quadrupole (RFQ) accelerator, a high speed beam chopper, and a comprehensive suite of diagnostics. The aim is to demonstrate production of a 60 mA, 2 ms, 50 pps, chopped  $\text{H}^-$  beam at 2.5 MeV with no partially chopped bunches. The test stand will be constructed in building R8 at RAL, reusing the space vacated by

decommissioning the ISIS RFQ test facility following installation of the new pre-injector on ISIS. Figure 1 shows a 3D layout of the RAL front-end test stand in building R8.

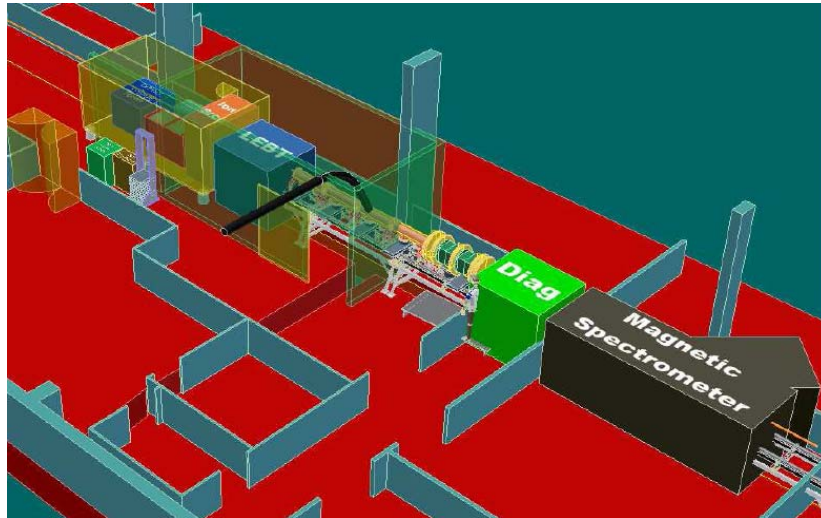


**Figure 1:** Proposed layout of the front-end test stand in building R8 at RAL.

#### 4.1.2.1 $H^-$ ion source

A review of  $H^-$  ion sources has been given in [5]. At RAL an ion source development programme [6], based on the highly successful ISIS  $H^-$  ion source [7], has been underway for several years, and has been funded in part by the European Union [8]. The intention is to increase the extracted  $H^-$  ion current from 35 mA to 60 mA and to increase the pulse length from 200 – 300  $\mu$ s to 2 ms. After extensive electromagnetic [9] and thermal [10] modelling (see figure 2) a re-engineered ISIS source has demonstrated the ability to sustain 1.75 ms long discharge pulses and peak currents of 60 mA have been achieved although not yet for the full 2 ms long pulses.

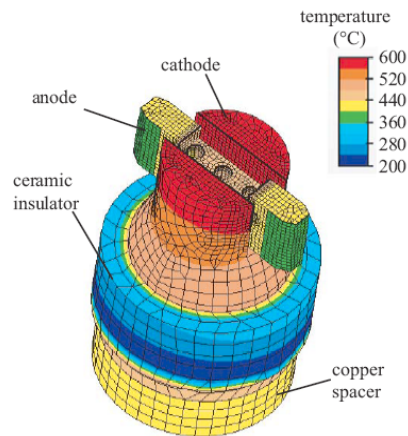


**Figure 2:** Finite element thermal model of the ISIS ion source showing steady state temperatures.

A planned increase in extraction voltage from 17 kV to 25 kV will further increase peak currents. This level of performance is not needed for routine ISIS operations but will be essential for the next generation of HPPAs.

#### 4.1.2.2 *LEBT*

The LEBT transports and matches the beam from the ion source into the RFQ. It is desirable that the LEBT minimises beam loss and emittance growth and there are two main options: a magnetic LEBT using solenoids or an electrostatic LEBT using Einzel lenses. The electrostatic LEBT is compact and its short length reduces beam loss due to stripping of the H<sup>-</sup> ions in the residual gas, and the high electric fields ensure that there is no space charge neutralisation. However the short length also precludes anything but the most rudimentary of LEBT diagnostics and the high electric fields may lead to sparking when operated in close proximity to the highly caesiated ion source. A magnetic LEBT, such as that used on the ISIS RFQ pre-injector upgrade and characterised on the RFQ test stand [11], has ample space for diagnostics and contains no high electric fields. However a high degree of space charge neutralisation leads to a transient mismatch at the RFQ input during the period over which neutralisation builds up and losses due to stripping are slightly higher than for the electrostatic designs.

On balance, a three solenoid magnetic LEBT is the preferred option for the RAL front end test stand. Three solenoids offer flexibility where the beam is not radially symmetric, such as in the case of the ISIS ion source. The space available between the solenoids will allow the installation of a variety of diagnostics to carry out a range of generic low energy beam experiments.

#### 4.1.2.3 *RF frequency choice*

A great deal of debate has taken place regarding the RF frequency to be adopted on the front-end test stand. Following the very successful testing and subsequent installation of a 202.5 MHz, 4-rod RFQ pre-injector upgrade on ISIS in 2004 [12], it was initially felt that a development of this technology at around 200 MHz was the natural way to go. Although the ISIS drift-tube linac frequency of 202.5 MHz is an historical legacy, this low frequency eases the design of the chopper pulser and makes perfect chopping, i.e. no partially chopped bunches, readily achievable. RAL also has a great deal of experience of high power RF systems at this frequency. However the desire for the front-end test stand to be as generic as possible rules out the ‘old fashioned’ frequency of 200 MHz because it is not being considered for any proposed HPPAs. A thorough review of RF frequencies proposed for other machines, the consequences of particular frequency choices for the front end test stand, the impact on the design of the following linac, and most importantly the availability now of a source of pulsed RF has led to the adoption of the J-PARC frequency of 324 MHz [4] based on the Toshiba E3740A 3 MW pulsed klystron [13].

#### 4.1.2.4 *RFQ*

The RFQ design will draw on the experience gained in the design and operation of the ISIS RFQ [11] (see figure 3) and on the 280 MHz RFQ designed (but not built) for the ESS (European Spallation [neutron] Source) project [14]. The input energy will be in the range 50 keV to 70 keV and the output energy will be 2.5 MeV. Modelling of the beam dynamics in the RFQ uses the RAL code [15] that has already had some

benchmarking against the ISIS RFQ [16].

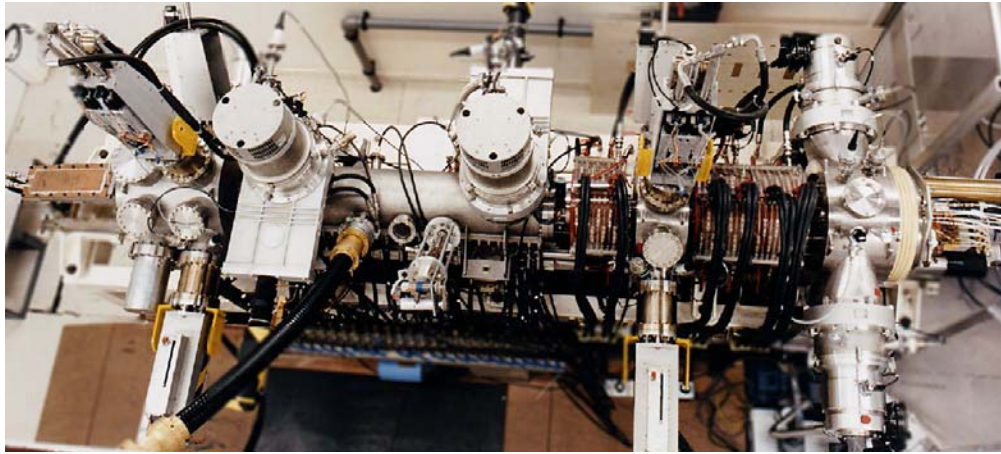


**Figure 3:** The ISIS RFQ test facility. The RFQ pre-injector has now been successfully installed on the ISIS accelerator.

Due to the experience already gained and some advantages in the manufacturing technique, the feasibility of a 4-rod resonator design at 324 MHz is being investigated. At the high RF duty cycles envisaged for the front-end test stand, cooling of the copper surfaces, particularly the rod electrodes, will be the critical factor in determining the practicality of a 4-rod RFQ at this frequency. Should this not prove feasible an alternative 4-vane resonator, based on the designs of SNS and J-PARC, will be adopted. The beam dynamics will be the same irrespective of resonator type.

#### 4.1.2.5 *The high-speed beam chopper*

For HPPAs, which utilise accumulator rings or synchrotrons, beam chopping is essential to reduce beam loss during trapping and extraction. The linac macro-pulse is chopped into micro-pulses at the ring revolution frequency to populate only the stable portion of the ring longitudinal phase space. Chopping duty factors are typically 60 – 70%. Because the linac macro-pulse contains bunches at the linac RF frequency, the chopper deflector must switch on between bunches if partially chopped bunches, which could lead to uncontrolled loss at higher energies, are to be avoided. In addition to very fast switching times, the chopper is required to maintain the deflecting field for periods up to some tens of microseconds. These two conflicting requirements are extremely challenging for the design of the high voltage pulser and at RAL an innovative tandem chopper design has been developed [17] to meet this challenge. A ‘fast’ chopper, which can switch between bunches but cannot maintain a long flat-top, removes two or three bunches leaving a gap in which a ‘slow’ chopper, which has a longer rise-time but can maintain a long flat-top, is switched. The fast chopper uses a slow wave meander transmission line deflector driven by a custom built high voltage pulser [18] and achieves 1.5 kV pulses with transition times of <2 ns (see figure 4). The slow chopper utilises 8 kV MOSFET switches driving an 8-element lumped deflector and achieves transition times of ~10 ns. Figure 5 shows a cut-away view of the tandem chopper

deflector. Work on the RAL tandem chopper has been partially supported by the EU [19].

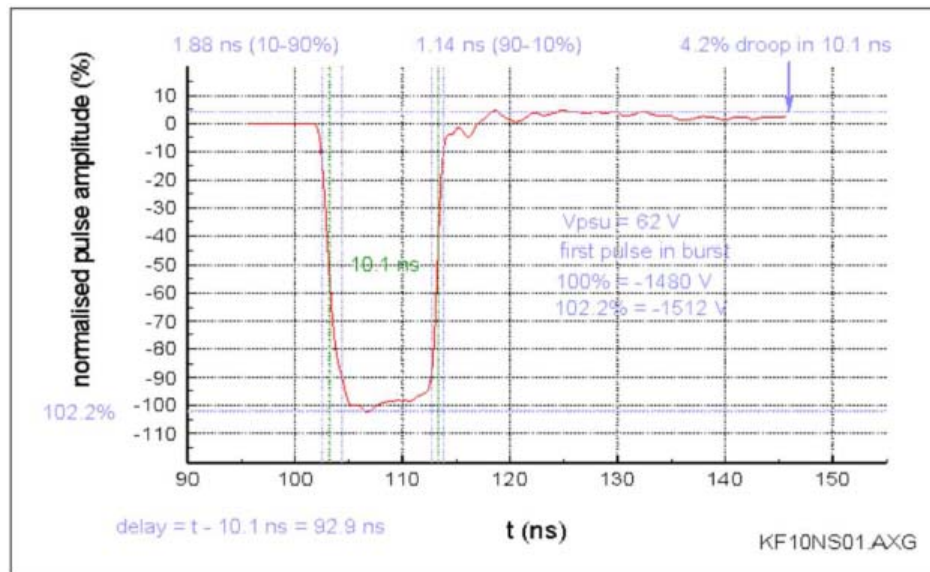


**Figure 4:** “Fast” chopper pulser waveform into a dummy load.

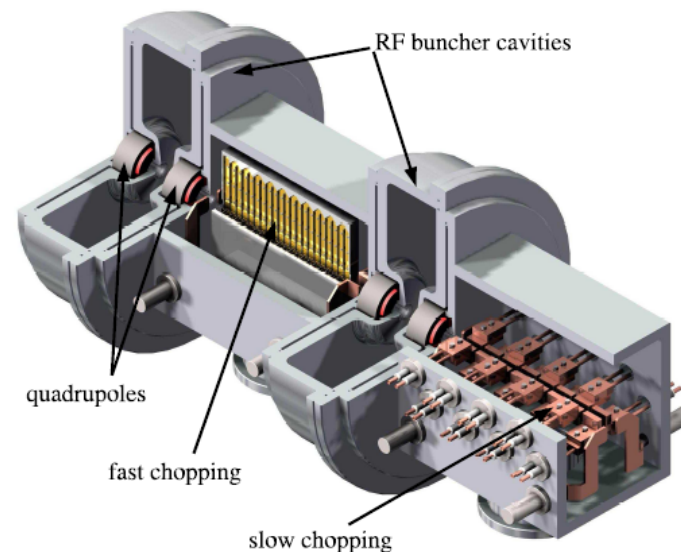


**Figure 5:** The RAL tandem chopper deflector.

#### 4.1.3 Diagnostics

The main purpose of the front-end test stand is to demonstrate the production of high quality chopped beams suitable for HPPAs, so the provision of suitable beam diagnostics is very important. The diagnostics to be used include those already used

satisfactorily on the ISIS RFQ test facility: beam current transformers, slit-and-cup emittance scanners, a fast coaxial Faraday cup, a magnetic energy spectrometer and a gas scattering energy spectrometer [20]. In addition, beam bunches will have to be measured with a dynamic range of  $\sim 10^4$  or better to suitably demonstrate the performance of the beam chopper. As well as diagnostics that are essential to the successful operation of the test stand, other diagnostics are planned which will provide a deeper understanding and contribute to generic HPPA front-end development. Such diagnostics include residual gas ion energy analysis [21] to quantify space charge neutralization in the LEBT and non-destructive laser profile measurements.

#### 4.1.4 Summary

The front-end test stand being built at RAL to contribute to the development of high power proton accelerators has been briefly described. Design and development work is well underway, with first beam through the LEBT being planned for 2006/7.

#### 4.1.5 References

1. Neutron News, vol. 5 no. 1 and no. 2 (2004), various pages. See also <http://www.isis.rl.ac.uk>
2. Neutron News, vol. 11, no. 3 (2000), p. 15. See also <http://sinq.web.psi.ch>
3. N. Holtkamp, "Proceedings of the 8<sup>th</sup> European Particle Accelerator Conference", p. 164, EPAC'02, Paris, June 2002. See also <http://www.sns.gov>
4. Y. Yamazaki, "Proceedings of the 8<sup>th</sup> European Particle Accelerator Conference", p. 169, EPAC'02, Paris, June 2002. See also <http://jki.tokai.jaeri.go.jp>
5. R. Scrivens, "Proceedings of the 9<sup>th</sup> European Particle Accelerator Conference", p. 103, EPAC'04, Lucerne, July 2004.
6. J. W. G. Thomason *et al.* Rev. Sci. Instrum. 73 (2002) 896.
7. J. W. G. Thomason and R. Sidlow, "Proceedings of the 7<sup>th</sup> European Particle Accelerator Conference", p. 1625, EPAC2000, Viena, June 2000.
8. EU network HPRI-CT-2001-50021.
9. D. C. Faircloth *et al.* Rev. Sci. Instrum. 75 (2004) 1735.
10. D. C. Faircloth *et al.* Rev. Sci. Instrum. 75 (2004) 1738.
11. C. P. Bailey *et al.* "Proceedings of the 7<sup>th</sup> European Particle Accelerator Conference", p. 933, EPAC2000, Viena, June 2000.
12. A. P. Letchford *et al.* to be presented at the 2005 Particle Accelerator Conference, Knoxville, May 2005.
13. See [http://www3.toshiba.co.jp/ddc/eng/electron/e\\_kly.htm](http://www3.toshiba.co.jp/ddc/eng/electron/e_kly.htm)
14. The ESS Project, Vol. III, Technical Report, ISBN 3-89336-303-3. See also [http://neutron.neutron-eu.net/n\\_ess](http://neutron.neutron-eu.net/n_ess)
15. A. P. Letchford and A. Schempp, "Proceedings of the 6<sup>th</sup> European Particle Accelerator Conference", p.1204, EPAC'98, Stockholm, June 1998.
16. A. P. Letchford *et al.* "Proceedings of the 8<sup>th</sup> European Particle Accelerator Conference", p. 927, EPAC'02, Paris, June 2002.
17. M.A. Clarke-Gayther, "Proceedings of the 9<sup>th</sup> European Particle Accelerator Conference", p. 1449, EPAC'04, Lucerne, July 2004.
18. Kentech Instruments Ltd, South Moreton, OX11 9AG, UK.
19. HIPPI/CARE/ESGARD programme, part funded by the EU under FP6 (Support for Infrastructures).
20. J. P. Duke *et al.* Nucl. Instr. Meth. A 538 (2005) 127.

21. R. Dölling *et al.* “Proceedings of the XVIII International Linear Accelerator Conference”, p. 83, LINAC96, Geneva, 1996.

## 4.2 Acceleration of beam in a four-cell Plane Wave Transformer (PWT) linac structure

Srinivas Krishnagopal  
[Centre for Advanced Technology](http://www.catech.ernet.in), Indore 452 013, INDIA  
 mail to: [skrishna@cat.ernet.in](mailto:skrishna@cat.ernet.in)

### 4.2.1 Introduction

The Beam Physics & FEL Laboratory at the Centre for Advanced Technology in Indore, India, is engaged in research and development in accelerators and free-electron lasers. We are working on a photocathode linac as well as a free-electron laser. We are building a Compact Ultrafast Terahertz Free-Electron Laser (CUTE-FEL), designed to lase between 50-100  $\mu\text{m}$ . The CUTE-FEL will require an electron beam of 15 MeV energy and 5 A peak current, with a normalized emittance of better than  $10\pi$  mm mrad. As injector to the CUTE-FEL, we have chosen to build a Plane Wave Transformer (PWT) linac. Here we give some details of the design of the linac, and the results of acceleration trials.

### 4.2.2 The Plane Wave Transformer (PWT) linac

V. G. Andreev in 1969 proposed the PWT linac as a part of linac injector for the Russian 1 TeV cybernetic accelerator project [1]. The first PWT structure was developed by Swenson in 1988 [2], which was followed by Pellegrini & Rosenzweig at the University of California at Los Angeles, where improved versions of the PWT linac structure have been developed, and where the only operating PWT linac is located [3].

The PWT linac we have built (Figure 1) is an S-band, standing-wave four-cell structure, designed to resonate at 2856 MHz in the  $\pi$  mode. It consists of a cylindrical cavity (tank) loaded with array of disks in a co-axial manifold, i.e. there is a gap between the disks and the cylindrical cavity. Four metallic tubes parallel to the axis support the disks within the cylindrical cavity. This structure supports a TEM mode, plane waves, in the region between the disks and the tank. These get converted, because of the boundary conditions, to a TM mode near the axis of the structure – which motivates the name. An advantage of using a PWT structure is its relatively greater tolerance to machining errors on account of the high inter-cell coupling of electromagnetic fields, which has been among the main reasons we chose to build it as the injector for the CUTE-FEL.

In the UCLA design, the disks are suspended on SS tubes. The disks themselves are made in two halves. A water channel is cut on the inside of the disks and the two halves are brazed together. This allows water to be flowed through the SS tubes and through the disks, to cool them and also to tune the resonant frequency. The disadvantage is that the braze joint between the disks and the tubes becomes crucial, since it has to provide not just structural stability, but also seal the water passage.

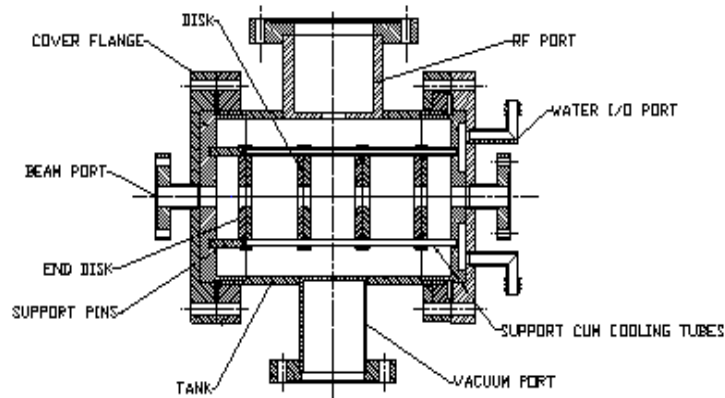


**Figure 1:** Schematic of a four-cell PWT linac structure.

We have therefore made a change to this design. We do not cut the disks in half to provide cooling channels. We have also replaced the SS tubes with copper rods. The braze joint is less crucial now. The rods can be machined to better tolerances than the tubes, which aids the brazing. Using copper allows for some conductivity to take the heat away from the disks to the reservoirs at the ends. Water can still be flowed through the reservoirs. We have done detailed thermal analyses using ANSYS to confirm that for the 1-2 Hz repetition rate we will be operating at initially, there are no thermal issues with this scheme, as shown in Figure 2.

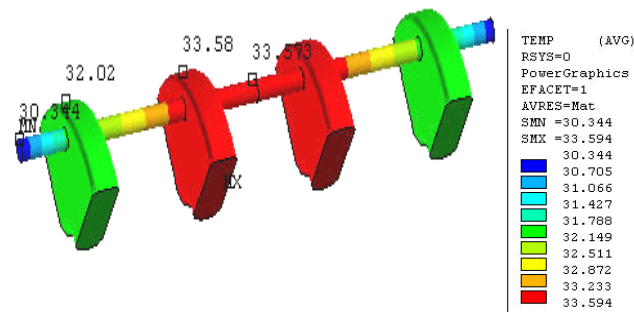


**Figure 2:** Steady-state temperature profile of the disk-array with copper rods.

#### 4.2.3 Simulations and cold tests

We have done detailed simulations and cold tests of the 4-cell PWT structure [4]. We did both two-dimensional electromagnetic simulations using SUPERFISH, and three-dimensional simulations using GDFIDL, to design the four-cell structure. Issues addressed included the diameter of the disks, the thickness of the disks, the location (on the disks) of the holes for the tubes, the diameter of the tubes, length of the structure, influence of the ports, etc. Figure 3 shows, as an example, the variation of the resonant

frequency with the length of the structure. More details can be found in Ref. 4.

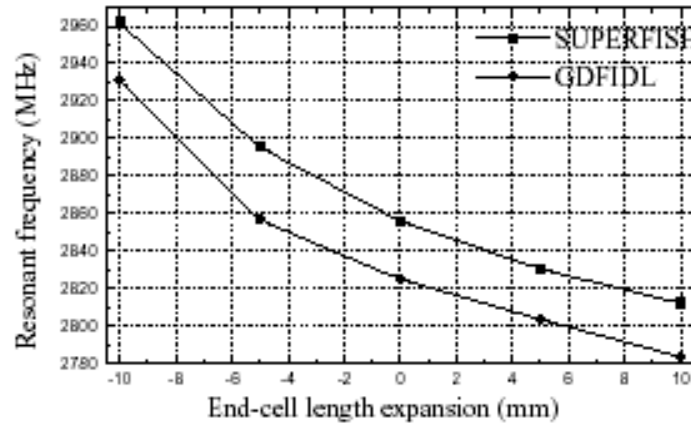


**Figure 3:** Variation of the resonant frequency as a function of the length of the structure. This feature is used to tune the PWT linac.

After this, we built dummy structures, with disks of varying diameters, to benchmark the simulations. The comparison between the simulations and cold tests, shown in Table 1, is good, typically of the order of a few MHz, and gave us the confidence to go ahead and build the structures.

**Table 1:** Comparison of predicted and measured resonant frequencies as a function of the disk diameter.

Disk diameter (mm)	Resonant Frequency (MHz)	
	GDFIDL Prediction	Cold-test Measurement
85.2	2916	2903
86.0	2911	2908
87.0	2905	2907
88.0	2897	2896
89.0	2892	2888
90.0	2883	2879

We also performed a number of beam dynamics simulations using PARMELA [4]. This included looking at the energy gain and emittance growth as a function of accelerating field, dependence on pulse charge, growth of emittance within the linac, etc. As an example, Figure 4 shows the emittance at the exit of the linac, as a function of the accelerating gradient. More details can be found in Ref. 4.

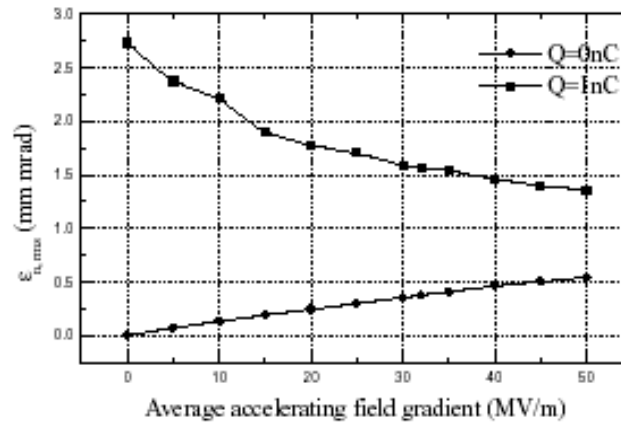


**Figure 4:** Emittance at the exit of the four-cell PWT linac, as a function of accelerating gradient.

#### 4.2.4 Acceleration trials

After building a number of prototypes and ascending a steep technology curve, we now have a structure (PWT3) that has been fabricated to the required tolerances (30  $\mu\text{m}$ ) and surface finish (0.2  $\mu\text{m}$  CLA), which can hold UHV ( $1 \times 10^{-8}$  Torr), resonates at the desired frequency of 2856 MHz, and has a loaded Q of 8,000.

We therefore built a beam-line (Fig. 5) to accelerate beam from a thermionic gun through the PWT3 structure. All elements of the beam-line, as also the klystron modulator that powers a 10 MW Russian klystron, have been built in-house.

In these trials we used an unbunched, 40 keV, 2  $\mu\text{s}$ , 20 mA DC beam from the thermionic gun. The beam-line was designed with two solenoids to focus the beam into the entrance of the linac. In the first set of trials we fed in around 4 MW of RF power to the structure. Since the electron beam was DC, we expected acceleration at all energies up to a maximum consistent with the accelerating gradient established in the linac. We therefore started by setting the magnetic field of the energy analyser to allow through only 40 keV electrons, and kept increasing the field. The results are shown in Figure 6.

These results show that electrons are accelerated to a maximum of around 3.5 MeV in the structure. We then increased the RF power to around 4.5 MW, and could observe electrons out to around 4 MeV. This corresponds to a gradient of around 20 MV/m. We also measured the current on a fast current transformer just before the Faraday cup. We found that at lower energies the current was below the sensitivity of the FCT (around 1 mA), but at the maximum energy of 4 MeV, the current was around 4 mA.

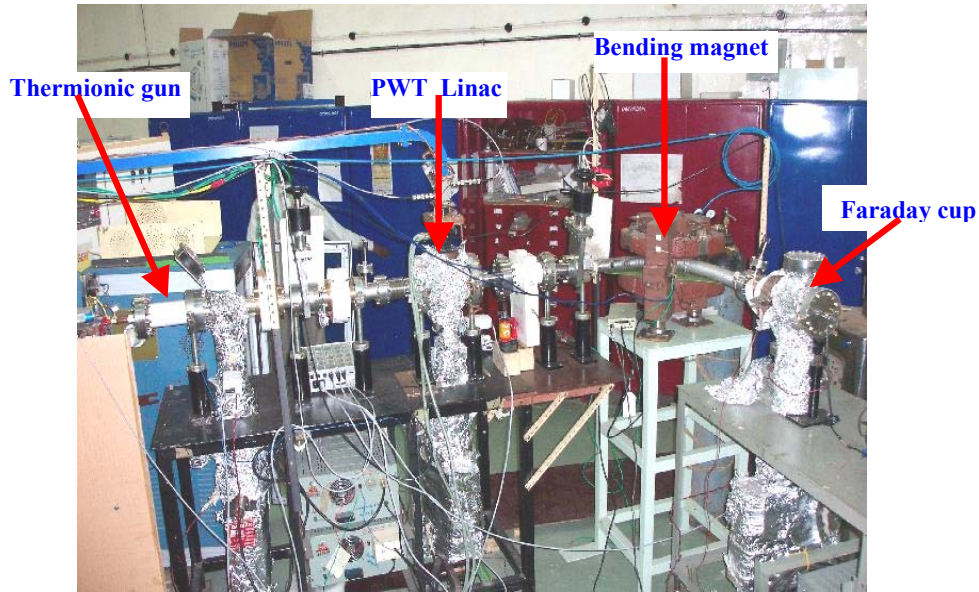


**Figure 5:** Photograph of the layout of the beam-line for the acceleration experiments

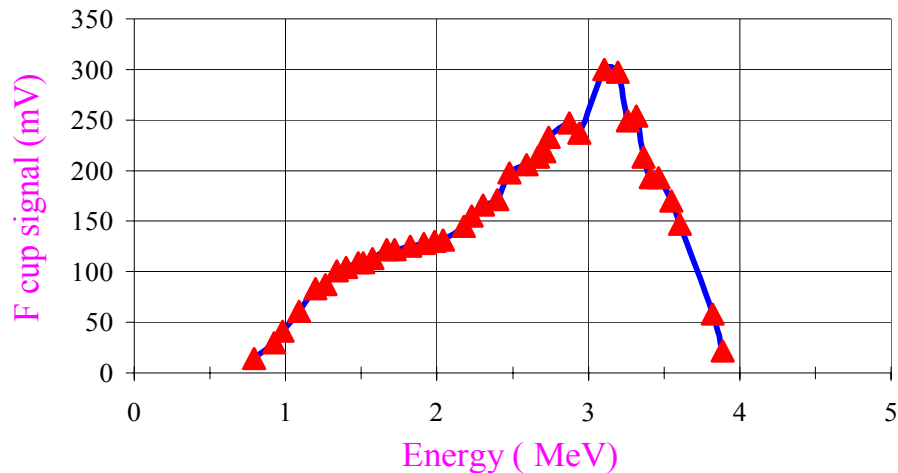


**Figure 6:** Energy spectrum of the beam accelerated in PWT3. The incoming beam is unbunched.

#### 4.2.5 Future plans

Now that we have successfully demonstrated acceleration in the indigenously built PWT structure, we plan to characterize the performance of the structure more thoroughly. One immediate goal would be to put in more power and explore the maximum gradient the structure can support. We are also developing a structure with cooling (identical to the UCLA one) so that we can also handle high repetition rate operation. Also, consistent with our plans for a free-electron laser, an immediate priority is to put the beam through a 5 cm period, 1.25 m long PPM undulator (which we have already built), and look for spontaneous emission. In parallel, we are also building a pre-buncher and buncher for the linac, so that we can accelerate a bunched, high-current

beam through the linac structures, put the beam through the undulator in an optical cavity, and look for lasing.

#### 4.2.6 Acknowledgements

This work has been presented on behalf of my colleagues in the Beam Physics & FEL Laboratory – Kamal Kumar Pant, Vinit Kumar, Arvind Kumar, Umesh Kale, Pravin Nerpagar, Bhaskar Biswas, Shankar Lal, Pratima Jain and V. Kodiarasan. We would like to acknowledge early help from Claudio Pellegrini, Jamie Rosenzweig and R. Zhang, from UCLA, in getting information about the PWT linac structure, including line drawings. We also thank S. Mahadevan of IGCAR for gifting to us the thermionic gun, S. Choukey and V. Prasad of CAT for engineering support, and numerous others for their various contributions.

#### 4.2.7 References

1. V. G. Andreev, "Accelerating structure for a high-energy linear proton accelerator", Soviet Physics- Technical Physics 13 (1969), 1070.
2. Donald A. Swenson, "The plane wave transformer linac structure", Proceedings of 1988 European Particle Accelerator Conference, Rome (world scientific, Singapore, 1988), 1418-1420.
3. R. Zhang, et al., 'Initial operations of the UCLA plane wave transformer (PWT) linac', Proceedings of Particle Accelerator Conference, 1995, 1102.
4. A. Kumar, K. K. Pant and S. Krishnagopal, "Simulations and cold-test results of a prototype plane wave transformer linac structure", Phys. Rev. ST Accel. Beams, **5**, 033501 (2002).

## 5 Workshop and Conference Reports

### 5.1 Summary of the 33rd ICFA Advanced Beam Dynamics Workshop on "High Intensity and High Brightness Hadron Beams" (ICFA-HB2004)

Ingo Hofmann, GSI Darmstadt, Germany  
[mail to: i.hofmann@gsi.de](mailto:i.hofmann@gsi.de)

The 33<sup>rd</sup> ICFA Advanced Beam Dynamics Workshop was held at the Conference Center of Bensheim, Germany, south of Darmstadt, in the week October 18-22, 2004. It was organized by GSI and co-sponsored by CEA and FZJ. The meeting was chaired by I. Hofmann (GSI) and J.-M. Lagniel (CEA). It was the second ICFA workshop fully dedicated to the theme "High Intensity and High Brightness Hadron Beams" and similar in format to its precursor, the 20<sup>th</sup> ICFA Advanced Beam Dynamics Workshop held at Fermilab, April 8-12, 2002. Topics have included accelerator and beam physics issues associated with high intensity and/or brightness, technical system designs, reviews of existing machines and overviews of planned projects for protons and ions.

The workshop was held at a very exciting phase of development of high-intensity accelerators worldwide:

- The Spallation Neutron Source (SNS) at Oakridge went into its commissioning phase for the linac and is approaching completion of construction in 2006
- For the Japan Proton Accelerator Research Complex (J-PARC) completion of construction is expected for the end of 2007
- The Large Hadron Collider (LHC) at CERN as the frontier of high-energy and high-brightness with unprecedented challenges to machine protection is coming to operation in 2007
- For the International Facility for Antiproton and Ion Research (FAIR) at GSI, with its challenges in high intensity of ions and cooling techniques of antiprotons, the expected start of construction (staged) is in 2008
- Plans for a diversity of new Megawatt-drivers in Europe and in the United States for applications in neutron scattering, neutrino physics, nuclear physics and energy.

130 participants from 14 countries, some new in the field, have reflected the broad interest worldwide. There have been 65 invited talks and over 40 working session contributions on the main topics of concern, in general not more than two parallel sessions. We are most grateful to the conveners of all sessions for their help and efforts. The interaction of experts in beam dynamics, commissioning, design, machine protection, vacuum, diagnostics, technical components both for circular and linear accelerators has turned out, as already in the HB2002, to be extremely fruitful and constructive. At this occasion we also thank the local organizing committee and conference secretaries, as well as the program committee and international advisory committee for their valuable input. On the last day a guided tour was organized to visit GSI in Darmstadt. Beyond the scientific program, the flair of the local environment could be enjoyed during a conference dinner at the "Schloss Auerbach", practicing medieval exercises and life-style.

The proceedings of this workshop will shortly appear (May/June 2005) as a special volume of the American Institute of Physics Conference proceedings (AIP) Series.

Viewgraphs of most talks are available on the web page of the conference under <http://www.gsi.de/ICFA-HB2004> (check *scientific program*)

The session topics and conveners are:

- Lattices, Beam Loss Handling & Collimation - *N. Catalan Lasheras (CERN), C. Warsop (RAL)*
- High Intensity Linacs & Front Ends - *R. Ferdinand (CEA), J. Galambos (ORNL)*
- Space Charge Simulation & Experiment - *S. Machida (KEK), R. Ryne (LBNL)*
- Diagnostics & Instrumentation - *J. Dietrich (FZJ), K. Wittenburg (DESY)*
- Ecloud & Ion Induced Desorption - *A. Krämer (GSI), S.Y. Zhang (BNL)*
- Proton Drivers - *W. Chou (FNAL), H. Haseroth (CERN)*
- Advanced Techniques - *J. Galambos (ORNL), K. Takayama (KEK)*
- FFAG & Cyclotrons - *R. Baartman (TRIUMF), S. Martin (FZJ)*

- Injection, Instabilities and Feedback - *Y.Y. Lee (BNL), E. Shaposhnikova (CERN)*
- High Brightness, IBS and Cooling - *O. Boine-Frankenheim (GSI), J. Wei (BNL)*

The program covered basically all aspects of high intensity beams and accelerators. The broad diversity of topics made it necessary to group presentations into 2-3 parallel sessions for both invited talks and working sessions, which included contributed talks and discussion topics. The summaries of the eight working sessions as compiled by the conveners (in part also referring to the related invited talks) are presented in the following:

### 5.1.1 Lattices, Beam Loss Handling and Collimation & Diagnostics and Instrumentation

N. Catalán Lasheras, J. Dietrich, C. Warsop, K. Wittenburg

Diagnostics and beam losses are intimately related when dealing with a high intensity accelerator. On one hand, operation is often limited by beam losses, so fast, reliable loss detection and protection systems become mandatory. On the other hand, the measurement of relatively low intensity halos and the detection of the minimum level of losses translate into very demanding specifications for instrumentation. The requirements imposed on the instrumentation of high intensity beams and some of the applied solutions were presented in the session on diagnostics and instrumentation. The joint working group of these sessions was mostly dedicated to the prevention of accidental beam losses. The participants showed examples of beam accidents and their identified causes. A list of hardware faults was drawn from participants' experience.

**Lattices, Beam loss handling and collimation:** The best moment to start thinking about avoiding losses is at the design stage of the accelerator. The final design should maximize acceptance, minimize space-charge and halo growth and avoid instabilities. Precise injection, stable ramping and clean extraction are also necessary. The low loss required will generally be achieved through precise beam control and practical experience during commissioning. Even when all possible sources of beam loss are minimized, dedicated collimation systems are still necessary restrict remaining loss to specified regions of the machine. Several kinds of collimation systems are usually found:

- *Beam choppers:* generally used to clean the beam gap at low energy. In these systems, the beam orbit is periodically deflected into an absorber that cleans the gap between nominal bunches.
- *Transfer line collimators:* used to define the beam before injection into a ring. The beam shape is defined by one or more blocks of material that cut in the transverse or longitudinal phase space by means of the phase advance and dispersion. In the special case of  $H^-$  injection, the removal of halo is made via electron stripping which allows much higher efficiencies.
- *Two-stage betatron collimation:* usually a multi-turn system in a circular accelerator designed to clean the transverse beam halo. Primary collimators intercept the beam and a secondary halo is formed that is, in turn, intercepted by

secondary collimators at a larger aperture. The phase advance between primary and secondary collimators determines the efficiency of the system together with the relative acceptance and the material choice. When beam power levels are very high (e.g. LHC), the survival of the collimator systems depends on controlled distribution of the losses among the jaws.

- *Longitudinal collimation:* untrapped particles need to be removed before they hit the vacuum pipe either during ramping or at extraction. For ramping losses, placing a two-stage transverse cleaning system in a dispersion area will simultaneously clean the transverse and longitudinal halo. Programmable dipolar kickers can be also excited resonantly with the betatron tune to remove longitudinal halo particles. These are generally useful in the absence of acceleration
- *Passive protection:* in critical locations such as injection and extraction areas, passive absorbers need to be located to capture beam losses that will otherwise not reach or escape from the cleaning system.

There are some important differences when collimating ions. Firstly, continuous ionization of the partially stripped ions by the residual gas leads to non-localized loss which is impossible to remove in one location. Secondly, even for bare nuclei, the fragmentation of the ions inside the collimator material makes optimization of the secondary collimators difficult. Out-scattering from the primary collimator has to be reduced and secondary locations depend strongly on the ion species and energy.

For many purposes, it is important to differentiate between the detailed instantaneous time structure of lost beam power, and the averaged values. In superconducting magnets, the temperature increase and likely hood of a quench depends on the rate of energy deposition and removal, as determined by loss, conductivity values and the heat removal capacity of the cryogenic system.

Hardware damage is similarly highly dependant on the time structure of loss. For higher repetition rate, medium energy machines it is often possible to design the hardware to withstand the stored power of the beam For the lower rep rate, higher energy case this may not be possible.

Residual activation, however, depends on average lost beam power. Hands on maintenance criteria (<100mrem/h) require very low levels of continuous losses in the order of 1W/m [4]. The final residual radiation will still depend on the exact geometry of the loss area, the materials surrounding the beam pipe, etc. The uncontrolled loss limits need to be estimated for each particular case.

**Accidental Loss Scenarios:** In terms of machine protection it is important to predict failure scenarios leading to accidental beam loss. These accidents may harm hardware components and cause costly and lengthy repairs or they may simply produce quenches in superconductor magnets preventing accelerator operation. As mentioned above, the effect of beam losses depends on its characteristic time. At the same time, the ability to intercept or dilute these losses also depends on it. We classify losses in three main regimes (R. Schmidt):

- Ultra fast losses: Losses over time scales of a few turns or less. Passive protection is needed as no collimation is possible.
- Very Fast losses (few turns <  $t$  < 5 ms): Losses happen in a time interval smaller than the diagnostic response time. Collimation systems are designed to intercept these losses.

- Fast losses ( $t > 5$  ms): The beam loss monitors and other diagnostics can detect the losses and apply a correction or even trigger a beam dump before any damage occurs.

The scenarios leading to accidental losses and quenches in existing accelerators have been explored during the workshop (K. Wittenburg).

A non-exhaustive list of the recurring hardware faults found is given below:

- Kicker failures: The asynchronous firing of a kicker may produce ultra fast losses lasting less than a turn.
- Magnet power supplies failures: The characteristic time of the loss is fast for most magnets but can be very fast for special magnets as at interaction regions.
- Instabilities: For example, those due to electron or ion clouds are usually in the fast regime and thus detectable by the instrumentation.
- Radio Frequency System failures: Losses driven by RF failures can be very fast or fast depending on the magnetic field ramping rate. RF faults may also drive very fast instabilities.
- Faulty Diagnostics: combined with automatic correction systems or feedback may lead to losses in the fast regime.
- Collimators: can be the cause of quenches because they localize the losses in a limited part of the accelerator. Wrong settings and electronic or mechanical failures have been the main causes. For this category of very fast loss, it is not expected that the collimators themselves will provide any protection.
- Human errors are the cause of a significant fraction of recorded accidents. They are not generally predictable and can have any time range.

Accidents are often a consequence of several faults in the accelerator hardware and protection systems. Interlock system failure, faulty diagnostics or inadequate thresholds are not a direct source of loss but can lead to accidental loss in the presence of otherwise controlled losses.

Dividing critical systems into smaller independent units, with built-in redundancy, was a useful approach, as used on the SNS kickers. Hardware alarms are also valuable, for example to notify a magnet power supply failure. The identification and continuous monitoring of a limited number of critical elements inside the interlock system has also proven to be very valuable.

Self-testing instrumentation was viewed as essential. Monitoring of additional diagnostics that could indicate a drift from normal conditions provides another layer of protection.

Experience presented at the workshop clearly demonstrated that post mortem logging of diagnostic systems and hardware status is a valuable tool. It allowed identification of the causes of accidents, and therefore helped improve safety systems, and reduce facility downtime.

**Diagnostics and Instrumentation:** As was illustrated during the workshop, space-charge painting, e-cooling, acceleration and accurate halo measurements require very large dynamic ranges. Access to instrumentation for servicing is often limited, for example due to high radiation, its location inside cryostats or e-cooling systems. Robustness is therefore mandatory.

Another important concern when considering the instrumentation for high intensity, high brightness beams is the survival of the detector itself. Non-destructive methods are necessary. Three profile measurement devices were presented during the workshop.

- *Beam induced fluorescence monitors:* The beam traverses a gas target and the excitation of the gas molecules produces visible light. A combined optical and light detection system provides the required beam information. In general, the solid angle seen by the detector is limited. The signal is generally small and the injected gas degrades the vacuum. These monitors are suitable in accelerators where a high-pressure bump is not critical.
- *Ionization profile monitors:* The beam ionizes the residual gas producing a cloud of charged ions and electrons, which are swept across the vacuum vessel by appropriate electric fields, to a detector. Signals are usually large. In the high intensity limit, the space charge between ions will distort the signal and correction via magnetic devices is needed. These monitors are more suitable for synchrotrons.
- *Laser wire scanners:* They are used for H<sup>-</sup> beam profiling mostly in transfer lines.

### 5.1.2 High Intensity Linacs / Front End & Proton Drivers

R. Ferdinand (CEA), W. Chou (FNAL) and J. Galambos (ORNL)

**High Intensity Linacs / Front End:** the session was divided in 3 major classes of topics:

- Improvement of existing facility (GSI)
- Projects under construction (SNS, J-PARC, IPHI)
- New projects (RIA, ADS)

Exciting new results were shown from the 2 new major projects SNS and J-PARC. Warm parts of the linacs were commissioned for both projects and beam was accelerated.

GSI was able to improve by a factor 5 the current of their reference ions in the past two years. They have plans for future upgrades of their linac.

RIA project is more or less ready for CD1 meaning they are awaiting approval of construction funds.

The ADS fault tolerance reliability study assesses the failure of cavities and the recovery process. It will be useful for other design.

**Proton Drivers:** There are numerous proton drivers around the world and the talks highlighted two kinds of projects:

- Upgrade of existing machines (ISIS, AGS, Main Injector)
- New machines (J-PARC, SPL, PEFP, FAIR, RAL driver, India driver, BNL 1.2 GeV linac, Fermilab 8 GeV linac)

Three types of drivers were presented: rapid cycling synchrotrons, warm RF linac and superconducting RF linac. All the designs presented show the same common features: high beam power, low losses, innovative design and state-of-the-art technology.

**Working sessions:** Topics from source development to experiment status were presented. Globally, one can say that many of the issues presented on new proton machines will be addressed with the European HIPPI project (Joint Research Activities – upgrades and R&D programme on pulse proton machine). No single approach was

observed in designing new projects. The old codes from Los Alamos are still in use, proving to be still acceptable for the community. New codes arise going deeper in detail. New types of SC cavities emerge, which is good for the accelerator community. One of the discussions commented the modelling and its impact on linac machine design. The designers use some “rule of thumb” judgment, for example on beam size to bore radius safety. Different approaches among the projects were presented. An analysis should be performed to assess this point and to provide rules agreed all over the world. An agreement among the participants was observed on front-end modelling (ion source and LEBT). Clearly, the simulations need improvement. Iteration on design is often empirical. Modelling from MEBT through accelerating structures could benefit from benchmarks with real machine data. The work will be achieved within HIPPI on the GSI Unilac. SNS will attempt to provide a set of beam conditions and measured profiles for the community. The last point was dedicated to express a desire for mini-workshop on linac Proton drivers. Among the issues to be covered, one can be the experience of superconducting cavities of low and medium beta. The idea is to provoke fair comparisons and offer choices of intermediate energy cavities. Too often, the designers use cavities development in their own lab without all the information needed to choose over a wide range of cavity types. The second topic, which could be covered with this mini-workshop, deals with number of cavities per klystron. FNAL, ANL, LBNL and CERN are among the interested parties to sponsor such a workshop.

### 5.1.3 Space Charge Simulation and Experiment

S. Machida (KEK) and R. Ryne (LBNL)

**Recommendations:** During the discussions several questions were raised and recommendations were proposed. These included the following: What do we have to do to make people trust code predictions? We need to systematically perform comparisons of codes with analytic results and comparisons of codes with other codes, and, most importantly, we need to systematically perform comparisons of codes with experiment. In regard to comparison with experiment, since many problems are initial value problems involving knowledge of the beam distribution function in phase space, we should make use of techniques for determining beam phase space data from real-space measurements. One example is the use of statistical methods to solve inverse problems in the presence of uncertainty in the data. What can we, as a community, do to facilitate code verification and validation (V&V)? We should develop community-wide standards. As an example, an initial effort is already under way to develop a standard for headers in particle data files to describe what is in the files and their units. We should also adopt standards for beam line descriptions, consistent with the Standard Input Format (SIF), but expanded to include systems not covered that are encountered in high intensity hadron systems. (For example, the SIF does not contain a widely accepted description of the accelerating structures encountered in high intensity linacs.) Another set of standards that should be developed is a set of analytical test problems. Finally, code V&V will be facilitated by good communication through workshops such as this and through publishing articles involving V&V on the e-print archive and in journals such as PRST-AB. Where can we get current or near-current data? Data can be obtained at accelerators such as the CERN PS, the FNAL booster, the J-PARC linac, the

SNS linac, the GSI linac and synchrotron, the University of Maryland electron ring, and others.

What are the most immediate challenging problems? Among the most immediate and challenging problems are: (1) predicting beam halos and losses in linacs, (2) predicting combined effects of weak space charge and nonlinear resonances on beam loss and dilution in rings, (3) self-consistent modelling intrabeam scattering and predicting the performance of electron cooling systems, (4) predicting electron-cloud effects, and (5) predicting beam-beam effects (a topic not covered at this workshop). Are there new computational algorithms that we should be aware of and using? Promising approaches include: (1) direct Vlasov methods that may someday prove useful for extremely low noise simulation and accurate simulation of beam halos, (2) Adaptive Mesh Refinement, which places grid points where they are most needed and has the potential to greatly reduce the number of required grid points for a specified resolution, especially in higher dimensions, and (3) self-consistent 3D Langevin simulations to solve the Fokker-Planck equation from first principles and accurately determine damping and diffusion coefficients.

**Working session:** A working session was held to discuss the ongoing effort to compare simulation and experiment at the CERN PS. A multi-step plan was formulated that started with idealized simulations and continued toward increasingly realistic models. The steps proposed were the following: (1) simulation of a coasting beam in a constant focusing channel, (2) simulation of a coasting beam in a periodic focusing, linear lattice, (3) simulation of a coasting beam in a periodic focusing, nonlinear lattice, and (4) simulation of a bunched beam in a periodic focusing nonlinear lattice with rf cavities. Detailed comparisons with experiment at the CERN-PS would involve three types of experiment: (1) the Montague resonance, (2) dynamic crossing of a resonance, and (3) an octupole experiment, including comparison of a frozen space charge model with self-consistent space charge. This effort is now well underway. The overall coordination is with I. Hofmann (GSI), points of contact for the experiment are E. Metral (CERN) and for simulation S. Cousineau (ORNL) and G. Franchetti (GSI).

**Conclusion:** There was unanimous agreement among the participants that meetings such as this serve an important and useful purpose, and that they should continue. The effort involving comparison of simulation with experiments at the CERN PS has become an important activity with international interest and participation. In the near future it is expected that experiments at the GSI Unilac and, in particular, the new projects SNS and J-PARC, will provide other important opportunities but in a different regime, namely, that of a high-intensity linac. The confluence of dedicated experiments, increasingly powerful computers, increasingly realistic computer models, and advances in beam theory and numerical algorithms, make this a time of tremendous opportunity. International collaboration involving all these elements are helping to make simulation a tool that can be used with confidence to facilitate decision making and design of the next generation of particle accelerators.

#### 5.1.4 Electron Clouds and Desorption

S.Y. Zhang (BNL) and A. Kraemer (GSI)

Electron cloud and ion desorption are currently intensity limit of several hadron machines in operation, such as RHIC, PSR, AGS Booster, SIS18, and possibly of concern for several accelerators in construction and planning, such as SNS, LHC, and GSI FAIR.

**Summary of ECLOUD'04:** R. Macek presented the summary of ECLOUD'04, where the progress in cures were summarized as: solenoids, NEG coating, grooved surface, beam scrubbing, feedback and Landau damping for electron cloud induced beam instabilities.

**Progress in cold scrubbing at SPS:** The inefficiency of cold scrubbing, which caused worry at ECLOUD'04, was confirmed due to water mono-layers, and the effective cold scrubbing has been demonstrated at the SPS. This is of importance to LHC commissioning, reported by J.M. Jimenez.

**Progress in studies toward GSI upgrade:** The results of ion desorption with respect to projectile's energy, per recommendation of Pressure Rise Workshop, was reported by H. Kollmus. Other efforts toward GSI upgrade such as the beam lifetime and vacuum model, were reported by G. Rumolo and E. Mustafin.

**RHIC pressure rise and electron cloud:** W. Fischer summarized the current understanding of RHIC luminosity limit due to the beam induced pressure rise. S.Y. Zhang reported the RHIC ion desorption observation and the test of anti-grazing ridges, which is designed to counteract the RHIC warm electron cloud.

**Progress in cold ion desorptions at CERN:** E. Mahner reported the results of ion desorption measurements at cold surfaces, studied at LINAC 3. The study is related to the LHC heavy ion program, where the lead beam ions may capture electrons from pair production, and the beam loss of the charge exchanged ions may cause magnet quench.

**Heavy ion fusion studies:** The progress of heavy ion fusion studies in recent one year was reported by P.A. Seidl. The electron physics were studied together with the beam dynamics. Simulation has been started to explain the experiment results.

**Progress in code development:** Efforts in the code CMEE to include ion stopping and ionization, etc. to accommodate the need of hadron machines, summarized by P. Stoltz, were presented by D. Bruhwiler. Further plans to include ion scattering etc. were also reported.

**Working session discussion:** Several topics were picked up for the working session discussion. These were electron cloud issues, ion desorption, cryogenic problem and surface issues. Brief descriptions about the topics and discussions are presented in the follows. Due to the time limit, some issues were not actually discussed, but these are still listed to show the concerns.

**Electron cloud issues:** Electron cloud is one of major intensity limits in hadron machines, and many progresses have been made in the beam studies, the test stand experiments, and simulations. There are still several open issues.

- Missing physics for hadron machines  
Contributions from residual gas at PSR are significantly larger than from simulations. Secondary electrons sometimes survive long time, observed at SPS (for fixed target program following the LHC beam) and in RHIC warm straight sections. Are ions playing a role?
- Quadrupole effect  
SPS observed strong electron multipacting at quadrupole, in a pattern predicted by simulation. For the same beam, the electron multipacting in a quadrupole is stronger than that in a dipole.
- Effect of electrons below 10eV

**Ion desorption:** The ion desorption has been a mechanism limiting the beam intensity in several low energy heavy ion accelerators. For high-energy hadron machines, it becomes of interest to understand the role it played for beam induced pressure rise, and also the role it played together with the electron cloud.

- GSI, CERN, BNL test stands.
- RHIC concerns and studies.
- Among many aspects, incident angle effect. RHIC study showed that  $\approx 1$  mrad, no dramatic increase of desorption rate. Even smaller angle?
- GSI plans tests of angular effect.
- Ions from other sources, ionization, low energy electrons.

**Cryogenic problem:** Electron cloud at the cryogenic regions is less well understood than that at warm regions. Also, the scrubbing at the cold region is more challengeable. The LHC and eRHIC are two examples of the concern.

- SPS COLDEX and cold scrubbing  
Scrubbing inefficiency at cold walls is identified due to water, opened door to LHC scrubbing. Some discrepancies between electron signal and heat load.
- RHIC cold pressure study  
Cold pressure rise observed at  $2 \times 10^{11}$  protons per bunch with 108 ns bunch spacing. Study is prepared. eRHIC, with  $10^{11}$  charges per bunch and 35 ns bunch spacing will have similar problem as LHC.

**Surface:** One of the most useful mitigations of the electron cloud and ion desorption is probably the surface and its treatment.

- NEG and problems of a large scale installation at RHIC.  
Activation, re-activation, saturation, and possible poisoning. RHIC activate at 250°C, 1 hour per CERN's recipe; but CERN is doing 230°C, 24hours now.
- TiN  
Serrated and grooved surfaces. Anti-grazing ridges are designed to counteract the RHIC warm electron cloud.

### 5.1.5 Injection, Instabilities and Feedback

Y. Y. Lee (BNL) and E. Shaposhnikova (CERN)

**Injection:** Simulation of losses and halo generation at the injection due to the injection mismatch were reported by Shimosaki. One novel idea to overcome space charge effect was reported by Derbenev. The idea is to create a smoke ring in the phase space using non-linearity to reduce the space charge force. Later the phase space is collapsed back by inverse resonance. Practicality of the scheme would be a subject of further study. Issues with high energy  $H^-$  injection were discussed by Chou. One surprising effect among usual injection issues was that a significant fraction of the  $H^-$  is stripped by the black body radiation from the vacuum chamber. As the velocity of the  $H^-$  ion approaches the speed of light, photons in black body radiation gain enough energy through the Doppler shift to strip the ion.

**Coherent effects:** Undamped longitudinal bunch shape oscillations were already noticed in the past. Recently they have also been observed in RHIC, Fermilab Main Ring and Tevatron, SIS and SPS. The observation time varies from hundreds of ms to hours but in all cases it is significantly longer than the decoherence time estimated (and observed) for a low intensity beam. Another common feature of these shapes or structures is that they are not the result of a growing perturbation. Usually they are created already before, in the injector, or at injection into a mismatched voltage or with a phase error.

Long-lived structures, usually bubbles, were observed in coasting beams (PS Booster, PSR...). For a bunched beam the situation seems to be paradoxical. Hot spots are observed below transition when space charge is dominant (Fermilab Main Injector, MacLachlan) and above transition for a dominant inductive wall impedance (RHIC, Blaskiewicz and Fischer, Tevatron, Lebedev) despite the fact that for a potential well distortion the space charge has a defocussing effect below transition and the inductive wall impedance is defocusing above transition. This phenomenon is explained analytically (Blaskiewicz and Fischer) and demonstrated in simulations as a nonlinear effect. In the Fermilab Main Injector the bunch itself forms a hot spot. Including space charge in simulations (MacLachlan) preserves a bunch injected out of center from dilution. Two hot spots would lead to undamped quadrupole oscillations.

In the case of RHIC these long-lived coherent structures are a potential danger for stochastic cooling, while for Main Injector this effect seems to be useful for injection oscillations damping.

A more traditional explanation of this phenomenon is based on the fact that the coherent frequency of a dipole or quadrupole oscillation is shifted at certain intensity out of the incoherent band and Landau damping is lost. The threshold found in this way agrees well with the threshold for persistent dipole oscillations for SIS18 (Boine-Frankenheim). Dancing bunches following coalescing are also observed in the Tevatron and can be damped by a longitudinal damper (Lebedev).

If these are the same phenomena, the intensity threshold for hot spots in both theory and simulations should agree with the loss of Landau damping obtained from the perturbation approach.

**Beam Loss Studies:** The problem of beam loss is one of the most important in high intensity accelerators (see also session A of this Workshop). The exact reasons for losses are not always obvious and careful measurements and studies are necessary to find them out. In the CERN SPS after preparation for the LHC beam (impedance reduction, feedback, feed-forward and longitudinal damping systems) capture losses of

LHC beam for nominal intensity were about 15% (Linnekar). At injection these losses are attributed to long bunches in reduced buckets due to energy loss in resistive impedance, while the origin of continuous loss on the flat bottom is less clear. Reduction of these losses with larger bunch spacing and a new working point on the tune diagram suggests that the effects of e-cloud and space charge could be involved. During acceleration the beam is unstable and this is cured by controlled emittance blow-up and a 4th harmonic RF system in bunch shortening mode.

The problem of beam loss at injection (energy mismatch, RF phasing...) and slow loss after adiabatic capture was also studied in SIS18 (Kirk). The exact reason for the losses is not clear and transverse resonances are also suspected. A possible reason for the large longitudinal increase measured with RF off (from Schottky spectrum) could be a longitudinal instability of the debunched beam. More accurate measurements during the ramp are being done now and compared with simulations taking into account the nonadiabaticity of RF gymnastics.

**Instabilities:** Transverse single bunch instability was observed recently in the Tevatron, RHIC, SPS and PS. In the six rings of Tevatron Complex only the Debuncher has no problems with beam stability (Lebedev). Suppression of instabilities is an important part of the luminosity increase. The weak head-tail instability in the Tevatron was cured by high chromaticity, also reducing the beam lifetime. The impedance of two laminated Lambertson magnets was identified as the main source of this instability. One magnet has been removed and one shielded so that the chromaticity can be significantly reduced. A theoretical model takes into account coupling between the planes and gives good agreement with observations.

In RHIC (Blaskiewicz and Fischer) this instability is observed at transition crossing when the chromaticity is changing sign and, depending on conditions, can have a fast growth rate, comparable to the synchrotron period. Simulations show that some impedance is missing in the model and space charge makes the situation worse.

Note that the strong head-tail or TMCI instability for proton bunches was also observed in the CERN PS at transition (Metral). However it seems that the same instability but far away from transition was observed for the first time in the CERN SPS (Burkhardt, Metral). The signature of this instability is that it is also observed for zero chromaticity. In the past TMCI was an intensity limitation for the lepton beam in the SPS. It was also predicted for protons, but was never seen before the impedance reduction, probably because the microwave instability had a lower threshold. Comparison of MOSES (Y. Chin) and Head Tail (G. Rumolo) codes for different parameters show good agreement for short bunches. In simulations the effect of space charge significantly increases the threshold for the flat chamber of the SPS.

Coherent tune shift measurements in the SPS were done to follow up the transverse impedance reduction and, unfortunately, the increase also (five kickers were reinstalled in 2003). TMCI can become an intensity limitation for the LHC beam with four more magnets installed in 2006. For a flat chamber there is no tune shift in the horizontal plane. Measurements of high-order modes, which shift as a function of intensity in the vertical plane, could verify the mode-coupling mechanism of this instability.

The particle motion in a barrier RF system is different from the traditional and consists of long drift and fast kick. The development of instabilities in barrier buckets was considered in several presentations. The origin of a resistive wall instability of a long bunch captured by a barrier RF system in the Fermilab Recycler was not clear from

the beginning and was studied in detail. Calculations are in good agreement with observations, including growth rate and mode structure (Lebedev). To suppress this instability a two-band damper is foreseen. The coasting beam theory was applied for a long bunch in a barrier bucket (Ng). The different behaviour of p and pbars can be explained by the difference in transverse size of the beam if space charge suppresses Landau damping.

The head-tail instability was also analysed for a superbunch in the induction synchrotron (Shimosaki, session G). Stability of cooled beams in barrier buckets is an important issue for HESR as well (Lehrach). In Hera-p the bunch length of the proton beam during acceleration is significantly larger than the expected theoretical value, lowering luminosity by 10%. Measurements of spectra and growth rates of different beam modes of longitudinal coupled bunch instabilities seen in HERA-p during acceleration (Kot) were done using the "Elmarmeter" (designed by Elmar Vogel, now at CERN).

**Impedance studies:** Shielding is an important issue for both existing offending elements in the ring and controlling impedance sources in future high-intensity accelerators. The longitudinal impedance found for resistive beam pipe (Hasse) allows the effectiveness of shielding to be estimated for different pipe thicknesses.

An accurate impedance model of HESR (FAIR) will be required in future to predict the stability of a cooled antiproton beam (Lehrach).

**Multi-harmonic RF System:** A double (lower) harmonic RF system is proposed as an upgrade for SIS18 to increase the bucket during acceleration and to lower the bunch peak current using bunchlengthening mode (BLM). Studies of intensity effects using nonlinear single particle dynamics (Boine-Frankenheim) showed good agreement between theory and simulation for the loss of Landau damping (dipole mode) due to space charge for both single and double RF systems. It was also found that with a double harmonic RF system the persistent dipole oscillations observed in SIS could only be worse in the presence of space charge below transition. The problem of long bunches in BLM in the region with  $dw(J) dJ = 0$  was not observed in simulations, but nevertheless created a problem for the low-level beam control in the CERN Booster. A large beam response for BLM was also measured in the SPS.

**Active Damping (Feedback/Feed-forward):** The single bunch head-tail instability in the Tevatron can be cured (Lebedev) using transverse feedback, since it is doing more than was expected due to the nonlinearity of the applied kick (which is also shifted in phase to contain both odd and even harmonics). This works for long bunches and a bunch-by-bunch feedback. Unfortunately it does not work for all dampers.

A proposal for a coasting beam feedback to cure instability due to some (unknown) impedance in the presence of space charge is based on the analogy between energy loss and the finite-impulse response filter, where the input signal is an earlier charge density and wake function - filter coefficients (Ziemann). Simulations showed that in this case accurate knowledge of the wake-function is required together with a well-adjusted gain - the system being closer to feed-forward than feedback. During discussions the solution of using direct measurement of the energy deviation (e.g. radial position, Schottky spectrum, etc.) was also proposed. Then this system would have a similarity to stochastic cooling but at only low frequencies.

### 5.1.6 Beam cooling and high brightness

O. Boine-Frankenheim (GSI) and J. Wei (BNL)

The many challenging beam cooling projects at high energies are the driving force behind the remarkable progress in modeling and experimental verification reported during the workshop.

At FNAL the 4.3 MeV electron cooler is presently being installed in the Recycler. Electron cooling at very high energies (55 MeV) is proposed for the RHIC upgrade (RHIC-II). Electron cooling up to 8 MeV is required for the proposed HESR as part of the FAIR project at GSI. Optimization of the proposed cooling scenarios, including studies on rf manipulations, stochastic and electron cooling, intrabeam scattering, gas scattering, as well as other processes, requires not only accurate but also fast numerical models. To make reliable predictions for the cooling dynamics at medium to high energies one has to critically check existing theoretical models.

**Intrabeam scattering (IBS):** The different IBS rate approximations can differ by factors of 2, depending on the application. In order to describe the detailed evolution of the bunch density profile and also the beam loss, direct analytical or numerical solutions of the Landau collision term, which has a Fokker-Planck structure, can be obtained (Zenkevich, Lebedev, Burov, Wei). Remarkable agreement between 1D Fokker-Planck simulations and the observed IBS driven bunch profile evolution in RHIC has been achieved (Wei).

**Electron cooling in combination with IBS results in non-Gaussian beam distributions:** The kinetic description of cooling dynamics requires at least 1D and preferably 3D kinetic IBS models. The 3D IBS map approach (Zenkevich) might be a way to include kinetic IBS in tracking codes. However, for long-term kinetic simulations of electron cooling scenarios reduced 1D Fokker-Planck models are still required. In summary, the theory behind IBS for “hot” beams (far away from crystallization) is considered as well understood.

Pertaining to IBS in “hot” beams, the following tasks are identified:

- Fast solvers for IBS rates including transverse coupling and arbitrary rf wave forms
- Fast numerical IBS models for simulations of kinetic cooling scenarios
- 3D kinetic IBS solvers using macro particle methods
- Benchmarking of kinetic IBS solvers with high resolution experiments, using beam echoes or other kinetic beam phenomena

**Electron cooling:** The cooling force estimations for the RHIC-II (Fedotov) project are based on the Parkhomchuk formula, which is an empirical generalization of the theoretical friction force for unmagnetized electrons. Magnetized electron cooling will be crucial for RHIC-II and also for the HESR in order to achieve the required cooling rates. Especially with regard to magnetized cooling at high energy, the existing theoretical cooling models are regarded as insufficiently accurate. Complications arise from the small Coulomb logarithm for magnetized cooling. Experimentally, the correction of field misalignments is a challenging technical problem.

The precise knowledge of the residual field errors is required for accurate simulations of beam cooling. All these complication will make accurate (within a factor of 2) predictions for magnetized cooling very difficult. On the other hand, macro-particle simulation codes, like VOPAL (Bruhwiler), allow the calculation of electron cooling forces from first principles. Using the tabulated forces extracted from a large number of simulation runs or fitting parameters one might be able in the future to achieve the required accuracy. Such simulations need to account for the various practical cooler imperfections and also for collective electron-ion effects. In addition, understanding of cooling forces through accurate measurements at the existing machines at low energies is important. It will also be worth re-investigating existing data under the light of the new project challenges. Transverse cooling forces are usually more difficult to measure. Recent results using kicked pencil beams in CELSIUS (Ziemann) look promising.

Pertaining to electron cooling, the following tasks are identified and questions raised:

- Large-scale simulation studies of magnetized cooling forces
- Measurement of magnetized cooling forces at low energy using existing machines with proper control of the relevant cooler and beam parameters
- Are non-ideal or non-linear electron plasma effects important at high energy? Do we expect deviation from the  $Z^2$  scaling law for the cooling force at high energy?

**Intensity limits:** Beam intensities in the existing cooler rings are mostly limited by various kinds of collective instabilities. Intensity limits discussed during the workshop were transverse coherent dipole oscillations (Meshkov), longitudinal microwave instabilities (Senichev, Steck) and two-stream instabilities induced by trapped ions (Meshkov). The transverse dipole modes observed in HIMAC and COSY can be damped by feedback systems, whereas the longitudinal microwave instability must be avoided by all means. Above transition energy the negative mass instability can effectively limit the equilibrium beam parameters (Steck). A lattice with imaginary  $\gamma_t$  is proposed for the HESR in order to enhance Landau damping to suppress longitudinal and transverse instabilities (Senichev). Pertaining to intensity limits, the following tasks are identified and questions raised:

- What is the driving impedance behind the coherent instabilities observed in HIMAC and COSY? A detailed stability analysis taking into account electron cooling, space charge and the resistive wall will be necessary.
- More accurate threshold calculations for the longitudinal microwave instability in electron-cooled beams are necessary. Is the microwave instability the main limitation for the achievable momentum spread in the proposed high-energy cooler rings?
- Comparison of the observed two-stream instability thresholds with theoretical predictions. What are the main intensity limitations with regard to high energy cooling?

### 5.1.7 Advanced Techniques

K. Takayama (KEK) and J. Galambos (ORNL)

The advanced techniques session covered a broad range of topics, and as such is not easily characterized. However, a common theme is the development of Proof of Principle experiments in many different areas. While generally not yet ready for production applications, the techniques discussed in this session could prove useful later for high intensity applications. One area is stripping foils. While the use of stripping foils has opened the door to accumulation of high intensity, low emittance beams in rings, the intrinsic limitation from large angle scattering is a concern for very low loss is important. Two papers were presented in the area of laser stripping (V. Danilov from ORNL and I. Yamane from KEK). The key issue being addressed for laser stripping is obtaining high stripping efficiencies for a real beam with a finite momentum spread, using a narrow band laser beam. Both two and three step processes are proposed to deal with this concern, and importantly proof of principle experiments on the BNL and SNS linac H- beamlines are being set up to investigate these ideas. Initial results should be available in the next year.

Another exciting paper was presented by Prof. K. Takayama from KEK, in the area of induction acceleration in rings. The first experimental results of beam accelerated in a ring by induction techniques (vs. RF) were presented for the KEK PS ring. This is a remarkably fast demonstration, from its first proposal four years ago. The technology for the cavities and voltage modulation were presented along with the initial measurements of the effect on the beam in the ring. In the same area of longitudinal acceleration, W. Chou (FNAL) presented a paper on the application of a barrier bucket RF system for the FNAL booster. A barrier RF system was installed and tested and successfully increased the beam intensity available to inject into the Main Injector. However the emittance is larger with the barrier RF system. Related to the topics of induction acceleration and a barrier bucket, Y. Shimosaki (KEK) addressed specific features in beam dynamics of super-bunches, such as diffusion caused by a steep barrier, significant modification of the barrier bucket by a droop in an acceleration voltage, emittance growth caused by a ripple in the accelerating voltage. The results obtained by computer simulations suggest a practical guideline on the performance of novel devices, which are being developed for the proposed scheme. In addition, his computer simulation assuming a water-bag model demonstrates that, as a length of the super-bunch becomes long, the head-tail instability in the super-bunch is more stable. It is extremely expected to explore physics behind it, as soon as possible.

In the area of beam extraction from rings, M. Giovannozzi (CERN) presented a talk on multi-turn extraction using stable island trapping. The key idea is to use nonlinear elements to create islands in which beam is trapped. This permits separation of the beam into distinct regions of transverse space, opening a new possibility for low loss extraction which is in between the presently used fast (single turn) extraction and slow extraction. Over the past two years the formation of islands and separation of beam into the islands has been demonstrated at CERN, with low loss.

D.R. Welch (Mission Research) reported key techniques in beam handling, such as pulse compression and neutralized transport of a heavy ion beam to a target, which are required in the recent Heavy Ion Fusion (HIF) scenarios. The Virtual National Laboratory, a formal collaboration of LBNL, LLNL, and PPPL, has been reorganizing their related activities in order to realize an intermediate state of HIF toward the final goal of inertial fusion, a small scale HIF driver, in which a  $\text{Ne}^+$  beam of 780A is accelerated up to 230MeV. So far the neutralized drift compression (NDC) has been investigated in extensive simulations of HIF driver. It was reported that the neutralized

transport experiment (NTX) with various plasma conditions at LBNL, which provides the first experimental validation of ballistic transport of a space-charge-dominated beam, were in good agreement with the electromagnetic PIC code LSP. Based on simulation results, NDC issues for the small scale HIF driver were addressed.

### 5.1.8 FFAGs and Cyclotrons

R. Baartman (TRIUMF) and S. Martin (FZJ)

Discussions centered on the special attributes of fixed-field magnetic focusing machines and their place in the context of high-brightness hadron machines. A complicating feature of machines of this type is that the orbit unavoidably grows with energy. There is thus no central reference orbit as there is with synchrotrons or linacs. At any energy, one must first find the equilibrium orbit before other Courant-Snyder functions can be found. There are no standard elements, instead the optics must be determined and fine-tuned by tracking through field maps. However, computation has improved by many orders of magnitude since the MURA days, and so calculation of the fields and tracking through them no longer represent a design constraint. During the 50s, when FFAGs were being developed by the MURA group as synchro-cyclotrons, cyclotrons also made the switch from weak-focusing “classical” machines to sector-focused. So since that time, cyclotrons can be considered as isochronous versions of FFAGs. 100's of these machines exist worldwide. They are the most economical way of producing low energy, high quality cw hadron beams. The fixed frequency allows the rf to be highly efficient, while the recirculating nature, in contrast to linacs, allows optimal use of the rf power.

The largest cyclotrons accelerate hadrons to relativistic energies. Examples are PSI (580MeV protons), TRIUMF (500MeV H<sup>-</sup>), and the RIKEN SRC (2500 Z<sup>2</sup>/A MeV heavy ions, under construction). The latter is superconducting with a peak magnetic field of 3.8 T. The most dramatic example in terms of efficiency is the PSI ring cyclotron. This machine produces 1.16 MW of protons at 580 MeV, from a total of 2.8 MW wall-plug power. After their rf upgrade is complete (they are switching from Al to higher- $Q$  Cu cavities), they expect to be able to produce 2MW beam from less than 4MW wall-plug power. The PSI group has also produced a conceptual design of a 10MW, 1GeV proton machine. At these intensities, space charge is not an issue as it would be in a synchrotron of similar power, since it is cw and not pulsed. So the extracted beam emittance can be very small. As well, in an isochronous machine  $\gamma = \gamma_t$ , longitudinal space charge cannot debunch the beam. The upper limit in energy is an economic one: for 10s of GeV protons, the amount of RF needed to maintain turn separation for clean extraction is so large that the total number of turns is small and thus a superconducting linac would be simpler.

The other kind of FFAG is called “scaling”: orbits of various energies are all congruent. This ensures that the betatron tunes do not vary with energy, but has the disadvantage that isochronism is no longer possible. Scaling FFAGs are magnetically “easier” than isochronous ones, since in the latter case, with  $\sim 10^3$  turns, the field must be correct to less than a part in  $10^4$ , while in the former case, 1% is sufficient to fix the tunes. In fact, the KEK 150 MeV proton FFAG's tunes vary by about 10%. This was found to be due to the fact that the tapered gap (needed to achieve the required field index) breaks the scaling. Scaling FFAGs are pulsed by having their rf frequency

modulated: they are in fact strong-focusing synchrocyclotrons. However, it is possible to pulse the rf frequency at a much higher rate than the magnetic field can be pulsed in a synchrotron. Advances in the magnetic materials used to load the rf cavities have made it possible to pulse in the kHz regime while maintaining reasonable rf efficiency. This makes the FFAG attractive as a proton driver in the many-GeV range. Furthermore, in either scaling or non-scaling form, FFAGs have very large acceptance, especially in the horizontal plane. Coupled with very fast cycling time, these features make FFAGs ideal for acceleration of muons.

**Discussion:** The discussion centered on trying to find the optimal machine for given applications. To narrow down the issue, we decided to focus on machines in the 1 to 2 GeV range. The following table contains our conclusions.

**Table 1.** Machine type vs. application at 1-2 GeV

Application	SC linac	RCS	FFAG	Cyclotrons
P = 10 MW (10 mA)	OK	Not OK unless $E \gg 1\text{ GeV}$	Not yet known, need a 1 MW demo first	OK
High rep rate (nu-fact)	OK	No	OK	Not yet known, need stacking
Low duty (neutron source)	OK, but compressor ring is ?	OK for $E \gg 1\text{ GeV}$	Not yet known	No
CW (e.g., ADS)	OK	No	Not yet known	OK

## 6 Forthcoming Beam Dynamics Events

### 6.1 Workshop Coulomb 05 – High Intensity Beam Dynamics

*Dates and place* Monday 12 to Friday 16 September 2005, Senigallia, Italy

*Motivation and goals* The workshop is intended to open a discussion panel on high intensity beams and space charge dynamics covering theoretical aspects, numerical techniques, recent experiments and machine designs. Attention will be devoted to collective instabilities, collisional effects, dynamic aperture, resonant extraction, adiabatic diffusion, emittance growth, CSR related effects. One of the goals is to promote a joint discussion between scientists from accelerators laboratories and academic institutions. Graduate students in beam dynamics or accelerator physics are invited to participate. We expect to focus the crucial open problems and to outline the analytical and computational techniques suitable to treat them.

*Official sponsors* University of Bologna and Istituto Nazionale di Fisica Nucleare.

Chairman G. Turchetti, Department of Physics, University of Bologna.

Logistic information Senigallia is located on the Adriatic coast in Italy, in the middle of Marche, a region rich of historical and natural beauties. Easily reachable by car, train, air.

Sessions The plenary sessions will take place at the IAT conference room, discussion meetings will also be organized at the hotel Duchi della Rovere conference room, a few minutes walk from the beach and from the centre of the town. There will be invited and contributed oral presentations. Poster sessions will be organized if necessary.

Registration Open on April 4.

Additional information available on <http://www.physycom.unibo.it/coulomb05>

### **International Advisory Board**

L. Calabretta (LNS INFN)  
 J. Ellison (Univ. of New Mexico)  
 Y. Elskens (Univ. of Marseille)  
 M. Giovannozzi (CERN)  
 I. Hofmann (GSI)  
 A. Lehrach (Juelich)  
 S. Lund (LBNL)  
 H. Mais (DESY)  
 R. Ryne (LBNL)  
 L. Serafini (INFN Milano)  
 E. Sonnendrücker (Univ. of Strasbourg)  
 G. Turchetti (INFN Bologna)  
 P. Zenkevich (ITEP)

### **Local organizing committee:**

A. Bazzani (Univ. of Bologna)  
 C. Benedetti (Univ. of Bologna)  
 N. Cufaro (Univ. of Bari)  
 M. Pusterla (Univ. of Padova)  
 R. Fedele (Univ. of Napoli)

### **Scientific Program**

#### **Monday 12** Morning session

Y. Elskens *From long-range interaction to collective behaviour,  
and from Hamiltonian chaos to stochastic models*  
 I. Hofmann *Nonlinear phenomena in space charge dominated beams*

#### Afternoon session

A. Neishtadt *Destruction of adiabatic invariance at resonances*

*in slow-fast Hamiltonian systems*

J. Ellison *Vlasov equation in beam dynamics: analysis and perturbation theory*

**Tuesday 13** Morning session

R. Warnock *Study of bunch instabilities by the nonlinear Vlasov-Fokker-Planck equation*

S. Lund *Title to be announced*

Afternoon session

Court Bohm *Chaotic dynamics and halo formation in charged particle Beams*

H. Mais *Stochastic Aspects of Beam Physics*

**Wednesday 14** Morning session

R. Kisheck *High-intensity beams at the UMER facility*

L. Serafini *Generation and transport of high brightness electron Beams for X-ray FEL's*

**Thursday 15** Morning session

M. Giovannozzi *Resonant multi-turn extraction: principle and experiments*

E. Metral *Observation of octupole driven resonance phenomena with spacecharge at the CERN Proton Synchrotron*

Afternoon session

A. Lerach *Intensity limits in HESR*

P. Zenkevich *New algorithms for kinetic analysis of intra-beam scattering in storage rings*

**Friday 16** Morning session

V. Malka *State of art of laser plasma accelerators*

S. Cousineau *Space charge issues in the SNS linac and ring*

G. Franchetti *Space charge challenges in the FAIR project*

**6.2 34<sup>TH</sup> ICFA Advanced Beam Dynamics Workshop - High Power Superconducting Ion, Proton, and Multi-Species Linacs, "HPSL 2005"**

The 34th ICFA Advanced Beam Dynamics Workshop will take place from May 22 to 24, 2005 at Northern Illinois University / Naperville Campus, Naperville, IL, USA.

The Workshop topic is "High Power Superconducting Ion, Proton, and Multi-Species Linacs" and aims to discuss common areas of beam dynamics and technology development required for a variety of next-generation high-power superconducting linacs.

The venue is the Naperville Campus of Northern Illinois University located between two National Laboratories, ANL and FNAL, near Chicago, USA. The workshop's website is available at <http://www.niu.edu/clasep/HPSLconf/>.

The goals of the workshop are to:

- Discuss common areas of beam dynamics and technology development required for a variety of next-generation high-power superconducting linacs (HPSL).
- Provide an excellent opportunity to involve the international SRF community in the design of machines, which may be on the "fast-track" for construction.

More specifically, the workshop will focus on the following topics:

- Discussion of current status of "standard" beam dynamics issues (e.g., beam quality preservation, halo, beam loss) in HPSL
- Lattice design for HPSL. Transition energy from RT to SC structures in proton and ion linacs
- Special issues related to multiple-charge-state acceleration
- Issues related to stripper foils in heavy ion linacs
- End-to-end simulations in the SC linacs in the presence of machine errors
- Controlled and uncontrolled beam losses. Beam losses due to H-minus stripping. Collimation and beam dump in HPSL
- Superconducting accelerating structures for cw or pulsed high-current applications to cover wide velocity range of ions from 0.02c to 1.0c.
- Power couplers
- RF power distribution systems
- LLRF, fast high-powered phase shifters and IQ modulators

The program consists of a review, opening, and a closing plenary sessions, and three parallel Working Group sessions with the following topics and conveners:

1. Beam Dynamics – Jean-Michel Lagniel (CEA-Saclay), Richard Baartman (TRIUMF)
2. Superconducting Radiofrequency Resonators for Ion Linacs – Jean Delayen (JLAB), Kenneth Shepard (ANL)
3. RF Systems – Mark Champion (SNS), Brian Chase (FNAL)

We are now encouraging the submission of contributed papers for the Working Group sessions. Proceedings will be published for both invited and contributed papers. For further information and registration, please visit:

<http://www.niu.edu/clasep/HPSLconf/>

#### **Executive Committee**

C.L. Bohn (NIU)

G.W. Foster (FNAL)

P.N. Ostroumov (ANL)

**Scientific Advisory Panel**

W. Barletta (LBNL)  
 W. Chou (FNAL & ICFA)  
 S. Chattopadhyay (TJNAF)  
 G. Dutto (TRIUMF)  
 A. Facco (INFN/LNL-Legnaro)  
 R. Garoby (CERN)  
 N. Holtkamp (ORNL SNS)  
 K.-J. Kim (ANL)  
 J.-M. Lagniel (CEA-Saclay)  
 S. Ozaki (BNL)  
 V. Sahni (CAT, India)  
 K. Shepard (ANL)  
 D. Trines (DESY)  
 Y. Yamazaki (JAERI-Tokai)  
 R. York (Michigan State University)  
 C. Zhang (IHEP China)  
 ICFA Beam Dynamics Panel

**Local Organizing Committee**

J. Bergman (ANL)  
 B. Erdelyi (NIU-ANL, Chair)  
 K. Gordon (NIU)  
 S. Johnson (NIU)  
 D. Mihalcea (NIU)  
 B. Mustapha (ANL)  
 I. Sideris (NIU)  
 B. Terzic (NIU)

**6.3 Joint 38th ICFA Advanced Beam Dynamics and 9th Advanced & Novel Accelerators Workshop on Laser-Beam Interactions and Laser and Plasma Accelerators**

4th LBI Workshop and 7th LPA Workshop, December 12 - 16, 2005 National Taiwan University, Taipei, Taiwan Jointly organized by NTU, Taiwan, and KEK, Japan

Co-chairs: W.-Y. Pauchy Hwang, NTU and Shin-ichi Kurokawa, KEK

Introduction

You are cordially invited to participate in the ICFA Workshop on Laser-Beam Interactions and Laser Plasma Accelerators, to be held at National Taiwan University in Taipei on December 12-16, 2005. National Taiwan University (NTU) and High Energy Accelerator Research Organization (KEK) will jointly host the workshop.

Up to now two workshops, namely, Laser-Beam Interactions Workshop (LBI) and Laser Plasma Accelerators Workshop (LPA), have been held independently. This time, we have decided that the Fourth LBI and the Seventh LPA Workshops will be jointly

held as the ICFA Workshop on Laser-Beam Interactions and Laser Plasma Accelerators for Celebrating the United Nations International Year of Physics.

Recent advancements on ultra-intense and relativistic lasers and particle accelerators have inspired a broad range of applications to science and technology. On the technology side, one exciting development has been the laser and plasma based novel accelerators, with the promise of extending the energy of high-energy accelerators far beyond what the conventional technology can provide. On the science side, the tremendous energy density provided by state-of-the-art laser and particle beams opens an exciting new window of opportunity for the investigations of frontier fundamental physics ranging from particle physics, nuclear physics, condensed matter physics, to astrophysics.

This joint workshop will focus on recent developments of the fundamental physics as well as the advanced accelerator technology based on ultra intense laser and particle beams. Inspired by the centenary celebration of Albert Einstein's magic year of 1905, new visions, novel concepts, and future prospects will be emphasized in this meeting. Your participation and support are certainly crucial to the success of this conference. We are looking forward to hearing from you.

#### Conference Topics

- Physics and applications of laser-beam and plasma interactions, including the generation of energetic particles, high-energy Gamma rays, short-pulse X-rays and Tera Herz radiations.
- Laser applications for beam and plasma diagnoses, and beam cooling and handling.
- Laser and plasma particle acceleration concepts and experiments including computer modeling of experiments.
- Mono energetic high quality particle beam generation in laser-plasma accelerators: mechanism, control and applications.
- Over-GeV laser-plasma accelerator technology.
- Extreme high-energy accelerator and collider concepts.
- High energy density beam-plasma physics including Laboratory astrophysics.
- High energy density astrophysics including ultrahigh energy cosmic ray acceleration, Gamma ray burst and Cosmic jet.
- Fundamental physics related to laser and particle beams.

#### Public Lecture Series

For celebrating the United Nations International Year of Physics, we have plans to hold the Public Lecture, inviting Nobel laureates as the Lecturers.

- S. Chu, LBNL, USA
- T. D. Lee, Columbia U., USA
- C. Cohen-Tannoudji, France
- S. Ting, MIT, USA
- S. Hawking, Cambridge, UK
- C. Wiemann, U. Colorado, USA
- W. Ketterle, MIT, USA
- C. N. Yang, Tsing-Hua, Beijing, China
- M. Koshiya, U. Tokyo, Japan

Registration Deadline for reduced rate: Oct. 30, 2005 (Beginning: Aug. 15)

Call for abstract Deadline: Sep. 12, 2005 (Beginning: Aug. 15)

Conference webpage <http://hep1.phys.ntu.edu.tw/~ytshen/icfa/index.html>

**International Advisory Committee** (\*to be confirmed)

F. Amiranoff, LULI, France  
 W. Namkung, POSTECH, Korea  
 I. Ben-Zvi, BNL, USA  
 A. Noda, Kyoto U., Japan  
 R. Bingham, RAL, UK  
 P. P. Pashinin, IGP, Russia  
 J. Chen, Peking U., China  
 F. Pegoraro, Pisa, Italy  
 P. Chen, SLAC, USA \*  
 M. Roth, Darmstadt, Germany  
 C. Joshi, UCLA, USA \*  
 F. Ruggiero, CERN, Switzerland  
 I.-S. Ko, PAL, Korea \*  
 V. C. Sahni, CAT, India  
 W. Leemans, LBNL, USA \*  
 P. Sprangle, NRL, USA \*  
 K. S. Liang, NSRRC, Taiwan  
 T. Tajima, JAERI, Japan  
 C. S. Liu, NCU, Taiwan  
 H. Takabe, Osaka, U., Japan \*  
 T. Mendonca, U. Lisbon, Portugal  
 M. Uesaka, U. Tokyo, Japan  
 H. O. Moser, SSSL, Singapore \*  
 J. M. Vehn, MPI-G, Germany  
 G. Mourou, LOA, France \*  
 J. Zhang, IOP, China  
 ICFA Beam Dynamics Panel  
 ICFA Advanced and Novel Accelerators Panel

**International Program Committee** (\*to be confirmed)

S. Bulanov, IGP, Russia  
 S. Kurokawa, KEK, Japan (Co-Chair)  
 T. Hirose, Waseda U., Japan  
 M. Lontano, CNR, Italy  
 Y.-K. Ho, Fudan U., China  
 V. Malka, LOA, France  
 Y. Hsiung, NTU, Taiwan  
 K. Nakajima, KEK, Japan  
 Y.-C. Huang, NTHU, Taiwan  
 J. S.-T. Ng, SLAC, USA

W-Y. P. Hwang, NTU, Taiwan (Co-Chair)  
 P. Norreys, RAL, UK  
 T. Katsouleas, USC, USA  
 L. Schachter, IIT, Israel  
 Y. Kitagawa, Osaka U., Japan  
 H. Suk, KERI, Korea  
 S. Krishnagopal, CAT, India \*  
 Y. Takahashi, UAH, USA  
 G. R. Kumar, TIFR, India A. Ting, NRL, USA

**Local Organizing Committee (\*to be confirmed)**

P.-T. Chang, NTU, Taiwan  
 W-Y. P. Hwang, NTU, Taiwan (Co-Chair)  
 S. Y. Chen, AS, Taiwan  
 S. Kurokawa, KEK, Japan (Co-Chair) \*  
 T. Chiueh, NTU, Taiwan  
 K. Nakajima, KEK, Japan  
 Y. Hsiung, NTU, Taiwan  
 J. Wang, AS, Taiwan \*  
 K.-T. Hsu, NSRRC, Taiwan  
 M. Z. Wang, NTU, Taiwan  
 Y.-C. Huang, NTHU, Taiwan \*  
 J.H.P. Wu, NTU, Taiwan

## **7 Announcements of the Beam Dynamics Panel**

### **7.1 ICFA Beam Dynamics Newsletter**

#### **7.1.1 Aim of the Newsletter**

The ICFA Beam Dynamics Newsletter is intended as a channel for describing unsolved problems and highlighting important ongoing works, and not as a substitute for journal articles and conference proceedings that usually describe completed work. It is published by the ICFA Beam Dynamics Panel, one of whose missions is to encourage international collaboration in beam dynamics.

Normally it is published every April, August and December. The deadlines are 15 March, 15 July and 15 November, respectively.

#### **7.1.2 Categories of Articles**

The categories of articles in the newsletter are the following:

1. Announcements from the panel.
2. Reports of beam dynamics activity of a group.

3. Reports on workshops, meetings and other events related to beam dynamics.
4. Announcements of future beam dynamics-related international workshops and meetings.
5. Those who want to use newsletter to announce their workshops are welcome to do so. Articles should typically fit within half a page and include descriptions of the subject, date, place, Web site and other contact information.
6. Review of beam dynamics problems: This is a place to bring attention to unsolved problems and should not be used to report completed work. Clear and short highlights on the problem are encouraged.
7. Letters to the editor: a forum open to everyone. Anybody can express his/her opinion on the beam dynamics and related activities, by sending it to one of the editors. The editors reserve the right to reject contributions they judge to be inappropriate, although they have rarely had cause to do so.
8. Editorial.

The editors may request an article following a recommendation by panel members. However anyone who wishes to submit an article is strongly encouraged to contact any Beam Dynamics Panel member before starting to write.

### **7.1.3 How to Prepare a Manuscript**

Before starting to write, authors should download the template in Microsoft Word format from the Beam Dynamics Panel web site:

<http://www-bd.fnal.gov/icfabd/news.html>

It will be much easier to guarantee acceptance of the article if the template is used and the instructions included in it are respected. The template and instructions are expected to evolve with time so please make sure always to use the latest versions.

The final Microsoft Word file should be sent to one of the editors, preferably the issue editor, by email.

The editors regret that LaTeX files can no longer be accepted: a majority of contributors now prefer Word and we simply do not have the resources to make the conversions that would be needed. Contributions received in LaTeX will now be returned to the authors for re-formatting.

In cases where an article is composed entirely of straightforward prose (no equations, figures, tables, special symbols, etc.) contributions received in the form of plain text files may be accepted at the discretion of the issue editor.

Each article should include the title, authors' names, affiliations and e-mail addresses.

### **7.1.4 Distribution**

A complete archive of issues of this newsletter from 1995 to the latest issue is available at

<http://icfa-usa.jlab.org/archive/newsletter.shtml>

This is now intended as the primary method of distribution of the newsletter.

Readers are encouraged to sign-up for electronic mailing list to ensure that they will hear immediately when a new issue is published.

The Panel's Web site provides access to the Newsletters, information about future and past workshops, and other information useful to accelerator physicists. There are links to pages of information of local interest for each of the three ICFA areas.

Printed copies of the ICFA Beam Dynamics Newsletters are also distributed (generally some time after the Web edition appears) through the following distributors:

Weiren Chou	<a href="mailto:chou@fnal.gov">chou@fnal.gov</a>	North and South Americas
Rainer Wanzenberg	<a href="mailto:rainer.wanzenberg@desy.de">rainer.wanzenberg@desy.de</a>	Europe* and Africa
Susumu Kamada	<a href="mailto:Susumu.Kamada@kek.jp">Susumu.Kamada@kek.jp</a>	Asia** and Pacific

\* Including former Soviet Union.

\*\* For Mainland China, Jiu-Qing Wang ([wangjq@mail.ihep.ac.cn](mailto:wangjq@mail.ihep.ac.cn)) takes care of the distribution with Ms. Su Ping, Secretariat of PASC, P.O. Box 918, Beijing 100039, China.

To keep costs down (remember that the Panel has no budget of its own) readers are encouraged to use the Web as much as possible. In particular, if you receive a paper copy that you no longer require, please inform the appropriate distributor.

### 7.1.5 Regular Correspondents

The Beam Dynamics Newsletter particularly encourages contributions from smaller institutions and countries where the accelerator physics community is small. Since it is impossible for the editors and panel members to survey all beam dynamics activity worldwide, we have some Regular Correspondents. They are expected to find interesting activities and appropriate persons to report them and/or report them by themselves. We hope that we will have a "compact and complete" list covering all over the world eventually. The present Regular Correspondents are as follows:

Liu Lin	<a href="mailto:liu@ns.lnls.br">liu@ns.lnls.br</a>	LNLS Brazil
S. Krishnagopal	<a href="mailto:skrishna@cat.ernet.in">skrishna@cat.ernet.in</a>	CAT India
Sameen Ahmed Khan	<a href="mailto:rohelakhan@yahoo.com">rohelakhan@yahoo.com</a>	MECIT Middle East and Africa

We are calling for more volunteers as *Regular Correspondents*.

## 7.2 ICFA Beam Dynamics Panel Members

Caterina Biscari	<a href="mailto:caterina.biscari@lnf.infn.it">caterina.biscari@lnf.infn.it</a>	LNF-INFN, Via E. Fermi 40, C.P. 13, Frascati, Italy
<u>Swapan Chattopadhyay</u>	<a href="mailto:swapan@jlab.org">swapan@jlab.org</a>	Jefferson Lab, 12000 Jefferson Avenue, Newport News, VA 23606, U.S.A.
Pisin Chen	<a href="mailto:chen@slac.stanford.edu">chen@slac.stanford.edu</a>	SLAC, 2575 Sand Hill Road, MS 26 Menlo Park, CA 94025, U.S.A.
Weiren Chou (Chair)	<a href="mailto:chou@fnal.gov">chou@fnal.gov</a>	Fermilab, MS 220, P.O. Box 500, Batavia, IL 60510, U.S.A.
Yoshihiro Funakoshi	<a href="mailto:yoshihiro.funakoshi@kek.jp">yoshihiro.funakoshi@kek.jp</a>	KEK, 1-1 Oho, Tsukuba-shi, Ibaraki-ken, 305-0801, Japan
Miguel Furman	<a href="mailto:mafurman@lbl.gov">mafurman@lbl.gov</a>	Center for Beam Physics, LBL, Building 71, R0259, 1 Cyclotron Road, Berkeley, CA 94720-8211, U.S.A.
Jie Gao	<a href="mailto:gaoj@ihep.ac.cn">gaoj@ihep.ac.cn</a>	Institute for High Energy Physics, P.O. Box 918, Beijing 100039, China
Ingo Hofmann	<a href="mailto:i.hofmann@gsi.de">i.hofmann@gsi.de</a>	High Current Beam Physics, GSI Darmstadt, Planckstr. 1, 64291 Darmstadt, Germany
Sergei Ivanov	<a href="mailto:ivanov_s@mx.ihep.su">ivanov_s@mx.ihep.su</a>	Institute for High Energy Physics, Protvino, Moscow Region, 142281 Russia
Kwang-Je Kim	<a href="mailto:kwangje@aps.anl.gov">kwangje@aps.anl.gov</a>	Argonne Nat'l Lab, Advanced Photon Source, 9700 S. Cass Avenue, Bldg 401/C4265, Argonne, IL 60439, U.S.A.
In Soo Ko	<a href="mailto:isok@postech.ac.kr">isok@postech.ac.kr</a>	Pohang Accelerator Lab, San 31, Hyoja- Dong, Pohang 790-784, South Korea
Alessandra Lombardi	<a href="mailto:Alessandra.Lombardi@cern.ch">Alessandra.Lombardi@cern.ch</a>	CERN, CH-1211, Geneva 23, Switzerland
Yoshiharu Mori	<a href="mailto:mori@kl.rii.kyoto-u.ac.jp">mori@kl.rii.kyoto-u.ac.jp</a>	Research Reactor Inst., Kyoto Univ. Kumatori, Osaka, 590-0494, Japan
Chris Prior	<a href="mailto:c.r.prior@rl.ac.uk">c.r.prior@rl.ac.uk</a>	ASTeC Intense Beams Group, Rutherford Appleton Lab, Chilton, Didcot, Oxon OX11 0QX, U.K.
David Rice	<a href="mailto:dhr1@cornell.edu">dhr1@cornell.edu</a>	Cornell Univ., 271 Wilson Laboratory, Ithaca, NY 14853-8001, U.S.A.
Yuri Shatunov	<a href="mailto:Yu.M.Shatunov@inp.nsk.su">Yu.M.Shatunov@inp.nsk.su</a>	Acad. Lavrentiev, prospect 11, 630090 Novosibirsk, Russia
Junji Urakawa	<a href="mailto:junji.urakawa@kek.jp">junji.urakawa@kek.jp</a>	KEK, 1-1 Oho, Tsukuba-shi, Ibaraki-ken, 305-0801, Japan
Jie Wei	<a href="mailto:wei1@bnl.gov">wei1@bnl.gov</a>	BNL, Bldg. 911, Upton, NY 11973- 5000, U.S.A.
Jiu-Qing Wang	<a href="mailto:wangjq@mail.ihep.av.cn">wangjq@mail.ihep.av.cn</a>	Institute for High Energy Physics, P.O. Box 918, 9-1, Beijing 100039, China
Rainer Wanzenberg	<a href="mailto:rainer.wanzenberg@desy.de">rainer.wanzenberg@desy.de</a>	DESY, Notkestrasse 85, 22603 Hamburg, Germany

*The views expressed in this newsletter do not necessarily coincide with those of the editors. The individual authors are responsible for their text.*